UNIVERSIDADE DE LISBOA
INSTITUTO SUPERIOR TÉCNICO

A Bridge Between Development and Engineering: Creating Liver Organoids from Human Induced Pluripotent Stem Cells

João Pedro Brinquete Cotovio

Supervisor: Doctor Tiago Paulo Gonçalves Pinheiro Fernandes

Thesis approved in public session to obtain the PhD Degree in
Bioengineering

Juri Final Classification: **Pass with Distinction**

2024

UNIVERSIDADE DE LISBOA
INSTITUTO SUPERIOR TÉCNICO

A Bridge Between Development and Engineering: Creating Liver Organoids from Human Induced Pluripotent Stem Cells

João Pedro Brinquete Cotovio

Supervisor: Doctor Tiago Paulo Gonçalves Pinheiro Fernandes

Thesis approved in public session to obtain the PhD Degree in
Bioengineering

Jury Final Classification: **Pass with Distinction**

Jury

Chairperson:
Doctor João Pedro Estrela Rodrigues Conde, Instituto Superior Técnico, Universidade de Lisboa

Members of the Committee:
Doctor Joaquim Manuel Sampaio Cabral, Instituto Superior Técnico, Universidade de Lisboa
Doctor Lino da Silva Ferreira, Faculdade de Medicina, Universidade de Coimbra
Doctor José Eduardo Marques Bragança, Faculdade de Medicina e Ciências Biomédicas, Universidade do Algarve
Doctor Tiago Paulo Gonçalves Pinheiro Fernandes, Instituto Superior Técnico, Universidade de Lisboa

Funding Institution
FCT: Fundação Para a Ciência e Tecnologia

2024

ABSTRACT

Liver disease is one of the main causes of death worldwide, leading to the death of approximately 2 million people per year. Current therapies include orthotopic liver transplantation, however, donor organ shortage remains a great challenge. In addition, the development of novel therapeutics has been limited due to the lack of *in vitro* models that mimic *in vivo* liver physiology. Accordingly, the development of new culture systems such as liver organoids derived from human induced pluripotent stem cells (hiPSCs), represent a promising tool for liver cell therapy, disease modelling, and drug discovery. Still, current methods to generate liver organoids from hiPSCs are laborious and give rise to structures with limited complexity. In this work it was developed a culture system that is able to generate liver bud organoids with increased complexity and vascularization. By integrating activin A gradients to direct spatial patterning, it was possible to recreate not only the diversity of cell types that constitute the human liver bud during development, but also key events of liver organogenesis. Therefore, this work provides a suitable platform to study liver development and to explore the emerging fields of disease modeling and drug screening based on hiPSC-derived organoids.

Keywords: pluripotent stem cells, hepatic differentiation, liver organoids, activin A, morphogenesis.

RESUMO

A doença hepática é uma das principais causas de morte no mundo, levando à morte cerca de 2 milhões de pessoas por ano. As terapias existentes incluem o transplante de fígado, no entanto, a escassez de doadores de órgãos continua a ser um dos grandes desafios a ultrapassar. Além disso, o desenvolvimento de novas terapias tem sido limitado pela falta de modelos *in vitro* que mimetizem a fisiologia hepática *in vivo*. Assim, o desenvolvimento de novas tecnologias, como organoides hepáticos derivados de células estaminais pluripotentes induzidas de humanos (hiPSCs), representam uma ferramenta promissora para as terapias celulares, para a modelação de doenças e para a descoberta de novos medicamentos. Contudo, os métodos atuais para gerar organoides hepáticos a partir de hiPSCs são trabalhosos e dão origem a estruturas com complexidade limitada. Neste trabalho foi desenvolvido um sistema de cultura capaz de gerar organoides de divertículo hepático com maior complexidade e vascularização. Ao integrar gradientes de activina A para direcionar padrões espaciais, foi possível recriar não apenas a diversidade dos tipos celulares que constituem o divertículo hepático humano durante o desenvolvimento, mas também eventos chave da organogénese do fígado. Desta forma, este trabalho fornece uma plataforma adequada para o estudo do desenvolvimento do fígado e fomenta a investigação em áreas emergentes como a modelação de doenças e o rastreio de fármacos com base em organoides derivados de hiPSCs.

Palavras-chave: células estaminais pluripotentes, diferenciação hepática, organoides hepáticos, activina A, morfogénese.

ACKNOWLEDGEMENTS

As I reach the culmination of this significant academic journey, I am filled with immense gratitude for the support and encouragement that have guided me throughout this work. I am deeply appreciative of the numerous individuals who have contributed to my growth and success.

First, I would like to thank to Professor Joaquim Cabral. Your pioneering work in stem cell engineering in Portugal and your dedication to building this exceptional research group have been truly inspiring. Thank you for providing us with the resources and opportunities to push the boundaries of knowledge in this field.

I would also like to express my heartfelt thanks to my supervisor, Professor Tiago Fernandes, whose guidance and unwavering belief in my potential have been invaluable. The degree of freedom you granted me in pursuing my research has been instrumental in fostering my creativity and scientific independence. Your insightful feedback, encouragement, but specially your positivity, have shaped this work and my development as a researcher.

Special thanks go to my colleagues and friends Mariana Branco and Carina Maranga. Navigating the challenges of a PhD is not always the lightest journey, but your companionship made the work in the lab a joy and turned my days much brighter. I will always cherish those moments in my heart, and I cannot imagine all these years without you. I am also grateful to Teresa Silva, Ana Rita Gomes and Cláudia Miranda, for all the adventures and lessons. To all of you girls, thank you for inspiring me.

I would also like to extend my sincere thanks to all my colleagues at SCERG, for your camaraderie and support. I am fortunate to have shared this experience with such a remarkable group of individuals. A special note of gratitude to Professor Margarida Diogo and Carlos Rodrigues who allowed me to initiate my journey in the stem cell field.

To my family, to my dad, and specially to my mother, sister and Eduardo, your love and support have been my backbone. I cannot describe in words how grateful I am, for everything. Thank you for your patience, encouragement, and, above all, for always being there during these difficult times. You are the foundation upon which this achievement stands.

Lastly, I extend my appreciation to all those who have, in various ways, supported me throughout this journey. Your contributions have been deeply felt and are sincerely acknowledged.

TABLE OF CONTENTS

LIST OF ABBREVIATIONS

2D - Two-dimensional
3D - Three-dimensional
ACC - Accutase
AAT - Alpha-1-Antitrypsin
ALB - Albumin
AFP - Alpha-fetoprotein
ATRA - All-Trans Retinoic Acid
ADME - Absorption, Distribution, Metabolism, and Excretion
BMP - Bone Morphogenetic Protein
BSA - Bovine Serum Albumin
CDM - Chemically Defined Medium
CER1 - Cerberus 1
cGMP - Current good manufacturing practice
CHIR - CHIR99021
CXCR4 - C-X-C Motif Chemokine Receptor 4
DAPI - 4',6-Diamidino-2-Phenylindole
DE - Definitive Endoderm
Dex - Dexamethasone
DILI - Drug-Induced Liver Injury
DMSO - Dimethyl Sulfoxide
DNL - De Novo Lipogenesis
EBs - Embryoid Bodies
ECs – Endothelial Cells
ECM - Extracellular Matrix
EDTA - Ethylenediaminetetraacetic Acid
ESCs - Embryonic Stem Cells
FB1 - Flow Cytometry Buffer 1
FB2 - Flow Cytometry Buffer 2
FC - Flow Cytometry3d
FGF - Fibroblast Growth Factor
FGS - Fetal Goat Serum
FOXA2 - Forkhead Box A2
GAPDH - Glyceraldehyde-3-Phosphate Dehydrogenase
GATA6 - GATA Binding Protein 6
GO - Gene Ontology
GRNs - Gene Regulatory Networks
GSC – Goosecoid
HBV - Hepatitis B Virus
HCM - Hepatocyte Culture Medium
HCV - Hepatitis C Virus
HGF - Hepatic Growth Factor
hiPSCs - Human Induced Pluripotent Stem Cells
HNF4a - Hepatocyte Nuclear Factor 4 Alpha
HSCs - Hepatic Stellate Cells
HTSeq - High-Throughput Sequencing
ICM - Inner Cell Mass
ICC - Immunocytochemistry
KLF4 - Kruppel Like Factor 4
LDN - LDN-193189l
LDL - Low-Density Lipoprotein
MESP1 - Mesoderm Posterior BHLH Transcription Factor 1
MIXL1 - Mix Paired-Like Homeobox
MMPs - Matrix Metalloproteinases
NaB - Sodium Butyrate
OCT4 - Octamer-Binding Transcription Factor 4
OSM - Oncostatin M
PBS - Phosphate Buffered Saline
PFA - Paraformaldehyde
PS - Primitive Streak
PSC - Pluripotent Stem Cell
qRT-PCR - Quantitative Real-Time Polymerase Chain Reaction
RA - Retinoic Acid
RNA-seq - RNA Sequencing
ROCKi - Rho Kinase Inhibitor
rpm – rotation per minute
RPMI - Roswell Park Memorial Institute Medium

RT - Room Temperature

SDF1 - Stromal Cell-Derived Factor 1

SHH - Sonic Hedgehog

SOX17 - SRY-Box Transcription Factor 17

SR - Serum Replacement

STM - Septum Transversum Mesenchyme

TGF-β - Transforming Growth Factor Beta

TFs - Transcription Factors

VEGF - Vascular Endothelial Growth Factor

1

INTRODUCTION

Part of the content of this chapter was adapted from the following publications:

Cotovio, J. P., Fernandes, T. G., Diogo, M. M., & Cabral, J. M. (2020). Pluripotent stem cell biology and engineering. In *Engineering Strategies for Regenerative Medicine* (pp. 1-31). Academic Press.

Cotovio, J. P., & Fernandes, T. G. (2020). Production of Human Pluripotent Stem Cell-Derived Hepatic Cell Lineages and Liver Organoids: Current Status and Potential Applications. *Bioengineering*, 7(2), 36.

STEM CELLS

In 1868, Ernst Haeckel (Haeckel, 1868), a notable biologist from Germany, came up with the term *Stammzelle* to describe the unicellular ancestor from which all multicellular organisms evolved, a concept very different from the one existing today. Later, he used the same term to describe the fertilized egg, or the zygote, capable of giving rise to all cell types of an organism (Haeckel, 1877). This was the cradle for the English term *stem cell* (Ramalho-Santos & Willenbring, 2007). After previous studies on the continuity of the germ-plasm and on the origin of the hematopoietic system, Till and McCulloch proposed in the 1960s what are still today the two gold standard features of stem cells: (1) undifferentiated cells that are capable of self-renewal and (2) production of specialized progeny through differentiation (Becker et al., 1963). To accomplish such attributes, it is now known that stem cells undergo asymmetric cell division, by which the cell divides to generate one stem cell and one differentiating cell. Therefore, it may be added that stem cells are of major importance in the maintenance of homeostasis through a balance between self-renewal and differentiation (Blanpain & Simons, 2013; Knoblich, 2008; Morrison & Kimble, 2006).

From conception to death, as cells develop derived from embryonic tissue, they become progressively restricted in their developmental potency, reaching the point when each cell can only differentiate into a single specific cell type. In the beginning, the earliest cells in ontogeny are totipotent, giving rise, in mammals, to all embryonic and extra-embryonic tissues, i.e., only a totipotent cell can originate an entire organism (De Los Angeles et al., 2015; Inoue et al., 2014; Sánchez Alvarado & Yamanaka, 2014). Through embryogenesis, when the pluripotent state is reached, a pluripotent stem cell (PSC) can originate all the cells from all the tissues of the body, though the contributions to the extra-embryonic membranes or placenta are limited (De Los Angeles et al., 2015). On the other hand, a multipotent stem cell is restricted to the generation of the mature cell type of its tissue of origin and finally, a unipotent stem cell displays limited developmental potential, giving rise to only a single-cell type. In an adult organism, stem cells can be found in most tissues throughout the body, even within relatively dormant tissues. These stem cells experience low or no division in normal homeostasis, remaining quiescent for extended periods of time. However, these cells can respond efficiently to stimuli upon initiation of homeostasis or injury (Hsu & Fuchs, 2012).

Altogether, in both plant and animal kingdoms, the multicellularity of highly regulated tissues is dependent of the generation of new cells for growth and repair. Therefore, biological systems are driven by a balance between cell death and cell proliferation, preserving form and function in tissues. From this point of view, stem cells are the units of the following attributes: development, regeneration and evolution (Sánchez Alvarado & Yamanaka, 2014; Weissman, 2000).

Pluripotent Stem Cells

Mammalian embryogenesis starts with a single totipotent cell, the zygote. After the first cell division, the two-cell embryo is composed by two equal blastomeres. In the earlier stages, including two-cell and four-cell embryos, cells are still considered totipotent. Later, when the zygote is already divided in numerous

blastomeres in a structure that can be called blastocyst, it is possible to distinguish the extraembryonic trophectoderm (TE) on the outside and the inner cell mass (ICM) (J. Wu et al., 2016; J. Wu & Izpisua Belmonte, 2016). It is in the ICM that pluripotent stem cells first arise.

Pluripotency can be defined as a transient property of cells within the early embryo, where PSCs have the capacity to form tissues of all three germ layers of the developing embryo - ectoderm, mesoderm and endoderm - and still the germ lineage. As previously mentioned, PSCs typically provide little or no contribution to the trophoblast layers of the placenta (De Los Angeles et al., 2015; M. Li & Belmonte, 2017).

The first PSCs to be isolated and investigated in culture were derived from mouse teratocarcinomas – a tumor of germ cell origin that maintain a wide variety of differentiated tissues – known as embryonal carcinoma cells (De Los Angeles et al., 2015; Solter & Solter, 2006). Nevertheless, PSCs can be isolated from several sources through development (J. Wu et al., 2016), as murine (Evans & Kaufman, 1981; Martin, 1981) and human blastocyst (Brons et al., 2007; Tesar et al., 2007; Thomson, 1998) or even from the post-implantation epiblast (Brons et al., 2007; Tesar et al., 2007) or germ line (Matsui et al., 1992; Shamblott et al., 1998). Also, pluripotency can be recapitulated in vitro by reprogramming somatic cells to become induced pluripotent stem cells (iPSCs) (Takahashi et al., 2007; Takahashi & Yamanaka, 2006; Yu et al., 2007).

There are specific molecular mechanisms that characterize PSCs anchored by a selected set of core transcription factors (TFs) essential to establish pluripotency. As part of the core pluripotency TFs encoding genes are octamer-binding transcription factor 4 (OCT4), SRY-box 2 (SOX2) and NANOG. In certain circumstances, the loss of SOX2 or NANOG or their substitution can be tolerated (De Los Angeles et al., 2015; Li and Belmonte, 2017). Despite that, PSCs can be classified into different states of pluripotency based on molecular signatures, with the terms *naive* and *primed* being introduced to describe early and late phases of ontogeny, respectively (Weinberger et al., 2016).

Pluripotency can be suggested by such molecular signatures, but only functional assays can reveal the developmental potential of a cell. Functional assays to assess pluripotency include differentiation into three germ layers *in vitro*, teratoma formation *in vivo*, chimaera formation, germline transmission through blastocyst injection, tetraploid complementation and single-cell chimaera formation (De Los Angeles et al., 2015). For human PSCs (hPSCs), teratoma formation remains the gold standard of functional assays.

To fully comprehend the nature of pluripotent stem cells is to unravel the genesis of every organ in the human body and particularly the process of differentiation from pluripotent stem cells to the liver, which is the organ that this thesis will focus on. By exploring this process, a deeper understanding on how to recreate such mechanisms that drive organ development and function can be obtained.

LIVER DEVELOPMENT

Since 1828, when one of the founders of modern embryology, Von Baer, published his classic work *Ueber Entwicklungsgeschichte der Thiere* (On the Developmental History of Animals), that general knowledge in liver development emerged (early works summarized in Lewis, 1912). From these early studies performed in chick but also mammal embryos, including human, it is possible to build the idea that the liver has its origins in the gut tube with the formation of a liver bud, and soon "liver cords" grow into mesenchymal tissue, named by His as *Septum Transversum* or primary diaphragm (Brachet, 1895; Bremer, 1906; His, 1885; Thompson, 1908). However, knowledge on this topic has grown immensely since then, and accordingly, detailed description of liver development from pluripotency to the adult organ is presented next.

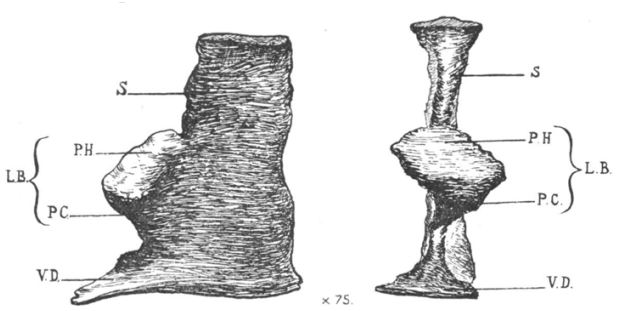

FIG. 3.—Model of entodermal tube showing the hepatic bud. ×75. Seen from the left side and the front.

S., stomach; L.B., liver bud; P.H., pars hepatica; P.C., pars cystica; V.D., vitelline duct.

Figure 1.1. One of the first representations of liver development with emphasis on the emergence of the liver bud. S., stomach; L.B., liver bud; P.H., pars hepatica; P.C., pars cystica; V.D., vitelline duct. (Thompson, 1908).

Origin and Fates of Hepatic Cells

A defining characteristic common to all metazoan, i.e. common to all animals, is their unique capability to undergo gastrulation, a series of cellular rearrangements of the blastomeres during the early stages of embryonic development (more recently, studies have demonstrated that sponges are the only exception (Ereskovsky & Dondua, 2006; Nakanishi et al., 2014)). It is during this process that the ICM experiences the first segregation of cells giving rise to two layers. The lower layer, named primitive endoderm (or hypoblast), and the upper layer that constitutes the epiblast, expressing *Nanog* and *Gata6*, respectively (Chazaud et al., 2006), depending on the levels of FGF (Yamanaka et al., 2010).

In the epiblast region, there is the formation of a transient structure known as primitive streak (PS). Throughout the gastrulation process, uncommitted cells migrate through the PS and undergo an epithelial-to-mesenchymal transition (EMT), ending in the generation of the three germ layers: ectoderm, mesoderm, and endoderm (Burdsal et al., 1993; Lawson et al., 1991; Pander, 1817). These three germ layers can be found in the embryos of most animal *phyla* and each one will give rise to different specific cell types. Therefore, it can be stated that the developmental path of the liver has its origin prior to, or shortly after, the beginning of gastrulation. As confirmed by experimental analysis of chick embryos, only the endoderm is competent for hepatic induction (Fukuda-Taira, 1981; Le Douarin, 1964, 1975). These principles were

confirmed later using mouse embryos (Gualdi et al., 1996). However, the formation of endoderm results not only from the definitive endoderm that migrates through the PS but also minimally by intercalation with visceral endoderm (cells from the primitive endoderm that were in contact with the epiblast) (Kwon et al., 2008; Viotti et al., 2014).

Molecularly, Nodal, a member of the transforming growth factor beta (TGFβ) family, is responsible for mammalian endoderm specification (Lowe et al., 2001), with high levels of Nodal promoting endoderm and low levels promoting mesoderm specification (Vincent et al., 2003). This signaling gradient activates the expression of key TFs like EOMES (in high levels) and T (in low levels), leading to the cooperation between EOMES with NODAL-SMAD2/3 signaling to induce the expression of endodermal markers such as CER1, FOXA2, and SOX17 (Faial et al., 2015).

After gastrulation, endoderm undergoes a series of morphogenetic movements resulting in the formation of the gut tube. In mammals, the gut tube begins to exhibit regional specification resulting in a patterned structure along the anterior–posterior axis into three regions, comprising the foregut, midgut, and hindgut (Tremblay & Zaret, 2005). This patterning starts around the third week of human embryonic development. It results from the action of Wnts, bone morphogenetic proteins (BMPs), and fibroblast growth factors (FGFs), that in a gradient from low levels in the anterior region to high levels in the posterior region, results in an anterior foregut, posterior foregut, and midgut-hindgut fate, respectively (Gordillo et al., 2015). The posterior foregut endoderm contains progenitor cells that can give rise to pancreas, liver, and gallbladder.

Concurrently during ontogeny, part of the mesoderm that emerges from the PS - the lateral plate mesoderm - undergoes a crucial process of splitting in somatic mesoderm and splanchnic mesoderm. It is the splanchnic mesoderm that surrounds the definitive endoderm of the naïve gut tube and, through a series of inductive interactions, directs its patterning into distinct progenitor domains (Funayama et al., 1999). This idea has its origins in the 1960s, in pioneer work from Le Douarin, which demonstrated the crucial role of specific mesoderm derivatives in determining the identity of endodermal tissues (Le Douarin, 1968). More specifically, it is known that for hepatic specification, it is required the convergence not only of the cardiac mesoderm (Gualdi et al., 1996) but also of a specific derivative of the splanchnic mesoderm, the septum transversum mesenchyme (STM) (J. M. Rossi et al., 2001). FGFs, like FGF1 and FGF2, from the cardiac mesoderm (Calmont et al., 2006; Serls et al., 2005), as well as BMPs, like BMP4 and BMP2, from the STM are key players in this process (J. M. Rossi et al., 2001). In light of recent findings, however, it appears that these paracrine signals arise from both the endodermal and mesodermal layers, promoting synchronized development of the adjacent tissues (Han et al., 2020).

After specification, hepatic endoderm thickens to form a liver diverticulum into the STM, initiating what can be called a budding process. This budding process is vital for the development of numerous metazoan organs and structures during embryonic development (Hogan, 1999), but only now start to be understood the cellular mechanisms that enable epithelial progenitor cells to bud away into their mesenchymal stromal environment. After the specific site is established, bud formation involves proximal-distal outgrowth,

usually associated with increased cell proliferation. In the case of the liver, this process starts with the hepatic endoderm transitioning from a columnar to a pseudostratified epithelium (Bort et al., 2006). In other words, the hepatic endoderm epithelium transitions into a state that creates the illusion of stratification, i.e. that is arranged in multiple layers, but in reality, each cell is in contact with the underlying basement membrane. It is now known that this epithelial transition is controlled by the TF HHEX (Bort et al., 2006).

At this stage in ontogeny, the pseudostratified epithelium constitutes the hepatic progenitor cells, the so-called hepatoblasts, that soon start to proliferate (Ober & Lemaigre, 2018). Accordingly, the generated liver bud is constituted by an outgrowth of hepatoblasts into the STM that is delineated by a basal lamina enriched in laminin, collagen IV and fibronectin (Shiojiri & Sugiyama, 2004). Adjacent to the basal lamina, outlining the liver bud, endothelial cells are also present, playing a crucial role in promoting the subsequent migration of hepatoblasts into the surrounding STM (Matsumoto et al., 2001). Concomitantly, there is a loss of contact between hepatoblast resulting from a downregulation of E-cadherin and by their turn, matrix metalloproteinases (MMPs) degrade the basal lamina, thereby facilitating hepatoblast migration (Margagliotti et al., 2008). This process of hepatoblast migration is controlled by a gene network comprising the TFs TBX3, PROX1, HNF6/OC-1 and OC-2 migration (Lüdtke et al., 2009; Margagliotti et al., 2007; Sosa-Pineda et al., 2000). HNF4a is equally essential for further development of the liver bud structure (Parviz et al., 2003). However, the role of endothelial cells and their direct regulation of hepatoblast migration remains poorly understood. Research in chicken embryos highlights a potential role for neurturin (NRTN) (Tatsumi et al., 2007). Known primarily for its functions in the nervous system, NRTN is also cited in the literature as a chemoattractant and may be secreted by endothelial cells to guide the migration of hepatoblasts from the liver bud.

Hepatoblasts are bipotent, having the potential to differentiate into either hepatocytes or cholangiocytes (biliary epithelial cells) in a process regulated by transforming growth factor-beta (TGFβ), Notch, Wnt, BMP, and FGF signaling (Clotman et al., 2005; Gordillo et al., 2015). The arrangement of these cells into functional liver architecture is influenced by the developing vascular network, as the lineage fate of hepatoblasts is influenced by their position relative to the portal vein. Moreover, a triad of vessels composed by a portal vein, hepatic artery, and bile ducts begin to form an intricate network within the liver as organogesis proceeds (Si-Tayeb, Lemaigre, et al., 2010).

As development progresses, hepatocytes, together with cholangiocytes and non-parenchymal cell types, mature and begin to take on their full range of functions (for extended review on liver development see (Ober & Lemaigre, 2018; Si-Tayeb, Lemaigre, et al., 2010)). This sequence of events, from a simple section of the gut tube to a fully functioning liver, highlights the complexity of organogenesis and the highly orchestrated interactions between different cell types and signaling pathways (Figure 1.2).

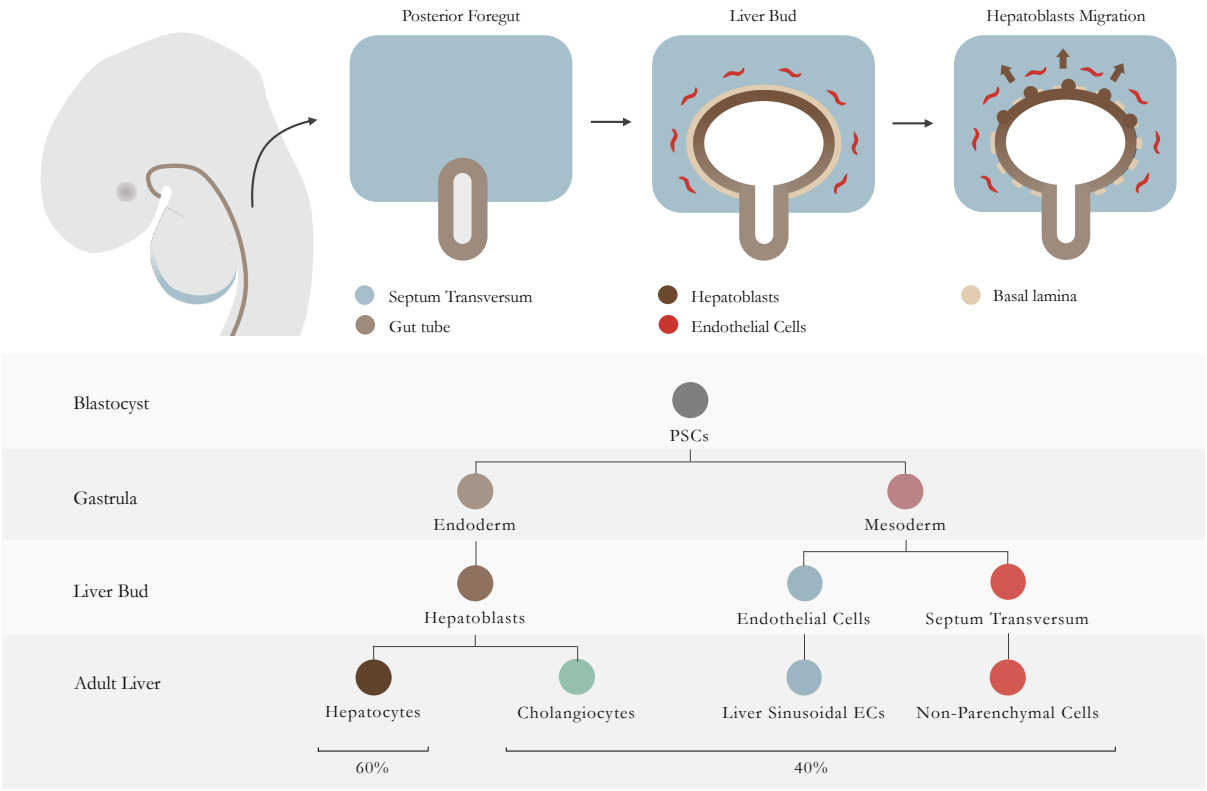

Figure 1.2. Liver bud formation during human embryonic development and cell lineage differentiation of the different components of the liver.

Hepatic Function and Disease

From all the internal organs that constitute the human body, the liver is the largest one, and its endocrine and exocrine properties make it also the largest gland. As an endocrine gland, the liver is responsible for the secretion of several hormones, while the bile constitutes the major exocrine secretion. The liver is therefore a central organ in our body that is responsible for homeostasis throughout the human lifespan, performing a complex array of functions (Miyajima et al., 2014; Si-Tayeb, Lemaigre, et al., 2010). Such functions include glycogen storage, drug detoxification, control of metabolism, regulation of cholesterol synthesis and transport, urea metabolism, immunological activity, and secretion of plasma proteins like albumin (Si-Tayeb, Lemaigre, et al., 2010). The liver is such an essential player in homeostasis, that liver disease due to genetic or environmental factors, such as hepatitis, fibrosis, cirrhosis, and hepatocellular carcinoma, often results in morbidity and mortality (Bhatia et al., 2014). Actually, liver disease is one of the leading causes of death worldwide and it is estimated that approximately 2 million people die per year, representing 3.5% of global deaths. From the 2 million, 1.16 million deaths are caused by cirrhosis (11th cause of death worldwide) and 0.79 million deaths are caused by hepatocellular carcinoma (16th cause of death worldwide) (Asrani et al., 2019). In addition to mortality rates, liver disease is estimated to have an impact on over 600 million people around the world (Schwartz et al., 2014). Besides that, for end-stage liver failure and other disorders, orthotopic liver transplantation is the only possible solution, making the liver the second most common solid organ transplantation. Still, transplantation needs are poorly met (Asrani et al., 2019).

Unfortunately, the discovery of novel therapeutics for liver disease is still a major challenge, as *in vitro* modeling of the *in vivo* physiological functions of the liver is still not accurate. *In vitro* models are traditionally based on hepatocyte cultures since they are the major parenchymal cell type, accounting for 60% of the total cells in the organ (80% of the volume), mediating almost all liver functions and being its functional metabolic unit (Miyajima et al., 2014). The gold standard source of hepatocytes for scientific investigation has been freshly isolated primary human hepatocytes (PHHs). However, when in culture these cells lose their ability to proliferate and most of their functions are impaired. Additionally, they have limited supply and present batch-to-batch variability, which greatly limit their potential for clinical applications (Corbett & Duncan, 2019; Hannoun et al., 2016). Other hepatocyte sources usually rely on immortalized or cancer cell lines, as well as fetal liver progenitors or adult liver stem cells. Nevertheless, these sources also present major drawbacks, like the fact that their metabolic enzymes do not entirely resemble the ones in adult hepatocytes, in addition to poor cell survival, proliferation, and availability (Corbett & Duncan, 2019; Hannoun et al., 2016).

Accordingly, the generation of hepatocytes derived from human pluripotent stem cells (hPSCs) represents a promising cell source to transform our understanding of liver disease and to change the way it is treated (Hannoun et al., 2016).

STEM CELL ENGINEERING

For the past decades, since the isolation and culture of human PSCs *in vitro*, the intention has been to engineer every cell, niche, tissue and organ-like structures, recreating the complexity and architecture of the human body. This technology has grown immensely since then, bringing an exciting new era for the fields of disease modelling, drug discovery and regenerative medicine, but nevertheless many more questions need to be further addressed. It is in the intersection of stem cell biology and engineering that new advances are being accomplished, applying bioengineering strategies to study each of the layers of the biological complexity of the human body.

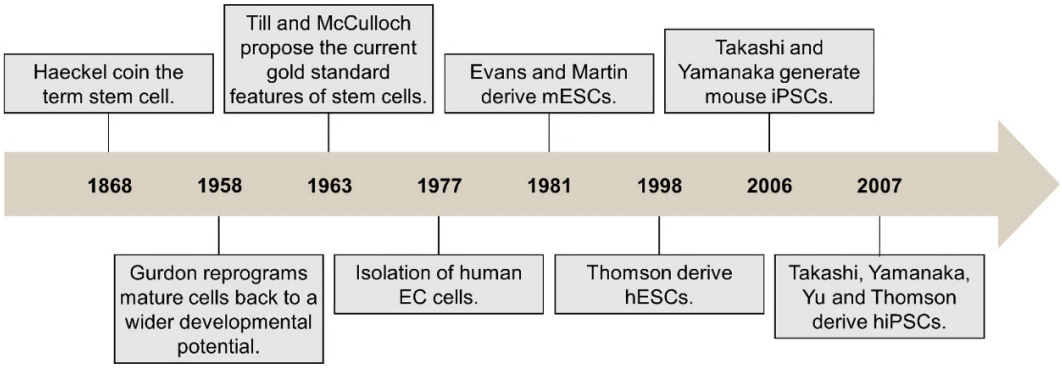

Figure 1.3 - Stem cell research timeline. Key events and technological breakthroughs in stem cell research. EC, embryonal carcinoma; mESCs, mouse embryonic stem cells; hESCs, human embryonic stem cells; iPSCs, induced pluripotent stem cells; hiPSCs, human induced pluripotent stem cells.

Embryonic Stem Cells

ICM cells cultured in conditions that allow indefinite self-renewal and maintenance of the pluripotent state, are known as embryonic stem cells (ESCs) and were first derived from mouse (mESCs) in 1981 by Martin Evans (Evans and Kaufman, 1981) and Gail Martin (Martin, 1981). These cultures proved to have all the properties previously established for embryonal carcinoma cell cultures, as well as a completely normal karyotype (Evans, 2011). Only by the year 1998, Thomson derived the first ESC lines from human blastocysts (Thomson, 1998), the so called human embryonic stem cells (hESCs).

Throughout normal development, the amount of ESCs is limited and their existence is constrained in the time course of development, being present for only a short period of time. In contrast, tissue culture allows the generation and maintenance of millions of ESCs indefinitely, preserving their pluripotent state (Evans, 2011).

Induced Pluripotent Stem Cells

The molecular mechanisms "by which the genes of the genotype bring about phenotypic effects" – the epigenetics concept – was captured by Conrad Waddington (Waddington, 1957) in the iconic image of the epigenetic landscape that influences cellular fate during development, analogously to the movement of a marble (Figure 1.4). Since then, the possibility that cells can change their identity has fascinated scientists (Merrell & Stanger, 2016). This notion was first suggested by Sir John Gurdon in 1958, establishing that *in vivo* plasticity of the differentiated state can be induced artificially by directly manipulating cells and their environment (Gurdon et al., 1958). It was demonstrated that the marble can be rolled back to the top of the hill, i.e., committed or differentiated cells can be reprogrammed back to a wider developmental potential (de-differentiation).

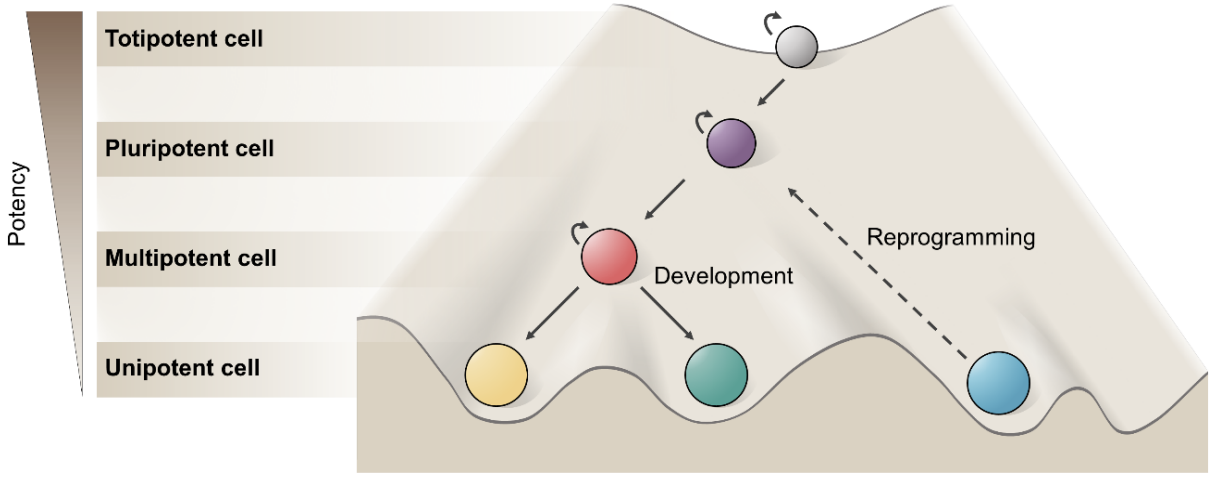

Figure 1.4 - Cell fate plasticity. Contemporary version of Waddington landscape depicting an analogy between a marble rolling downhill as development leads undifferentiated cells to a mature state. Cellular reprogramming has shown that it is possible to make the marble roll back to the top of the hill as mature cells can be reprogrammed back to a wider developmental potential.

As the possibility to reprogram cells, not by transplanting their nuclei, but by introducing pluripotency factors into cells became a reality, cells with a gene expression profile and developmental potential similar to ESCs were generated in 2006. This accomplishment was reached using mouse somatic cells together with a cocktail of four TFs (Takahashi & Yamanaka, 2006). The resulting reprogrammed cells were termed induced pluripotent stem cells (iPSCs) and were generated after retrovirally introducing four TFs encoding genes, OCT4, SOX2, Kruppel like factor 4 (KLF4) and the MYC proto-oncogene, bHLH transcription factor (MYC) – the "Yamanaka factors". After successfully generating mouse iPSCs, in 2007 iPSCs were generated from human fibroblasts, using the same four factors and alternatively NANOG and Lin-28 homolog A (LIN28) instead of KLF4 and MYC (Takahashi et al., 2007; Yu et al., 2007). It was the establishment of human induced pluripotent stem cells (hiPSCs). Since then, cellular reprogramming became a robust method to convert differentiated cells to a pluripotent stem cell state (Shi et al., 2016; Takahashi & Yamanaka, 2016).

Afterwards, besides the initially used retroviral or lentiviral vectors, non-integrating methods have been developed and include reprogramming using episomal DNAs, adenovirus, Sendai virus, PiggyBac transposons, minicircles, recombinant proteins, synthetically modified mRNAs, microRNAs and, more recently, small molecules (Shi et al., 2016). These new techniques, in addition to lower variability between cell lines, can lead to safer reprogramming of iPSCs and to more suitable cells for clinical applications by avoiding insertional mutagenesis and transgene reactivation.

Applications of Human Pluripotent Stem Cells

Since the isolation of ESCs from human embryos, the use of pluripotent stem cells as a potential tool for research and medicine has been growing. Besides that, after finding that somatic cells can revert all the way back to an embryonic stem cell state through TF activation, manipulation of signaling pathways aiming for cell differentiation has been studied contributing to hiPSCs applications in biomedicine. Accordingly, several protocols have been described for *in vitro* direct differentiation of neurons, hematopoietic cells, hepatocytes, smooth muscle cells and cardiomyocytes, among other cell types across the three germ layers (Tabar & Studer, 2014).

An obvious application of hPSCs in medicine is in cell therapy. Regenerative medicine strategies based on the use of stem cells to promote regeneration or to replace damaged tissues after cellular transplantation has been shown to successfully induce functional recoveries (Shi et al., 2016). In fact, several clinical trials were already established using hPSC-based therapies (Kimbrel & Lanza, 2015). In the particular case of hiPSCs, an important advantage of using these cells is the capability to generate autologous differentiated cells, i.e. patient-specific cells, theoretically suppressing the risk of immune rejection. For instance, the first clinical study using hiPSC-derived products was performed in 2014 by Masayo Takahashi and Yasuo Kurimoto, in which these two Japanese physicians successfully transplanted autologous retinal pigment epithelium sheets derived from hiPSCs into a woman with macular degeneration (Mandai et al., 2017). Besides all this progress in hPSC-based therapies, the acquisition of chromosomal aberrations, due to the

reprograming process and subsequent culture, represent one of the disadvantages of these cells (Lamm et al., 2016). Moreover, due to hPSC tumorigenicity, it is critical to ensure that the transplanted product does not contain undifferentiated cells with the potential to generate teratomas (Shi et al., 2016).

Another important biomedical application of hPSCs is in disease modelling (Rowe & Daley, 2019a). It is expected that *in vitro* hPSC-based disease models help to identify the pathological mechanisms underlying human diseases. Both hESCs and hiPSCs have been used for modelling human genetic diseases, establishing isogenic cell lines with novel gene editing tools (e.g. CRISPR-Cas9), to induce disease-causing mutations or to silence mutations carried by patient-specific cells (Avior et al., 2016; Sterneckert, Reinhardt, & Scholer, 2014).

Modelling of human diseases is motivated by the necessity of developing novel therapeutic agents allowing the diseases to be treated, alleviated or cured. Therefore, drug screening and toxicological assays is also considered as a potential application of hPSCs (Rowe & Daley, 2019a). Animal models have been used in drug screening but differences from the actual human setting lead to an inaccurate forecasting of their effects. Moreover, animal models are not suitable for high-throughput screening of small-molecule libraries (Avior et al., 2016; Sayed et al., 2016). Until now, many drug screens have been conducted using hiPSC-based models and potential drug candidates have been identified. Also, it is not only important to assess efficacy but also toxicity, predicting the likelihood of candidate drugs to cause serious side effects (Shi et al., 2016). A specific patient has a specific genetic background and this fact implies different responses to medication for each individual. Accordingly, hiPSC-based drug screening is the key for a personalized therapy, an emerging approach known as precision medicine (Sayed et al., 2016).

Just as new technologies are being developed, the greater will be the potential applicability of hPSCs in the emerging fields of regenerative medicine, disease modelling, and drug screening.

Engineering at the Cellular Level

In the past, only a few molecular techniques were able to provide information at the single-cell level, like patch-clamping electrophysiology (Sakmann & Neher, 1984), fluorescence *in situ* hybridization (Langer-Safer et al., 1982) or flow cytometry (Julius et al., 1972), potentially analysing 1 to 3 parameters from a given cell. Nevertheless, major breakthroughs in molecular biology like next-generation sequencing and novel omics technologies have provided transformative ways to comprehensively analyse the single-cell at the molecular level in recent years (Heath et al., 2016). Consequently, these technologies have been used in favour of stem cell engineering, generating large datasets not only by capturing transcriptional information, but also by disclosing protein interactions, enabling computational techniques to construct and simulate cellular GRNs, and to increase the efficiency resolution of differentiation processes of so many stem cell derivatives. In this context, the use of this information to build improved *in vitro* cellular systems is known as reverse engineering (Tewary et al., 2018).

From among a bewildering palette of omics technologies, transcriptomic analysis is being widely used at the moment. Gene expression analysis at the single-cell level has its origins back in the 1990's (Eberwine

et al., 1992) but single-cell RNA sequencing (scRNA-seq) revolutionized the way one can profile gene expression of PSCs and its derivatives at a given time (Tang et al., 2009). The underlying technique of scRNA-seq has been subjected to a remarkable amount of improvements, and new approaches are now being reported very frequently with low-cost methods and increased number of sequenced cells arising at the scRNA-seq landscape (for review: Kumar et al., 2017; Papalexi & Satija, 2018). Standard approaches for scRNA-seq include: plate-based approaches using micropipettes or fluorescence-activated cell sorting (FACS); the commercial microfluidic approach Fluidigm C1; pooled approaches applying a barcode to the cells; and massively parallel approaches that isolate single-cells into droplets thanks to the advances in droplet microfluidics enabling the profiling of thousands of cells in a single experiment (Papalexi & Satija, 2018). In a recent publication, the need for single-cell isolation required by previous methods was even eliminated by not partitioning cells into individual compartments but relying on cells themselves as compartments (Rosenberg et al., 2018). Moreover, due to the complex data output of these procedures, numerous algorithms have been developed to analyse the amount of multidimensional data generated (Grün & van Oudenaarden, 2015; Yuan et al., 2017). During cell differentiation and lineage commitment from pluripotency to a given cell type, scRNA-seq can capture different transcriptional states of the cells in different developmental stages. This analysis provides information of the cellular decision-making process leading to the prediction and reconstruction of the differentiation trajectories of the cells and at larger extent of the mapping of their developmental progression (Kester & van Oudenaarden, 2018). Prime examples of that are illustrated by the study of pairwise choices, or bifurcating lineage choices, to predict the developmental roadmap of mesodermal lineages from pluripotency to bone and heart (Loh et al., 2016), and to study cardiomyocyte maturation (C. E. Friedman et al., 2018).

Engineering at the Tissue Level

The growing knowledge about hiPSC differentiation triggered the development of new three-dimensional (3D) culture technologies that bring together multiple organ-specific cell types and to which the name organoids was given (Fatehullah et al., 2016a; Lancaster & Knoblich, 2014a). Nowadays, an organoid can be considered a stem cell-derived structure that through a self-organization process can recapitulate biological parameters like the spatial arrangement, cell-cell and cell-extracellular matrix (ECM) interactions, providing a better model of the *in vivo* anatomy and physiology of a given organ (G. Rossi et al., 2018a; Yin et al., 2016a). Organoid technology has its origins in the 1970's with 2D co-cultures of primary human keratinocytes and 3T3 fibroblasts originating epithelial colonies resembling human epidermis (Rheinwald & Green, 1975). Since then, the emergence of 3D culture systems has stimulated organoid research to the stage of what is today considered an organoid. Pioneer work was developed with 3D organoids of mammary gland by Mina Bissel (Barcellos-Hoff et al., 1989) but, the real step forward in this field was given by the work of the groups of Yoshiki Sasai and Hans Clevers on optic cup (Eiraku et al., 2011a) and intestinal organoids (Sato et al., 2009a), respectively. The knowledge to create such structures enabled scientists to generate organoids from a multiplicity of different cell sources and continues to nurture

numerous new efforts, driving forward the complexity of this technology (for review of main organoids types already developed: G. Rossi et al., 2018a).

Organoid self-organization occurs through self-assembly, self-patterning and self-morphogenesis (Sasai, 2013b, 2013a), but for the successful induction of these processes *in vitro*, culture conditions are determinant. Accordingly, biophysical characteristics must be taken into consideration. One can use solid ECMs to entrap 3D cell aggregates, which has been done with intestinal (Sato et al., 2009a), cerebral (Lancaster et al., 2013) and gastric organoids (McCracken et al., 2014), or follow a different strategy by simply using a scaffold-free approach, like in optic cup (Eiraku et al., 2011a), cerebellar (Muguruma et al., 2015) and liver bud organoid generation (Takebe et al., 2013b). Regarding biochemical signals, it is important to understand how self-governing the formation of a specific organoid is, since it can rely exclusively on endogenous signals, or may depend on the addition of exogenous cues at different time points and lengths. In fact, some organoids are exclusively driven by endogenous signals, e.g. mouse optic cup organoids (Eiraku et al., 2011a), while others are initially inducted by exogenous signals followed by self-organization solely relying on endogenous cues, e.g. human kidney organoids (Takasato et al., 2015), or alternatively be dependant of the continuous supplementation of exogenous signals, e.g. human gastric organoid (McCracken et al., 2014). Finally, another critical parameter is the starting cell population, since organoids can be derived from a single cell, e.g. intestinal organoids (Sato et al., 2009a), from a homogeneous cell aggregate, e.g. optic cup organoids (Eiraku et al., 2011a), or from a co-culture of different cell types, e.g. liver bud organoids (Takebe et al., 2013b).

Bioengineering can provide new tools and technologies for organoid generation. Particularly, it can help addressing the unmet need of creating tissues and organoids that mimic the anatomical and physiological features of the different organs in the human body so they can be used in disease modelling and drug discovery (Rowe & Daley, 2019b). Below are summarized the most recent technological innovations in organoid engineering (Table 1.1).

Engineering biophysical signals

Matrigel is an obvious choice when supporting ECMs are used for organoid generation, but this matrix presents some critical limitations. Besides not being well defined in what concerns to chemical composition and facing lot-to-lot variation, Matrigel does not cooperate with morphogenesis, spatially limiting the development of complex structures (G. Rossi et al., 2018a; Yin et al., 2016a). Thus, to improve organoid architecture beyond the limits of self-organization, the bioengineering of chemically defined scaffolds and hydrogels with tuneable stiffness are of great interest. Some of the materials already used include hyaluronic acid (HA), tested in cerebral organoids (Lindborg et al., 2016), or the synthetic polymer polyethylene glycol (PEG), tested for neural tube morphogenesis in organoids (Ranga et al., 2016). In fact, it is well known that the surrounding ECM can regulate stem cell fate (Vining & Mooney, 2017). Studies on the differentiation of hESCs into mesoderm derivatives were performed varying the stiffness of the scaffold and leading to distinct outcomes in terms of differentiation (Przybyla et al., 2016). Additionally, some synthetic hydrogels

are already being tested to transplant human intestinal organoids into mouse models (Cruz-Acuña et al., 2017).

Topographical features can also be added to these materials to mimic those found in the *in vivo* environment. To this end, micropatterning and microfabrication technologies play an important role controlling tissue geometry and environmental factors (Tewary et al., 2018). Examples of these technologies are soft lithography, using microcontact printing, replica moulding and photolithography techniques, and robotic printing (for a detailed review of microtechnologies see Chapter 7). A classic example is the use of microwells, usually made of PDMS by soft lithography, to control organoid shape and size (Murrow et al., 2017). For a more personalized design, microstructured collagen gels are a good example of the use of these technologies, where a soft lithography approach using the replica moulding technique is used to resemble the crypt architecture of the small intestine (Y. Wang et al., 2017; Y. Wang, Kim, et al., 2018). On the other hand, ECM design at the nanoscale can be achieved using electro-beam lithography, to create computer-guided surfaces with nanopaterns, or electrospinning, responsible for the formation of nanofibrous substrates (Yin et al., 2016a).

Besides topographical features, it is known that *in vivo* biophysical signals are presented in a spatiotemporal fashion, shaping the developmental process of tissues. For that reason, dynamic hydrogels whose biophysical properties can be modulated, in both space and time, have been developed (G. Rossi et al., 2018a). For scaffolds to match different developmental stages over time mechanically, several techniques have been applied based on chemical, light, magnetic or thermal stimuli (Bahlmann et al., 2017). An example of that was published by Lutolf and co-workers using a chemically induced change by hydrolysis from a static PEG to a mechanically dynamic PEG, allowing the alleviation of accumulated compressive forces (Gjorevski et al., 2016). Accordingly, this method initially favoured cell expansion and then supported organogenesis in intestinal organoids by temporal modulation of the matrix. Along with temporal modulation, some spatial control has also been tested over hydrogel mechanical properties using for example mechanical gradients (Bahlmann et al., 2017).

Spatial positioning of the different cell types within the generated tissue is another parameter on which bioengineers are focused, particularly trying to improve architecture and mimicking *in vivo* anatomical arrangements. Strategies like bioprinting are able to control not only cell-ECM but cell-cell interactions as well, using cells together with a biomaterial, the so-called bioink, to precisely positioning them in a layer-by-layer manner (Murphy & Atala, 2014; Yin et al., 2016a). Indeed, this technology has already been applied to many stem cell derivatives (Ong et al., 2018) and a good example of that is the bioprinting of hiPSC-derived hepatic tissue (Ma et al., 2016). In this work, the assembly of hiPSC-derived hepatocytes with other supportive cells, featured in the human liver, was performed using a microscale hexagonal architecture. This strategy led to improved morphological organization, up-regulation of liver-specific genes and enhanced functionality.

Delivery of biochemical signals

Most cellular functions, from the embryo to adulthood, depend on the continuous supply of nutrients and soluble factors to the cells (Figure 1.5.). Analogously, bioengineers have used different strategies to properly deliver such factors to stem cell-derived tissues and organoids (Yin et al., 2016a). One possible solution is the integration of endothelial cells (ECs) or their progenitors in the engineered constructs or tissues (G. Rossi et al., 2018a). In fact, vascularization facilitates the delivery of nutrients and soluble factors through the tissue, but desired soluble factors can be delivered as well using special platforms designed for this intent. Traditionally, these soluble signalling molecules are presented in a uniform fashion to the cells cultured *in vitro* but, once again, spatiotemporal control of biochemical signals is crucial. For example, delivery of such cues can be achieved by means of light-triggered activation of caged molecules that are masked by a photo-degradable moiety in a hydrogel (Bahlmann et al., 2017; T. T. Lee et al., 2015). Also, microbeads and nanoparticles, in all possible forms, play an important role in the spatiotemporal control of biochemical signals. These platforms can be loaded with required signalling molecules and conjugated on the surface of the cells (Yin et al., 2016a). The interesting part is that they can release its content in a bioresponsive manner, i.e., the content is only released when proper molecular cues are present.

Microfluidic devices can also be used to deliver soluble ligands mimicking signalling gradients present *in vivo*. This technology not only has the ability to manipulate the flow rate and flow profile, but also recent advances have shown its possible high-throughput nature (Murrow et al., 2017). In the past, several microfluidic devices were developed (B. Zhang et al., 2018a), to culture cells from blood vessels (J. W. Song et al., 2005), muscles (Lam et al., 2009), bones (K. Jang et al., 2008), airways (Huh et al., 2007), liver (Carraro et al., 2008; P. J. Lee et al., 2007), brain (Harris & Shuler, 2003), gut (Kimura et al., 2008) and kidney (K.-J. Jang & Suh, 2010).

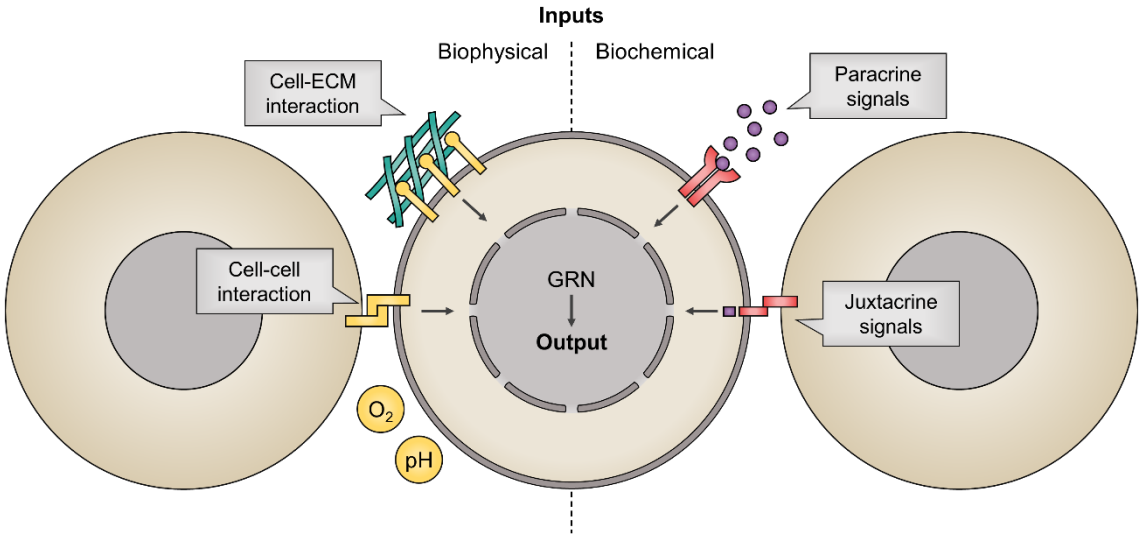

Figure 1.5. Regulatory microenvironment of biological systems and its biophysical and biochemical inputs. Biochemical signals include juxtacrine (contact-dependent) and paracrine (secreted) signals received from adjacent or neighbouring cells, while biophysical signals include cell–cell, cell-extracellular matrix (ECM) interactions and physiological factors (oxygen and pH). The GRN convert these signals (inputs) in controlled functional responses (output) according to the physiological needs.

All the above strategies are mainly focused on the delivery of diffusible molecules, but some biochemical signals like juxtacrine signals are contact-dependent. In order to study these signals in an insulated manner, droplet-based microfluidic devices are an alternative approach creating ordered cellular structures by controlled encapsulation and pairing of single cells in selected ECMs (Allazetta & Lutolf, 2015; Murrow et al., 2017). These techniques were tested in the past combining two different blood progenitor cell lines (Tumarkin et al., 2011) and more recently combining mesenchymal stem/stromal cells (MSCs) and human umbilical vein endothelial cells (HUVECs), as proof-of-concept studies on the utility of such platform to interrogate intercellular communications (L. Zhang et al., 2018). Additionally, micropatterning technologies can also be applied to study juxtracrine signals. Proof of this are cell-cell interaction arrays using DNA-programmed adhesion, used to study the dynamics of single adult neural stem cell fate decisions, based on the simultaneous presentation of juxtacrine signals (S. Chen et al., 2016).

Table 1.1. Engineering at the tissue level.

Approach		**Examples**	**References using Stem Cells**
Biophysical signals	Chemically defined scaffolds	Hyaluronic acid Polyethylene glycol	(Cruz-Acuña et al., 2017; Lindborg et al., 2016; Przybyla et al., 2016; Ranga et al., 2016)
	Topographically structured scaffolds	Micropatterning *Soft lithography* *Robotic printing* Nanopatterning *Electro-beam lithography* *Electrospinning*	(Maldonado et al., 2015; Takebe et al., 2017a; Y. Wang et al., 2017; Y. Wang, Kim, et al., 2018)
	Spatio-temporal dynamic scaffolds	Temporal control *Chemical, light, magnetic or thermal stimuli* Spatial control *Mechanical gradients*	(Gjorevski et al., 2016)
	Spatial positioned cells	Bioprinting	(Ma et al., 2016)
Biochemical signals	Vascularized tissues	Integration of endothelial cells	(Huch et al., 2013a; Takebe et al., 2013b, 2017a)
	Spatio-temporal delivered ligands	Light-triggered activation Microbeads Nanoparticles Microfluidics	(T. T. Lee et al., 2015)
	Controlled juxtacrine signalling	Droplet-based microfluidics Micropatterning	(S. Chen et al., 2016; Tumarkin et al., 2011; L. Zhang et al., 2018)

HEPATIC DIFFERENTIATION AND LIVER ORGANOIDS

Since the isolation of embryonic stem cells (ESCs) from the blastocyst (Evans & Kaufman, 1981; Martin, 1981; Thomson, 1998), and later with the recapitulation of pluripotency *in vitro* by reprogramming somatic cells into induced pluripotent stem cells (iPSCs) (Takahashi et al., 2007; Takahashi & Yamanaka, 2006; Yu et al., 2007), numerous protocols have been described for the direct differentiation of PSCs into many cell populations across the three germ layers, including neurons (Chambers et al., 2009), cardiomyocytes (Branco et al., 2019), and also hepatic cells (Table 1.2). Most of the research in differentiating hepatic cell types from hPSCs has been focused on hepatocytes, but differentiation strategies that originate other enriched populations of liver cells have also been developed. The design of such protocols should bring a new level of complexity to the study of liver development and medical research.

The majority of the differentiation protocols already published are at their core a recapitulation of the natural developmental processes that occur during embryogenesis. Thus, the differentiation of PSCs into a certain cell population can be achieved through the addition of extrinsic signals that guide the cells into a particular fate while repressing alternative ones. These extrinsic signals are usually presented as a combination of signaling pathway agonists and antagonists, added to the culture medium in a stepwise fashion in specific concentrations, sequence, and time (Bellin et al., 2012). To attain this, it is necessary to understand not only the signaling pathway kinetics, but also the developmental roadmap of the different cell types of the liver, and studying how different cell populations are segregated during fate transitions (Ang et al., 2018).

Hepatocytes

Since hepatocytes constitute the major cell type in the liver, there has been great interest in differentiating PSCs into this type of cell. The first reports date back to 1996 and relied on the spontaneous differentiation of mouse ESCs using embryoid bodies (EBs) (Abe et al., 1996). These EBs spontaneously recapitulate early steps of embryogenesis in an uncontrolled fashion, ending in a highly variable structure with differentiated cells of all three germ layers, where hepatocytes can be present. Only in the following decade the first direct differentiation of hPSCs was reported using hESCs (Rambhatla et al., 2003) and latter using hiPSCs (Z. Song et al., 2009). Since then, based on developmental signaling pathways and morphogens, many protocols have used similar growth factors and small molecules to generate hepatocytes in adherent culture conditions, leading to outstanding improvements in efficiency and functionality (Table 1.2).

As previously described, Nodal/Activin, members of the TGF-β superfamily of signaling molecules, are critical for definitive endoderm induction in mammals, and the same is true for *in vitro* differentiation of PSCs. Kubo and colleagues were the first to provide evidence that high concentrations of Activin A result in endoderm induction (Kubo et al., 2004). Since then, this growth factor has been widely used in the first steps of hepatocyte differentiation, sometimes associated with other signaling molecules that also promote endoderm development, like BMPs, FGFs, or WNT3A, among others. Afterwards, to recapitulate hepatic specification, BMPs and FGFs have been used to give rise to hepatic endoderm, FGF2, FGF4, BMP4, and BMP2 being the most commonly used. Finally, to trigger hepatoblast proliferation and subsequent

hepatocyte differentiation/maturation, hepatocyte growth factor (HGF), Oncostatin M (OSM), and Dexamethasone (DEX) are among the most frequent choices. These differentiation strategies result in the production of what can be called hepatocyte-like cells (HLCs), since current protocols still do not generate hepatocytes with fully mature phenotype when compared to adult hepatocytes. To simplify, in this work only the term "hepatocyte" will be used. Nevertheless, several approaches have been used for *in vitro* maturation of hPSC-derived hepatocytes, including growth factors, small molecules, TFs, and microRNAs (C. Chen et al., 2018). Examples of that are the already mentioned HGF and OSM. It is established that HGF can promote hepatoblast proliferation, migration, and survival, and in the presence of DEX it can upregulate several mature hepatocyte markers (Kamiya et al., 2001). On the other hand, it has also been proven that fetal hepatocytes in the presence of OSM acquire a similar morphology to mature hepatocytes, also contributing to hepatic functionality (Kamiya, 1999; Kamiya et al., 2001).

The majority of the differentiation methods to generate hepatocytes can then be divided into three main stages: endoderm induction, hepatic specification, and hepatocyte differentiation/maturation. However, these three-step approaches may not precisely mimic *in vivo* liver development, generating impure populations. Trying to overcome this challenge, recent studies attempt to recapitulate hepatocyte development through a sequence of six consecutive lineage choices (Ang et al., 2018). On the other hand, there are groups trying to overcome the lack of definition and reproducibility between protocols, relying for that purpose on methods solely driven by small molecules, following a growth-factor-free strategy (Siller et al., 2015). Additionally, some studies have been focused on the generation of scalable protocols for large-scale production of hPSC-derived hepatocytes (Farzaneh et al., 2018; Vosough et al., 2013; Yamashita et al., 2018).

Cholangiocytes

Apart from hepatocytes, cholangiocytes have a key role in the liver as they constitute the epithelium lining of the biliary tree, which processes bile production. Some of the first differentiation protocols of hPSCs into hepatocytes reported the presence of bile-duct structures formed by $CK7^+$ and $CK19^+$ cells, which are well known cholangiocyte cell markers (Cai et al., 2007; Zhao et al., 2009). However, the first defined protocol for cholangiocyte differentiation from hPSCs was only published several years later (Dianat et al., 2014). As mentioned before, during hepatic specification when cells become hepatoblasts, they can give rise to both hepatocytes and cholangiocytes. Therefore, existing protocols for cholangiocyte differentiation follow a similar strategy to obtain hepatoblasts. Once this stage is reached, different strategies have been applied for cholangiocyte specification, including the use of epidermal growth factor (EGF) (Dianat et al., 2014; Ogawa et al., 2015), FGF10 (Sampaziotis et al., 2015), TGF-β, and activation of NOTCH signaling (either by using Jagged1 or by the incorporation of OP9 stromal cells in a co-culture system) (De Assuncao et al., 2015; Ogawa et al., 2015).

Other Non-Parenchymal Cells

LSECs are also essential cells of the liver. They are highly specialized endothelial cells that constitute the permeable interface that controls the trafficking of molecules and cells between hepatocytes and the blood stream. Additionally, LSECs play an important role in immunity, liver disease, and regeneration (Poisson et al., 2017; Sørensen et al., 2015). Although important in the maintenance of normal liver functions, there are still few protocols for differentiation of hPSCs into LSECs. In fact, to our best knowledge, there is only one protocol using hPSCs that specifically generates LSECs (Koui et al., 2017), and a second one using mouse ESCs (Arai et al., 2011). Both studies assume that LSECs diverge at some point in ontogeny from endothelial progenitors. Therefore, Koui and colleagues used FLK1^{+}CD31^{+}CD34^{+} endothelial cells derived from hiPSCs as the starting point to generate and promote a LSEC mature phenotype by adding A83-01 (a TGFβRI inhibitor) under hypoxic conditions. This protocol was able to produce LSECs expressing specific markers like FCGR2B, STAB2, F8, and LYVE1. Generically, many research groups have focused their work on the differentiation of hPSCs into endothelial cells, thus indirectly contributing to future methods for LSEC derivation. For general reviews on this topic, please see (Williams & Wu, 2019; Xu et al., 2019).

Kupffer cells are the liver macrophages, the first line of defense against bacteria, microbial debris, and endotoxins with gastrointestinal origin (P. Li et al., 2017). In addition to their immunological role, they also cooperate with LSECs in blood clearance (Sørensen et al., 2015). Recently, one study was able to differentiate hiPSCs into Kupffer cells, recapitulating their ontogeny by firstly differentiating hiPSCs into macrophage-precursors and subsequent exposure to hepatic cues by simply culturing these precursors in hepatocyte culture medium (HCM) and advanced DMEM (Tasnim et al., 2019).

Finally, HSCs are specialized pericytes that reside in the perisinusoidal space (or space of Disse), between hepatocytes and LSECs. They are important in the maintenance of extracellular matrix homeostasis and its most distinctive feature is the accumulation of vitamin A. Additionally, they play a major role in liver fibrosis upon HSCs activation, i.e., HSCs transdifferentiate from quiescent, vitamin A storing cells into proliferative, fibrogenic myofibroblasts (Higashi et al., 2017; Tsuchida & Friedman, 2017). The embryonic origin of HSCs has been and still is elusive, creating a debate around whether these cells originate from the mesoderm, endoderm, or even the neural crest (S. L. Friedman, 2008). However, the hypothesis that HSCs originate from the mesoderm (more precisely from the STM) has gained acceptance (Asahina et al., 2011). This has prompted two studies (Coll et al., 2018; Koui et al., 2017) in which hPSCs are firstly differentiated into mesodermal cells, particularly ALCAM^{+} cell populations, and then divergent paths are used to generate HSCs. Koui and colleagues relied solely on the inhibition of the Rho signaling pathway using Y27632 to achieve an HSC phenotype, whereas Coll and colleagues adopted a more complex strategy adding FGF1, FGF3, palmitic acid, and retinol to the culture. This last study claims that not only cells with phenotypic and functional characteristics of mature HSCs are produced, but also that the method is highly robust with around 78% of PDGFRβ^{+} cells and 80% vitamin A-storing cells, a feature of mature HSCs.

Table 1.2. Methods for differentiation of human pluripotent stem cells into hepatic lineages.

Media	Molecules	Ref.
Hepatocytes		
KO-DMEM+FBS	NaB/DMSO – NaB/HGF	(Rambhatla et al., 2003)
StemPro34 – IMDM+SR	Act A – DEX	(Kubo et al., 2004)
RPMI+B27 – DMEM+SR+DMSO – L15	Act A/Wnt3a – HGF/OSM	(Hay et al., 2008)
RPMI – HCM – N2B27	Act A – FGF4/BMP2 – HGF/KGF – OSM/DEX	(Z. Song et al., 2009)
RPMI+B27 – HCM	Act A – BMP4/FGF2 – HGF – OSM	(Si-Tayeb, Noto, et al., 2010)
RPMI+B27 – DMEM+SR+DMSO – L15	Act A/Wnt3a – Act A – HGF/OSM	(Sullivan et al., 2010)
CDM	Act A/Ly/BMP4/FGF2 – FGF10 – FGF10/RA/ SB – FGF4/HGF/EGF	(Touboul et al., 2010)
RPMI+B27 – DMEM+SR+DMSO - HCM	Act A/Wnt3a/NaB – Act A/Wnt3a – HGF/OSM	(Kajiwara et al., 2012)
RPMI+B27 – DMEM+SR+DMSO – L15	CHIR – Dihexa/DEX	(Siller et al., 2015)
CDM	Act A/CHIR/PI – Act A/LDN – A83/BMP4/FGF2/ATRA – Act A/CHIR/BMP4/Forskolin – BMP4/OSM/DEX/ Forsk/Ro/AA/Insulin – DEX/Forskolin/Ro/AA/Insulin	(Ang et al., 2018)
Cholangiocytes		
RPMI	Act A/Ly – Act A/FGF2/BMP4 – FGF4/HGF/EGF/RA – EGF/GH/IL6	(Dianat et al., 2014)
RPMI – H69	Act A/Wnt3a – FGF2/BMP4/SHH – SHH/JAG1 – TGFβ	(De Assuncao et al., 2015)
RPMI – H16 – H16/Ham's F12 – H21/Ham's F12	Act A/CHIR – FGF2/BMP4 – HGF/OSM/DEX – HGF/EGF/TGFβ/OP9	(Ogawa et al., 2015)
CDM – RPMI – William's E	Act A/Ly/FGF2/BMP4 – Act A – BMP4/SB – Act A/FGF10/RA	(Sampaziotis et al., 2015)
Liver Sinusoidal Endothelial Cells		
StemPro34 SFM – EGM2	BMP4 – BMP4/Act A/FGF2 – VEGF/SB/Dorsomorphin – VEGF – A83	(Koui et al., 2017)
Kuppfer Cells		
mTeSR1 – X-VIVO – PHCM/Adv DMEM	BMP4/VEGF/SCF – MCSF/IL3 – MCSF	(Tasnim et al., 2019)
Hepatic Stellate Cells		
StemPro34 SFM – MSCGM	BMP4 – BMP4/Act A/FGF2 – VEGF/SB/Dorso – ROCKi	(Koui et al., 2017)
MCDB 201	BMP4 – BMP4/FGF1/FGF3 – FGF1/FGF3/PA/Retinol	(Coll et al., 2018)

The symbol "/" is used to separate media and molecules within the same differentiation step and the symbol "–" is used to separate the different differentiation steps. NaB, sodium butyrate; Act A, Activin A; Ly, Ly294002; SB, SB431542; CHIR, CHIR99021; PI, PI103; LDN, LDN193189; A83, A8301; Ro, Ro4929097; ROCKi, Y-27632.

Production of Liver Organoids from Human Pluripotent Stem Cells

The development of advanced 3D culture systems, triggered by the growing knowledge on hPSC differentiation, unlocks the possibility of bringing together multiple organ-specific cell types into a single structure, the so-called organoid, as already introduced above (Fatehullah et al., 2016b; Lancaster & Knoblich, 2014b). These structures can provide a much more reliable model of the *in vivo* anatomy and physiology of a given organ, not only when compared to a 3D cell aggregate composed of a single cell type, but even more when compared to a 2D monolayer culture system. Organoids are thus an emergent system that may serve as building block for tissue engineering applications.

This accumulated knowledge enabled a few groups to recently report the generation of liver organoids derived from hPSCs (Figure 1.6). The first report of liver organoids dates from 2001 by Michalopoulos and colleagues using several types of adult rat hepatic cells (Michalopoulos et al., 2001), but a more robust and long-term culture of human liver organoids was described later in 2013, using a progenitor population of adult mouse liver (Huch et al., 2013b). In the same year, Takebe and colleagues were pioneers in using hepatic cells derived from hPSCs, reporting the generation of human liver-like organoids that resemble the developing liver bud during early embryogenesis (Takebe et al., 2013a). These liver bud organoids were generated by mixing hepatic endodermal cells derived from hiPSCs, human umbilical vein endothelial cells (HUVECS) and human mesenchymal stem cells (MSCs). This approach recapitulated the early steps of liver organogenesis resulting in a vascularized human liver bud organoid with improved functionality by producing key liver enzymes. For the maturation of these liver bud organoids, the culture medium used was constituted by HCM and endothelial growth medium (EGM) in 1:1 proportion with the addition of HGF, OSM, and DEX. More recently, the same authors were able to generate fully hPSC-derived liver buds. They used hiPSCs as the cell source to generate hepatic endoderm cells, endothelial cells, and STM cells, and mixed them in a 10:7:2 ratio (Takebe et al., 2017b) (Figure 1.6A). To support the relevance of this approach, complementary *in vitro* studies demonstrated that besides homotypic interactions between human hepatocytes, heterotypic interactions between hepatocytes and other non-parenchymal cells are critical for self-organization, and that paracrine signals secreted by these cells are important for hepatic maturation (Asai et al., 2017; Camp et al., 2017), an idea previously explored in developmental studies using mouse embryos (Matsumoto et al., 2001). A similar system was described in 2019 by Pettinato and colleagues using co-cultures of hPSCs with human adipose microvascular endothelial cells (HAMECs) in a 3:1 ratio, that were then submitted to hepatocyte differentiation (Pettinato et al., 2019). This protocol resulted in liver organoids with 89% Albumin$^+$ and 15% CD31$^+$ cells and improved human hepatic functions associated to mature liver cells. Interestingly, HAMECs self-organized in rosette-like structures within the organoids (Figure 1.6B). Another strategy used 3D aggregates of hepatoblast-like cells derived from hPSCs that were then co-cultured with human fetal liver mesenchymal cells (hFLMCs) (S. Wang et al., 2019). By day 14 of differentiation, Albumin$^+$ cells were found in the peripheral region, whereas PDGFR-β^+ hFLMCs were found in the center of the organoids. Overall, co-culture of hepatoblast-like cells with hFLMCs, in a 2:1 ratio, generated organoids with increased levels of hepatic functions (Figure 1.6C).

Apart from co-culture of different cell types as a starting point for the generation of liver organoids, other studies have shown how to start with homogeneous cell populations to obtain complex organoids. Since 2017, two different protocols were published using this approach to produce hPSC-derived liver organoids constituted by hepatocytes and cholangiocytes (Guan et al., 2017; F. Wu et al., 2019). Both studies started with differentiation of hPSCs into hepatoblasts, but they diverge not only in the approach to get to that point, but also in the way they generate liver organoids. Guan and colleagues started with the production of hepatoblast aggregates that with the addition of exogenous growth factors and subsequent dissociation/reaggregation in Matrigel generated liver organoids with both hepatocytes and cholangiocytes (Figure 1.6D). On the other hand, Wu and colleagues developed a protocol capable of generating liver organoids with 60% ALB^+ hepatocytes and about 30% $CK19^+$ cholangiocytes. They claimed that the key factors for the success of their study were the inclusion of 25% mTeSR medium during differentiation and the addition of a cholesterol mixture for organoid functional maturation (Figure 1.6E). Based on a similar approach, a recent work describes the production of hPSC-derived liver organoids containing hepatocytes, HSCs, Kupffer cells, and cholangiocytes (Ouchi et al., 2019).

They initially differentiated hPSCs to foregut, collecting foregut spheroids released from the 2D culture and embedding them in Matrigel with further addition of retinoic acid, a molecule that reportedly plays and important role in the specification not only of parenchymal, but also non-parenchymal liver cells (Figure 1.6F). Apart from these examples using hPSC-derived cells, other human cell types have been used in the generation of human liver organoids in the past few years (Huch et al., 2013b, 2015). Likewise, liver organoids have been produced using mouse (Hu et al., 2018), rat (Kuijk et al., 2016), cat (Kruitwagen et al., 2017), and canine cells (Nantasanti et al., 2015).

It is important to note that organoid technology is becoming an increasing trend in biomedical research (G. Rossi et al., 2018b). However, some caution needs to be taken into consideration since by definition, an organoid is a reductionist cell construct that captures the cellular, structural, and physiological complexity of a given organ. Therefore, a clear distinction between 3D spheroids made up of a single cell type and without clear self-organization, and organoids needs to be made. In this section, the focus was placed only on reports that fit into this organoid concept.

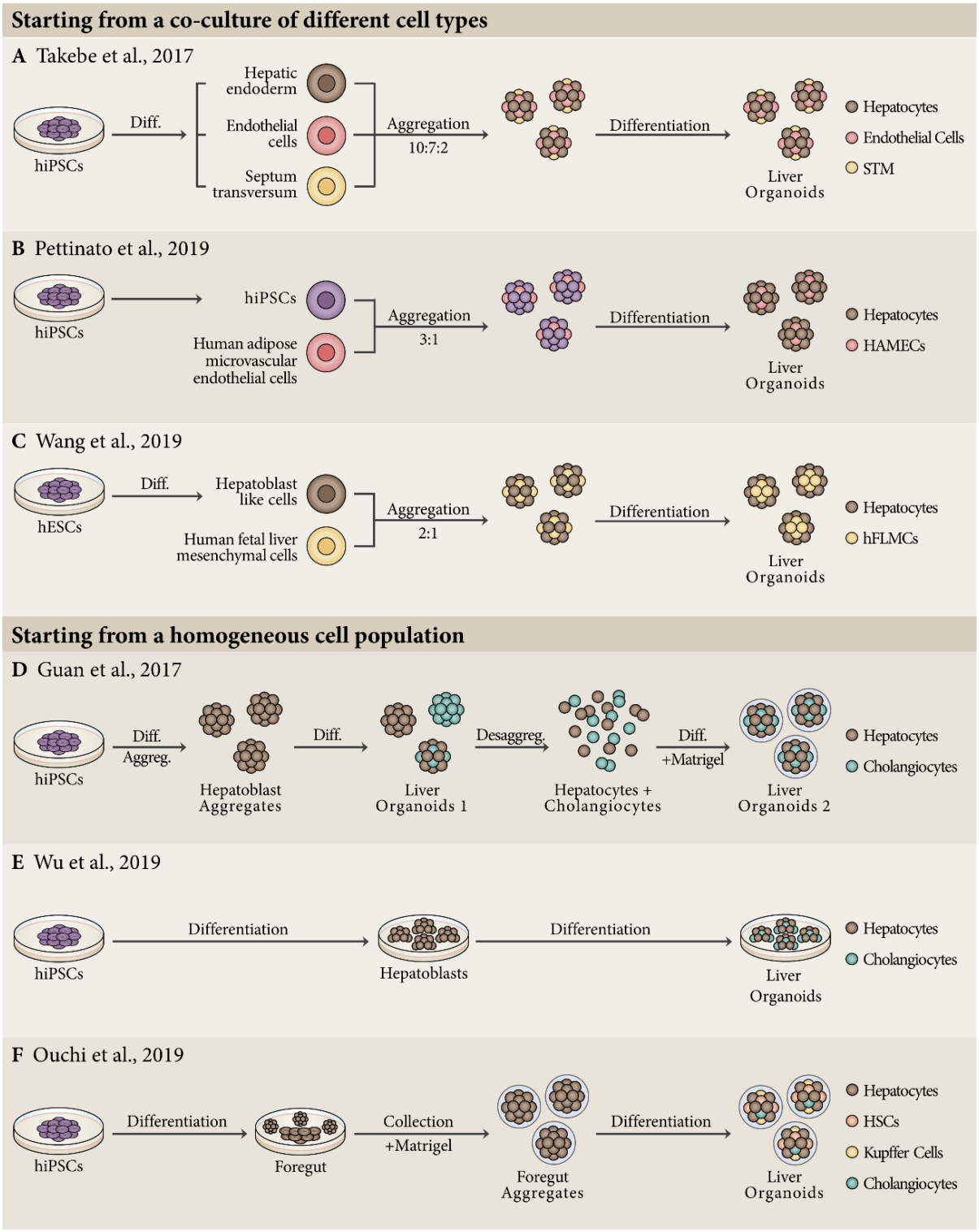

Figure 1.6. Current strategies for the generation of human pluripotent stem cell (hPSC)-derived liver organoids. So far, liver organoids have been generated by **(A-C)** co-culture of different cell types, including hPSCs, differentiated hepatic cell lineages, or isolated human cells with potential to promote liver organoid differentiation/maturation; **(D-F)** homogeneous cell populations that, through differentiation, are capable of generating cellular constructs with structural and physiological complexity. STM, septum transversum mesenchymal cells; HSCs, hepatic stellate cells.

Applications of hPSC-Derived Hepatic Cell Lineages and Liver Organoids

As demonstrated above, hPSCs have the capacity to establish human liver models giving researchers the opportunity to design human liver-based platforms for disease modeling, drug discovery, and hepatotoxicity. Furthermore, differentiated hepatic cells and liver organoids derived from hPSCs represent a renewable source for cell-based therapies aiming at the treatment of patients suffering from liver disease (Figure 1.7).

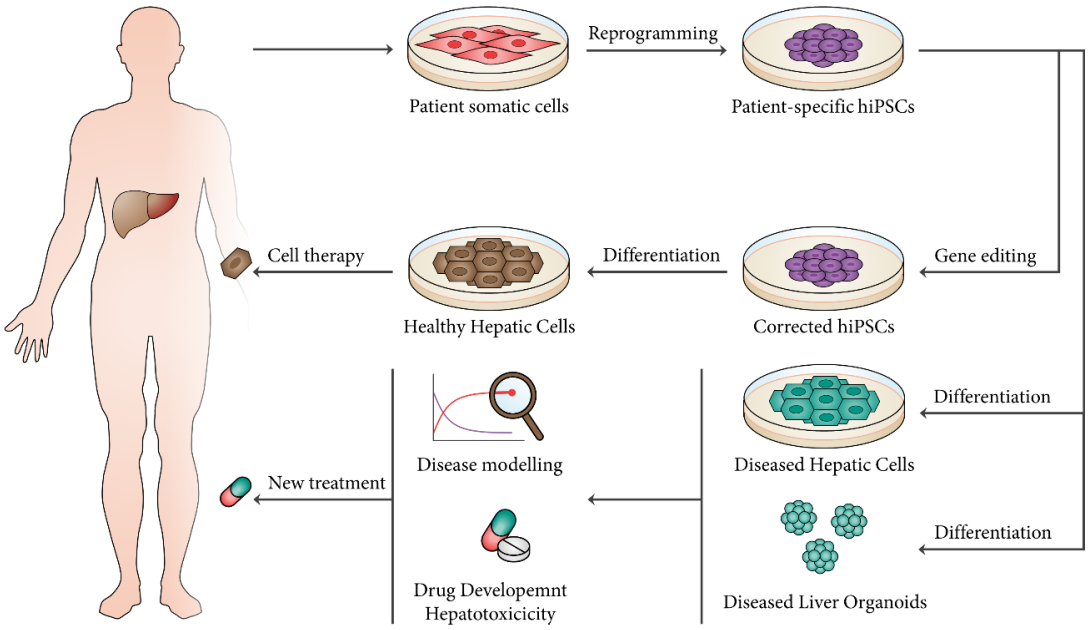

Figure 1.7 - Clinical applications for hPSC-derived hepatic cells and liver organoids. Isolated somatic cells from patients can be cultured and reprogrammed into patient-specific hiPSCs. These cells represent a promising cell source for cell therapy, as differentiated hepatocytes can be used for transplantation in regenerative medicine strategies. Additionally, differentiated hepatic cell lineages or generated liver organoids can be applied in disease modelling, as well as drug development and hepatotoxicity assays.

Regenerative Medicine

The use of hPSC-derived cells for regeneration or replacement of damaged tissue in regenerative medicine has been proposed to deliver functional recoveries (Shi et al., 2016). Indeed, hPSC-based therapies were already established in several clinical trials (Kimbrel & Lanza, 2015). hiPSCs in particular have the important advantage of their capability in generating differentiated patient-specific cells, allowing autologous cell transplantation and, theoretically, suppressing the risk of immune rejection. This milestone was achieved in 2014 with the successful transplantation of autologous retinal pigment epithelium sheets derived from hiPSCs (Mandai et al., 2017). Besides all this progress, chromosomal aberrations (due to cell reprograming and subsequent culture), as well as the tumorigenicity of undifferentiated cells, represent some of the hurdles that need to be taken into consideration when using hPSCs in cell therapies (Lamm et al., 2016; Shi et al., 2016).

As mentioned above, orthotopic liver transplantation is the single solution for end-stage liver failure and other liver disorders, making this organ the second most common solid transplantation after kidney. Still,

given the current transplantation rates, less than 10% of global organ transplantation needs are met [4]. This fact results in the need for alternative therapeutic strategies, and hepatocyte transplantation has been perceived as one (Iansante et al., 2018). The first attempt to use these cells for transplantation dates back to 1976 using Gunn rats as animal models for Crigler–Najjar syndrome (Matas et al., 1976). Still, it was only in 1992 that primary hepatocytes were transplanted into human patients (Mito & Kusano, 1993). Since then, numerous patients with liver disease have been treated with hepatocyte transplantation. However, this strategy still presents major hurdles like the limited source of hepatocytes, poor quality of isolated cells, and occasional hepatocyte rejection (Iansante et al., 2018). Therefore, hPSC-derived hepatocytes have been seen as a potential cell source for transplantation (Table 2). In fact, one of the most successful studies using hPSC-derived hepatocytes for transplantation was able to repopulate up to 15% of the liver of uPA immunodeficient mice after intrasplenic injection (Carpentier et al., 2014). In this study, the differentiated hepatocytes still presented fetal markers like AFP and they were largely negative for isoforms of CYP450. However, after transplantation, the transplanted cell population acquired mature features such as downregulation of AFP expression and cells positive for CYP450 isoforms. This transplantation strategy has also been successful in the alleviation of liver metabolic disorders (Y. Chen et al., 2015) and in acetaminophen-induced acute toxicity (Tolosa et al., 2015), with liver repopulation rates of 2.5–7.5% and 10%, respectively. Thus, hPSC-derived hepatocytes demonstrated their potential to become a relevant cell source for liver cell therapy. However, although initial studies are promising, the use of these cells for regenerative medicine applications needs to be more efficient and effective until it can be translated into human benefit. To accomplished that, recent studies have been using different strategies besides intrasplenic injection for hepatocyte transplantation. One of these strategies is the transplantation of hepatocyte sheets onto the surface of mice livers (Nagamoto et al., 2016). Additionally, different scaffolds have been used to support hPSC-derived hepatocytes for subsequent transplantation, namely PCL fibers (Rashidi et al., 2018) and decellularized livers (Lorvellec et al., 2017; Minami et al., 2019). Besides this, a recent study reported for the first time, to the best of our knowledge, the use of current good manufacturing practice (cGMP)-compliant hepatocytes generated from hPSCs for transplantation (Blackford et al., 2019). Liver regeneration will probably require more than simply injecting the right type of cells in the right place. The foundation of knowledge concerning liver regeneration mechanisms, both in normal development and after injury, seems to provide a strong platform to achieve this goal.

Table 2. Summary of recent studies on hPSC-derived hepatocyte transplantation in murine models.

Route	Cells	Nr of Cells	% Repopulation	Ref.
Intrasplenic injection	hPSC-hepatocytes	4×10^6	<1–20%	(Carpentier et al., 2014)
Intrasplenic injection	hPSC-hepatocytes	2×10^6	2.5–7.5%	(Y. Chen et al., 2015)
Intrasplenic injection	hPSC-hepatocytes	1×10^6	10%	(Tolosa et al., 2015)
Sheet transplantation	hPSC-hepatocyte sheet	8×10^5	-	(Nagamoto et al., 2016)
Intraperitoneal transplantation	hPSC-hepatocytes	1×10^6	-	(Takayama et al., 2017)
Renal subcapsular space	hPSC-hepatocyte aggregates	1×10^6	-	(Nie, Zheng, Ogawa, et al., 2018)
Intraperitoneal transplantation	hPSC-hepatocyte aggregates	2×10^6 (aggregates)	-	(Rashidi et al., 2018)
Subcutaneous transplantation	hPSC-hepatocytes in PCL fibers	-	-	(Rashidi et al., 2018)
Intraperitoneal transplantation	hPSC-hepatocyte aggregates	2×10^3 (aggregates)	-	(Blackford et al., 2019)

Disease Modeling

In addition to regenerative medicine, disease modeling constitutes another important biomedical application for hPSC derivatives. *In vitro* disease models based on hPSC technology should improve our knowledge regarding pathological mechanisms underlying human diseases, either genetic or acquired (Rowe & Daley, 2019a). Given the relevance of liver disease, several studies using hPSC-derived hepatocytes have been published in the last years (for extended review see (Corbett & Duncan, 2019)). However, the effort for improved maturity and greater complexity of *in vitro* culture systems for disease modeling has led to recent publications using liver organoids as a platform to study liver disease (Table 3).

With the advent of novel gene editing tools like CRISPR-Cas9, it is now possible to induce disease-causing mutations or silencing mutations carried by patient-specific hPSCs and evaluate their effects in differentiated cell phenotypes (Avior et al., 2016; Sterneckert, Reinhardt, & Schöler, 2014). To understand liver disease mechanisms at the organ level, at least two different studies have been published studying genetic diseases in hPSC-derived liver organoids. Guan and colleagues used patient-specific hPSCs to model Alagille Syndrome (ALGS) and Tetralogy of Fallotthis (TOF) genetic disorders (Guan et al., 2017). Firstly, they generated liver organoids from hPSCs reprogrammed from ALGS patients, where in contrast to healthy organoids, mature hepatocytes were developed, but cholangiocytes and bile ductular structure development was impaired. Additionally, they used CRISPR-Cas9 technology to introduce and revert an ALGS causing *JAG1* mutation, C829X, into control and ALGS hPSCs. Thus, ALGS liver pathology was

recapitulated, and it was also shown that *JAG1* haploinsufficiency alone does not produce pathology in liver organoids. Moreover, this team also modelled a disease caused by another mutation in *JAG1*, TOF, demonstrating that the type of *JAG1* mutation has a considerable effect in the onset of liver disease. More recently, another study has demonstrated that liver organoids are a suitable platform to model steatohepatitis, a condition that is, among others, characteristic of Wolman disease, caused by a defective activity of lysosomal acid lipase (LAL) (Ouchi et al., 2019). Firstly, these researchers induced steatohepatitis phenotype in liver organoids exposing them to free fatty acids, resulting in lipid accumulation, inflammation, and fibrosis. After that, to highlight the clinical relevance of modelling steatohepatitis, they used patient-derived hPSCs with LAL deficiency to generate liver organoids, thus recapitulating the Wolman disease phenotype with severe steatohepatitis. Additionally, it was demonstrated through liver organoid technology that the steatohepatitis phenotype could be rescued using FGF19, suppressing lipid accumulation and improving liver organoids survival. Besides these two examples of genetic disease modeling, organoids derived from adult liver tissue were already used to study A1AT deficiency and Alagille syndrome (Huch et al., 2015).

Recently, liver disease modelling has also been successfully performed to study acquired liver diseases. An example is hepatitis B virus (HBV) infection of hPSC-derived liver organoids (Nie, Zheng, Miyakawa, et al., 2018). This culture system proved to be more susceptible to HBV when compared to hepatocytes differentiated in a 2D culture system. Particularly, the infection of liver organoids with HBV resulted in hepatic dysfunction with downregulation of hepatic gene expression and emergence of hepatic injury markers, along with the alteration of hepatic structures. Therefore, this study suggested that liver organoids can be considered a good platform for HBV modelling, recapitulating the virus life cycle and consequent dysfunctions. Another example of disease modeling of acquired liver diseases using liver organoids is the study of alcoholic liver disease (ALD), the number one cause of liver-associated mortality in Western countries (S. Wang et al., 2019). Upon EtOH treatment for 7 days, liver organoids displayed liver damage and reduction in cell viability, as well as upregulation of gene expression of fibrogenic markers, thus recapitulating ALD pathophysiology. Additionally, EtOH treatment led to enhanced oxidative stress, an established characteristic of ALD that starts with the metabolism of EtOH by ADH and CYP2E1. Once more, liver organoids proved to be a reliable platform for disease modeling, encouraging its use to study new conditions and eventually contributing to the discovery of new therapeutics.

It is important to note that the cell composition of liver organoids can be of extreme importance when modeling liver diseases. In the examples above, it is possible to understand that given the biliary deficiencies in ALGS and TOF , the presence of cholangiocytes within these organoids it is an essential requirement (Guan et al., 2017); similarly, given the characteristic fibrosis of steatohepatitis, HSCs should also be present (Ouchi et al., 2019). Obviously, increasing the complexity of the model system will result in better recreating liver function, and it may even expose the role of the different hepatic cellular components in disease development. In fact, a very recent study shows how the crosstalk between hepatocytes, hepatic Kupffer cells, and HSCs play an important role in alcoholic liver disease (ALD), providing new insights into this pathology and identifying potential new targets for drug therapy (W. M. Choi et al., 2019; Kisseleva & Brenner, 2019).

Table 3. Reported studies for disease modeling in hPSC-derived liver organoids.

Study	Disease	Gene/Toxin	Approach	Ref.
Genetic Liver Diseases				
	Alagille syndrome	JAG1	Patient-derived/gene editing	(Guan et al., 2017)
	Tetralogy of Fallot	JAG1	Patient-derived	(Guan et al., 2017)
	Wolman disease	Free fatty acids	Patient-derived/induced	(Ouchi et al., 2019)
Acquired Liver Diseases				
	Hepatitis B	Hepatitis B virus	Induced	(Nie, Zheng, Miyakawa, et al., 2018)
	Alcoholic liver disease	EtOH	Induced	(S. Wang et al., 2019)

Drug Discovery and Hepatotoxicity

Modeling of human diseases is driven by the need for novel therapeutics aiming at disease treatments and cures. For this reason, drug discovery and toxicological assays are considered a potential application for hPSC derivatives (Miranda, Fernandes, Pinto, et al., 2018; Rowe & Daley, 2019a). To this end, animal models have been continuously used for drug screening. However, differences between the actual human setting and other animals result in inaccurate prediction of drug effects. Moreover, animal models are not suitable for high-throughput screening of small-molecule libraries (Avior et al., 2016; Sayed et al., 2016). As an alternative, the use of hPSC-based models for drug screens have been amply established, assessing not only the efficacy of potential drug candidates, but also their toxicity, predicting the likelihood of potential drugs to cause severe side effects (Shi et al., 2016). It is also important to bear in mind that each patient has a specific genetic background, and that this fact implies different responses to medication. Accordingly, hepatocytes and liver organoids generated from hPSCs can be used as a new tool to investigate not only disease mechanisms, but also therapeutic strategies, creating the foundation for personalized therapies, an emerging approach known as precision medicine (Sayed et al., 2016). Currently, pharmaceutical development is highly costly ($2.6 billion per drug that enters the market) and inefficient (89% of drugs that enter clinical trials will fail due to unforeseen toxicity) (Corbett & Duncan, 2019; Knowlton & Tasoglu, 2016). Part of this is due to inadequate screening during preclinical studies and so, the use of hPSC-derived hepatocytes and liver organoids in this field is of extreme relevance, as hepatotoxicity is the major type of toxicity associated to drug withdrawals (21% of the cases) (Siramshetty et al., 2016).

Given this context, there is the urgent need to create protocols that can generate hepatocytes or liver organoids in a scalable and miniaturized fashion, being suitable for high throughput screening of small molecule libraries. Examples of this have been already published (Carpentier et al., 2016; Takebe et al., 2017b). These high-throughput screening platforms were already used for identification of drugs for disease treatment with hPSC-derived hepatocytes. At least three studies used small molecules/drug libraries aiming

the attenuation or reversion of the effects of diseases like alpha-1-antitrypsin (AAT) deficiency (S. M. Choi et al., 2013), familial hypercholesterolemia (Cayo et al., 2017), and mitochondrial DNA depletion syndrome (MTDPS3) (Jing et al., 2018). The same platforms have also been used for toxicity screens evaluating the effect of certain drugs on hPSC-derived hepatocytes, typically testing compounds known to be toxic and non-toxic and assessing cell morphology and viability (Medine et al., 2013; Sirenko et al., 2016; Ware et al., 2015).

All of these studies are mainly focused on hepatocytes, but as described before non-parenchymal cells hold great importance in liver physiology. For instance, LSECs are implicated in most liver diseases making them an attractive therapeutic target (Poisson et al., 2017). Additionally, Kupffer cells play a crucial role in drug-induced liver injury (DILI) and other liver diseases. To demonstrate this, hepatocytes have been co-cultured with Kupffer cells resulting in a model that is more sensitive in detecting hepatotoxicity induced by different drugs (Tasnim et al., 2019). Thus, the development of more complex liver organoids composed of different hepatic cell types can substantially benefit drug discovery and hepatotoxicity assays.

Drug screening can also be performed using microfluidic devices like the so-called organ-on-a-chip or microphysiological systems (MPSs), where living cells can be cultured in continuously perfused chambers, modeling the physiological functions of a given tissue or organ (Ronaldson-Bouchard & Vunjak-Novakovic, 2018; B. Zhang et al., 2018b). Accordingly, organ-on-a-chip is also a valuable platform for drug development and toxicology giving insights into adsorption, distribution, metabolism, elimination, and toxicity (ADMET), mathematical pharmacokinetics (PK), pharmacodynamics (PD), and drug efficacy (Bhatia & Ingber, 2014). In fact, Wang and colleagues have recently achieved the in situ differentiation of hPSCs into liver organoids using a perfusable micropillar chip (Y. Wang, Wang, et al., 2018). The on-chip liver organoids displayed both hepatocytes and cholangiocytes, as well as increased cell viability and mature cell signature. Notably, the organoids generated in this platform not only presented high levels of cytochrome P450 enzyme expression, but also dose- and time-dependent hepatotoxic response to acetaminophen. These results support the notion that organ-on-a-chip technology constitutes a valid platform for drug testing. Moreover, organ-on-a-chip technology can rely not only on individual designs, but also in more complex interlinked multi-organ-on-chips, or body-on-a-chip platforms capable of mimicking multi-organ crosstalk (Miranda, Fernandes, Diogo, et al., 2018). Indeed, the study of an inter-tissue crosstalk between gut and liver during inflammatory processes was already reported (W. L. K. Chen et al., 2017), and more recently an interconnected MPS representing up to 10 organs, including liver, was established (Edington et al., 2018). Applying this technology to hPSC-derivatives is still, to the best of our knowledge, an unmet need.

REFERENCES

Abe, K., Niwa, H., Iwase, K., Takiguchi, M., Mori, M., Abé, S. I., Abe, K., & Yamamura, K. I. (1996). Endoderm-specific gene expression in embryonic stem cells differentiated to embryoid bodies. *Experimental Cell Research*, *229*(1), 27–34. https://doi.org/10.1006/excr.1996.0340

Allazetta, S., & Lutolf, M. P. (2015). Stem cell niche engineering through droplet microfluidics. *Current Opinion in Biotechnology*, *35*, 86–93. https://doi.org/10.1016/j.copbio.2015.05.003

Ang, L. T., Tan, A. K. Y., Autio, M. I., Goh, S. H., Choo, S. H., Lee, K. L., Tan, J., Pan, B., Lee, J. J. H., Lum, J. J., Lim, C. Y. Y., Yeo, I. K. X., Wong, C. J. Y., Liu, M., Oh, J. L. L., Chia, C. P. L., Loh, C. H., Chen, A., Chen, Q., … Lim, B. (2018). A Roadmap for Human Liver Differentiation from Pluripotent Stem Cells. *Cell Reports*, *22*(8), 2190–2205. https://doi.org/10.1016/j.celrep.2018.01.087

Arai, T., Sakurai, T., Kamiyoshi, A., Ichikawa-Shindo, Y., Iinuma, N., Iesato, Y., Koyama, T., Yoshizawa, T., Uetake, R., Yamauchi, A., Yang, L., Kawate, H., Ogawa, S., Kobayashi, A., Miyagawa, S., & Shindo, T. (2011). Induction of LYVE-1/stabilin-2-positive liver sinusoidal endothelial-like cells from embryoid bodies by modulation of adrenomedullin-RAMP2 signaling. *Peptides*, *32*(9), 1855–1865. https://doi.org/10.1016/j.peptides.2011.07.005

Asahina, K., Zhou, B., Pu, W. T., & Tsukamoto, H. (2011). Septum transversum-derived mesothelium gives rise to hepatic stellate cells and perivascular mesenchymal cells in developing mouse liver. *Hepatology*, *53*(3), 983–995. https://doi.org/10.1002/hep.24119

Asai, A., Aihara, E., Watson, C., Mourya, R., Mizuochi, T., Shivakumar, P., Phelan, K., Mayhew, C., Helmrath, M., Takebe, T., Wells, J., & Bezerra, J. A. (2017). Paracrine signals regulate human liver organoid maturation from induced pluripotent stem cells. *Development (Cambridge)*, *144*(6), 1056–1064. https://doi.org/10.1242/dev.142794

Asrani, S. K., Devarbhavi, H., Eaton, J., & Kamath, P. S. (2019). Burden of liver diseases in the world. *Journal of Hepatology*, *70*(1), 151–171. https://doi.org/10.1016/j.jhep.2018.09.014

Avior, Y., Sagi, I., & Benvenisty, N. (2016). Pluripotent stem cells in disease modelling and drug discovery. *Nature Reviews Molecular Cell Biology*, *17*(March), 170–182. https://doi.org/10.1038/nrm.2015.27

Bahlmann, L. C., Fokina, A., & Shoichet, M. S. (2017). Dynamic bioengineered hydrogels as scaffolds for advanced stem cell and organoid culture. *MRS Communications*, *7*(03), 472–486. https://doi.org/10.1557/mrc.2017.72

Barcellos-Hoff, M. H., Aggeler, J., Ram, T. G., & Bissell, M. J. (1989). Functional differentiation and alveolar morphogenesis of primary mammary cultures on reconstituted basement membrane. *Development (Cambridge, England)*, *105*(2), 223–235. https://doi.org/10.1038/nrclinonc.2010.139.Delivering

Becker, A. J., McCulloch, E. A., & Till, J. E. (1963). Cytological demonstration of the clonal nature of spleen colonies derived from transplanted mouse marrow cells. *Nature*, *197*(4866), 452–454. https://www.ncbi.nlm.nih.gov/pubmed/13970094

Bellin, M., Marchetto, M. C., Gage, F. H., & Mummery, C. L. (2012). Induced pluripotent stem cells: The new patient? *Nature Reviews Molecular Cell Biology*, *13*(11), 713–726. https://doi.org/10.1038/nrm3448

Bhatia, S. N., & Ingber, D. E. (2014). Microfluidic organs-on-chips. *Nature Biotechnology*, *32*(8), 760–772. https://doi.org/10.1038/nbt.2989

Bhatia, S. N., Underhill, G. H., Zaret, K. S., & Fox, I. J. (2014). Cell and tissue engineering for liver disease. *Science Translational Medicine*, *6*(245), 245sr2. https://doi.org/10.1126/scitranslmed.3005975

Blackford, S. J. I., Ng, S. S., Segal, J. M., King, A. J. F., Austin, A. L., Kent, D., Moore, J., Sheldon, M., Ilic, D., Dhawan, A., Mitry, R. R., & Rashid, S. T. (2019). Validation of Current Good Manufacturing Practice Compliant Human Pluripotent Stem Cell-Derived Hepatocytes for Cell-Based Therapy. *Stem Cells Translational Medicine*, *8*(2), 124–137. https://doi.org/10.1002/sctm.18-0084

Blanpain, C., & Simons, B. D. (2013). Unravelling stem cell dynamics by lineage tracing. *Nature Reviews Molecular Cell Biology*, *14*(8), 489–502. https://doi.org/10.1038/nrm3625

Bort, R., Signore, M., Tremblay, K., Pedro, J., Barbera, M., & Zaret, K. S. (2006). Hex homeobox gene controls the transition of the endoderm to a pseudostratified , cell emergent epithelium for liver bud development. *Developmental Biology*, *290*(1), 44–56. https://doi.org/10.1016/j.ydbio.2005.11.006

Brachet, A. (1895). Recherches sur le développement du diaphragme et du foie. *Journ. De L'Anatomie Et De La Phys.*

Branco, M. A., Cotovio, J. P., Rodrigues, C. A. V., Vaz, S. H., Fernandes, T. G., Moreira, L. M., Cabral, J. M. S., & Diogo, M. M. (2019). Transcriptomic analysis of 3D Cardiac Differentiation of Human Induced Pluripotent Stem Cells Reveals Faster Cardiomyocyte Maturation Compared to 2D Culture. *Scientific Reports*, *9*(1), 1–13. https://doi.org/10.1038/s41598-019-45047-9

Bremer, J. L. (1906). Description of a 4 mm Human Embryo. *Amer. Journ. of Anat.*, *5*, 459–480.

Brons, I. G. M., Smithers, L. E., Trotter, M. W. B., Rugg-Gunn, P., Sun, B., Chuva de Sousa Lopes, S. M., Howlett, S. K., Clarkson, A., Ahrlund-Richter, L., Pedersen, R. A., & Vallier, L. (2007). Derivation of pluripotent epiblast stem cells from mammalian embryos. *Nature*, *448*(7150), 191–195. http://www.ncbi.nlm.nih.gov/pubmed/17597762\nhttp://www.nature.com/nature/journal/v448/n7150/pdf/nature05950.pdf\nhttp://www.nature.com/doifinder/10.1038/nature05950\nhttp://www.ncbi.nlm.nih.gov/pubmed/17597762

Burdsal, C. A., Damsky, C. H., & Pedersen, R. A. (1993). The role of E-cadherin and integrins in mesoderm differentiation and migration at the mammalian primitive streak. *Development*, *118*(3), 829–844.

Cai, J., Zhao, Y., Liu, Y., Ye, F., Song, Z., Qin, H., Meng, S., Chen, Y., Zhou, R., Song, X., Guo, Y., Ding, M., & Deng, H. (2007). Directed differentiation of human embryonic stem cells into functional hepatic cells. *Hepatology*, *45*(5), 1229–1239. https://doi.org/10.1002/hep.21582

Calmont, A., Wandzioch, E., Tremblay, K. D., Minowada, G., Kaestner, K. H., Martin, G. R., & Zaret, K. S. (2006). An FGF Response Pathway that Mediates Hepatic Gene Induction in Embryonic Endoderm Cells. *Developmental Cell*, *11*(3), 339–348. https://doi.org/10.1016/j.devcel.2006.06.015

Camp, J. G., Sekine, K., Gerber, T., Loeffler-Wirth, H., Binder, H., Gac, M., Kanton, S., Kageyama, J., Damm, G., Seehofer, D., Belicova, L., Bickle, M., Barsacchi, R., Okuda, R., Yoshizawa, E., Kimura, M., Ayabe, H., Taniguchi, H., Takebe, T., & Treutlein, B. (2017). Multilineage communication regulates human liver bud development from pluripotency. *Nature*, *546*(7659), 533–538. https://doi.org/10.1038/nature22796

Carpentier, A., Nimgaonkar, I., Chu, V., Xia, Y., Hu, Z., & Liang, T. J. (2016). Hepatic differentiation of human pluripotent stem cells in miniaturized format suitable for high-throughput screen. *Stem Cell Research*, *16*(3), 640–650. https://doi.org/10.1016/j.scr.2016.03.009

Carpentier, A., Tesfaye, A., Chu, V., Nimgaonkar, I., Zhang, F., Lee, S. B., Thorgeirsson, S. S., Feinstone, S. M., & Liang, T. J. (2014). Engrafted human stem cell-derived hepatocytes establish an infectious HCV murine model. *Journal of Clinical Investigation*, *124*(11), 4953–4964. https://doi.org/10.1172/JCI75456

Carraro, A., Hsu, W. M., Kulig, K. M., Cheung, W. S., Miller, M. L., Weinberg, E. J., Swart, E. F., Kaazempur-Mofrad, M., Borenstein, J. T., Vacanti, J. P., & Neville, C. (2008). In vitro analysis of a hepatic device with intrinsic microvascular-based channels. *Biomedical Microdevices*, *10*(6), 795–805. https://doi.org/10.1007/s10544-008-9194-3

Cayo, M. A., Mallanna, S. K., Di Furio, F., Jing, R., Tolliver, L. B., Bures, M., Urick, A., Noto, F. K., Pashos, E. E., Greseth, M. D., Czarnecki, M., Traktman, P., Yang, W., Morrisey, E. E., Grompe, M., Rader, D. J., & Duncan, S. A. (2017). A Drug Screen using Human iPSC-Derived Hepatocyte-like Cells Reveals Cardiac Glycosides as a Potential Treatment for Hypercholesterolemia. *Cell Stem Cell*, *20*(4), 478-489.e5. https://doi.org/10.1016/j.stem.2017.01.011

Chambers, S. M., Fasano, C. A., Papapetrou, E. P., Tomishima, M., Sadelain, M., & Studer, L. (2009). Highly efficient neural conversion of human ES and iPS cells by dual inhibition of SMAD signaling. *Nature Biotechnology*, *27*(3), 275–280. https://doi.org/10.1038/nbt.1529

Chazaud, C., Yamanaka, Y., Pawson, T., & Rossant, J. (2006). Early Lineage Segregation between Epiblast and Primitive Endoderm in Mouse Blastocysts through the Grb2-MAPK Pathway. *Developmental Cell*, *10*(5), 615–624. https://doi.org/10.1016/j.devcel.2006.02.020

Chen, C., Soto-Gutierrez, A., Baptista, P. M., & Spee, B. (2018). Biotechnology Challenges to In Vitro Maturation of Hepatic Stem Cells. *Gastroenterology*, *154*(5), 1258–1272. https://doi.org/10.1053/j.gastro.2018.01.066

Chen, S., Bremer, A. W., Scheideler, O. J., Na, Y. S., Todhunter, M. E., Hsiao, S., Bomdica, P. R., Maharbiz, M. M., Gartner, Z. J., & Schaffer, D. V. (2016). Interrogating cellular fate decisions with high-throughput arrays of multiplexed cellular communities. *Nature Communications*, *7*, 10309. https://doi.org/10.1038/ncomms10309

Chen, W. L. K., Edington, C., Suter, E., Yu, J., Velazquez, J. J., Velazquez, J. G., Shockley, M., Large, E. M., Venkataramanan, R., Hughes, D. J., Stokes, C. L., Trumper, D. L., Carrier, R. L., Cirit, M., Griffith, L. G., & Lauffenburger, D. A. (2017). Integrated gut/liver microphysiological systems elucidates inflammatory inter-tissue crosstalk. *Biotechnology and Bioengineering*, *114*(11), 2648–2659. https://doi.org/10.1002/bit.26370

Chen, Y., Li, Y., Wang, X., Zhang, W., Sauer, V., Chang, C. J., Han, B., Tchaikovskaya, T., Avsar, Y., Tafaleng, E., Madhusudana Girija, S., Tar, K., Polgar, Z., Strom, S., Bouhassira, E. E., Guha, C., Fox, I. J., Roy-Chowdhury, J., & Roy-Chowdhury, N. (2015). Amelioration of Hyperbilirubinemia in Gunn Rats after Transplantation of Human Induced Pluripotent Stem Cell-Derived Hepatocytes. *Stem Cell Reports*, *5*(1), 22–30. https://doi.org/10.1016/j.stemcr.2015.04.017

Choi, S. M., Kim, Y., Shim, J. S., Park, J. T., Wang, R. H., Leach, S. D., Liu, J. O., Deng, C., Ye, Z., & Jang, Y. Y. (2013). Efficient drug screening and gene correction for treating liver disease using patient-specific stem cells. *Hepatology*, *57*(6), 2458–2468. https://doi.org/10.1002/hep.26237

Choi, W. M., Kim, H. H., Kim, M. H., Cinar, R., Yi, H. S., Eun, H. S., Kim, S. H., Choi, Y. J., Lee, Y. S., Kim, S. Y., Seo, W., Lee, J. H., Shim, Y. R., Kim, Y. E., Yang, K., Ryu, T., Hwang, J. H., Lee, C. H., Choi, H. S., … Jeong, W. Il. (2019). Glutamate Signaling in Hepatic Stellate Cells Drives Alcoholic Steatosis. *Cell Metabolism*, *30*(5), 877-889.e7. https://doi.org/10.1016/j.cmet.2019.08.001

Clotman, F., Jacquemin, P., Plumb-Rudewiez, N., Pierreux, C. E., Van der Smissen, P., Dietz, H. C., Courtoy, P. J., Rousseau, G. G., & Lemaigre, F. P. (2005). Control of liver cell fate decision by a gradient of TGF beta signaling modulated by Onecut transcription factors. *Genes & Development*, *19*(16), 1849–1854. https://doi.org/10.1101/gad.340305

Coll, M., Perea, L., Boon, R., Leite, S. B., Vallverdú, J., Mannaerts, I., Smout, A., El Taghdouini, A., Blaya, D., Rodrigo-Torres, D., Graupera, I., Aguilar-Bravo, B., Chesne, C., Najimi, M., Sokal, E., Lozano, J. J., van Grunsven, L. A., Verfaillie, C. M., & Sancho-Bru, P. (2018). Generation of Hepatic Stellate Cells from Human Pluripotent Stem Cells Enables In Vitro Modeling of Liver Fibrosis. *Cell Stem Cell*, *23*(1), 101-113.e7. https://doi.org/10.1016/j.stem.2018.05.027

Corbett, J. L., & Duncan, S. A. (2019). iPSC-Derived Hepatocytes as a Platform for Disease Modeling and Drug Discovery. *Frontiers in Medicine*, *6*(November), 1–12. https://doi.org/10.3389/fmed.2019.00265

Cotovio, J. P., Fernandes, T. G., Diogo, M. M., & Cabral, J. M. S. (2020). Pluripotent stem cell biology and engineering. In *Engineering Strategies for Regenerative Medicine* (pp. 1–31). Elsevier. https://doi.org/10.1016/B978-0-12-816221-7.00001-X

Cruz-Acuña, R., Quirós, M., Farkas, A. E., Dedhia, P. H., Huang, S., Siuda, D., García-Hernández, V., Miller, A. J., Spence, J. R., Nusrat, A., & García, A. J. (2017). Synthetic hydrogels for human intestinal organoid generation and colonic wound repair. *Nature Cell Biology*, *19*(11), 1326–1335. https://doi.org/10.1038/ncb3632

De Assuncao, T. M., Sun, Y., Jalan-Sakrikar, N., Drinane, M. C., Huang, B. Q., Li, Y., Davila, J. I., Wang, R., O'Hara, S. P., Lomberk, G. A., Urrutia, R. A., Ikeda, Y., & Huebert, R. C. (2015). Development and characterization of human-induced pluripotent stem cell-derived cholangiocytes. *Laboratory Investigation*, *95*(6), 684–696. https://doi.org/10.1038/labinvest.2015.51

De Los Angeles, A., Ferrari, F., Xi, R., Fujiwara, Y., Benvenisty, N., Deng, H., Hochedlinger, K., Jaenisch, R., Lee, S., Leitch, H. G., Lensch, M. W., Lujan, E., Pei, D., Rossant, J., Wernig, M., Park, P. J., & Daley, G. Q. (2015). Hallmarks of pluripotency. *Nature*, *525*(7570), 469–478. https://doi.org/10.1038/nature15515

Dianat, N., Dubois-Pot-Schneider, H., Steichen, C., Desterke, C., Leclerc, P., Raveux, A., Combettes, L., Weber, A., Corlu, A., & Dubart-Kupperschmitt, A. (2014). Generation of functional cholangiocyte-like cells from human pluripotent stem cells and HepaRG cells. *Hepatology*, *60*(2), 700–714. https://doi.org/10.1002/hep.27165

Eberwine, J., Yeh, H., Miyashiro, K., Cao, Y., Nair, S., Finnell, R., Zettel, M., & Coleman, P. (1992). Analysis of gene expression in single live neurons. *Proceedings of the National Academy of Sciences of the United States of America*, *89*(7), 3010–3014. https://doi.org/10.1073/pnas.89.7.3010

Edington, C. D., Chen, W. L. K., Geishecker, E., Kassis, T., Soenksen, L. R., Bhushan, B. M., Freake, D., Kirschner, J., Maass, C., Tsamandouras, N., Valdez, J., Cook, C. D., Parent, T., Snyder, S., Yu, J., Suter, E., Shockley, M., Velazquez, J., Velazquez, J. J., … Griffith, L. G. (2018). Interconnected Microphysiological Systems for Quantitative Biology and Pharmacology Studies. *Scientific Reports*, *8*(1), 1–18. https://doi.org/10.1038/s41598-018-22749-0

Eiraku, M., Takata, N., Ishibashi, H., Kawada, M., Sakakura, E., Okuda, S., Sekiguchi, K., Adachi, T., & Sasai, Y. (2011a). Self-organizing optic-cup morphogenesis in three-dimensional culture. *Nature*, *472*(7341), 51–56. https://doi.org/10.1038/nature09941

Eiraku, M., Takata, N., Ishibashi, H., Kawada, M., Sakakura, E., Okuda, S., Sekiguchi, K., Adachi, T., & Sasai, Y. (2011b). Self-organizing optic-cup morphogenesis in three-dimensional culture. *Nature*, *472*(7341), 51–56. https://doi.org/10.1038/nature09941

Ereskovsky, A. V., & Dondua, A. K. (2006). The problem of germ layers in sponges (Porifera) and some issues concerning early metazoan evolution. *Zoologischer Anzeiger*, *245*(2), 65–76. https://doi.org/10.1016/j.jcz.2006.04.002

Evans, M. J., & Kaufman, M. H. (1981). Establishment in culture of pluripotential cells from mouse embryos. *Nature*, *292*(5819), 154–156. https://doi.org/10.1038/292154a0

Faial, T., Bernardo, A. S., Mendjan, S., Diamanti, E., Ortmann, D., Gentsch, G. E., Mascetti, V. L., Trotter, M. W. B., Smith, J. C., & Pedersen, R. A. (2015). Brachyury and SMAD signalling collaboratively orchestrate distinct mesoderm and endoderm gene regulatory networks in differentiating human embryonic stem cells. *Development*, *142*(12), 2121–2135. https://doi.org/10.1242/dev.117838

Farzaneh, Z., Najarasl, M., Abbasalizadeh, S., Vosough, M., & Baharvand, H. (2018). Developing a Cost-Effective and Scalable Production of Human Hepatic Competent Endoderm from Size-Controlled Pluripotent Stem Cell Aggregates. *Stem Cells and Development*, *27*(4), 262–274. https://doi.org/10.1089/scd.2017.0074

Fatehullah, A., Tan, S. H., & Barker, N. (2016a). Organoids as an in vitro model of human development and disease. *Nature Cell Biology*, *18*(3), 246–254. https://doi.org/10.1038/ncb3312

Fatehullah, A., Tan, S. H., & Barker, N. (2016b). Organoids as an in vitro model of human development and disease. *Nature Cell Biology*, *18*(3), 246–254. https://doi.org/10.1038/ncb3312

Friedman, C. E., Nguyen, Q., Lukowski, S. W., Helfer, A., Chiu, H. S., Miklas, J., Levy, S., Suo, S., Han, J.-D. J., Osteil, P., Peng, G., Jing, N., Baillie, G. J., Senabouth, A., Christ, A. N., Bruxner, T. J., Murry, C. E., Wong, E. S., Ding, J., … Palpant, N. J. (2018). Single-Cell Transcriptomic Analysis of Cardiac Differentiation from Human PSCs Reveals HOPX-Dependent Cardiomyocyte Maturation. *Cell Stem Cell*, *23*(4), 586-598.e8. https://doi.org/10.1016/j.stem.2018.09.009

Friedman, S. L. (2008). Hepatic stellate cells: Protean, multifunctional, and enigmatic cells of the liver. *Physiological Reviews*, *88*(1), 125–172. https://doi.org/10.1152/physrev.00013.2007

Fukuda-Taira, S. (1981). Hepatic induction in the avian embryo: specificity of reactive endoderm and inductive mesoderm. *Journal of Embryology and Experimental Morphology*, *63*, 111–125. http://www.ncbi.nlm.nih.gov/pubmed/7310284

Gjorevski, N., Sachs, N., Manfrin, A., Giger, S., Bragina, M. E., Ordóñez-Morán, P., Clevers, H., & Lutolf, M. P. (2016). Designer matrices for intestinal stem cell and organoid culture. *Nature*, *539*(7630), 560–564. https://doi.org/10.1038/nature20168

Gordillo, M., Evans, T., & Gouon-Evans, V. (2015). Orchestrating liver development. *Development*, *142*(12), 2094–2108. https://doi.org/10.1242/dev.114215

Grün, D., & van Oudenaarden, A. (2015). Design and Analysis of Single-Cell Sequencing Experiments. *Cell*, *163*(4), 799–810. https://doi.org/10.1016/j.cell.2015.10.039

Gualdi, R., Bossard, P., Zheng, M., Hamada, Y., Coleman, J. R., & Zaret, K. S. (1996). Hepatic specification of the gut endoderm in vitro: cell signaling and transcriptional control. *Genes & Development*, *10*(13), 1670–1682. https://doi.org/10.1101/gad.10.13.1670

Guan, Y., Xu, D., Garfin, P. M., Ehmer, U., Hurwitz, M., Enns, G., Michie, S., Wu, M., Zheng, M., Nishimura, T., Sage, J., & Peltz, G. (2017). Human hepatic organoids for the analysis of human genetic diseases. *JCI Insight*, *2*(17). https://doi.org/10.1172/jci.insight.94954

Gurdon, J. B., Elsdale, T. R., & Fischberg, M. (1958). Sexually mature individuals of Xenopus laevis from the transplantation of single somatic nuclei. *Nature*, *182*(4627), 64–65. https://doi.org/10.2307/3280933

Haeckel, E. (1868). *Natürliche Schöpfungsgeschichte*. George Reimer.

Haeckel, E. (1877). *Anthropogenie* (3rd edn). Wilhelm Engelmann.

Hannoun, Z., Steichen, C., Dianat, N., Weber, A., & Dubart-Kupperschmitt, A. (2016). The potential of induced pluripotent stem cell derived hepatocytes. *Journal of Hepatology*, *65*(1), 182–199. https://doi.org/10.1016/j.jhep.2016.02.025

Harris, S. G., & Shuler, M. L. (2003). Growth of endothelial cells on microfabricated silicon nitride membranes for an In Vitro model of the blood-brain barrier. *Biotechnology and Bioprocess Engineering*, *8*(4), 246–251. https://doi.org/10.1007/BF02942273

Hay, D. C., Fletcher, J., Payne, C., Terrace, J. D., Gallagher, R. C. J., Snoeys, J., Black, J. R., Wojtacha, D., Samuel, K., Hannoun, Z., Pryde, A., Filippi, C., Currie, I. S., Forbes, S. J., Ross, J. A., Newsome, P. N., & Iredale, J. P. (2008). Highly efficient differentiation of hESCs to functional hepatic endoderm requires ActivinA and Wnt3a signaling. *Proceedings of the National Academy of Sciences of the United States of America*, *105*(34), 12301–12306. https://doi.org/10.1073/pnas.0806522105

Heath, J. R., Ribas, A., & Mischel, P. S. (2016). Single-cell analysis tools for drug discovery and development. *Nature Reviews Drug Discovery*, *15*(3), 204–216. https://doi.org/10.1038/nrd.2015.16

Higashi, T., Friedman, S. L., & Hoshida, Y. (2017). Hepatic stellate cells as key target in liver fibrosis. *Advanced Drug Delivery Reviews*, *121*, 27–42. https://doi.org/10.1016/j.addr.2017.05.007

His, W. (1885). *Anatomie menschlicher Embryonen*. Vogel. https://doi.org/10.5962/bhl.title.1229

Hogan, B. L. M. (1999). Morphogenesis. *Cell*, *96*(2), 225–233. https://doi.org/10.1016/S0092-8674(00)80562-0

Hsu, Y.-C., & Fuchs, E. (2012). A family business: stem cell progeny join the niche to regulate homeostasis. *Nature Reviews Molecular Cell Biology*, *13*(2), 103–114. https://doi.org/10.1038/nrm3272

Hu, H., Gehart, H., Artegiani, B., LÖpez-Iglesias, C., Dekkers, F., Basak, O., van Es, J., Chuva de Sousa Lopes, S. M., Begthel, H., Korving, J., van den Born, M., Zou, C., Quirk, C., Chiriboga, L., Rice, C. M., Ma, S., Rios, A., Peters, P. J., de Jong, Y. P., & Clevers, H. (2018). Long-Term Expansion of Functional Mouse and Human Hepatocytes as 3D Organoids. *Cell*, *175*(6), 1591-1606.e19. https://doi.org/10.1016/j.cell.2018.11.013

Huch, M., Dorrell, C., Boj, S. F., Van Es, J. H., Li, V. S. W., Van De Wetering, M., Sato, T., Hamer, K., Sasaki, N., Finegold, M. J., Haft, A., Vries, R. G., Grompe, M., & Clevers, H. (2013a). In vitro expansion of single Lgr5 + liver stem cells induced by Wnt-driven regeneration. *Nature*, *494*(7436), 247–250. https://doi.org/10.1038/nature11826

Huch, M., Dorrell, C., Boj, S. F., Van Es, J. H., Li, V. S. W., Van De Wetering, M., Sato, T., Hamer, K., Sasaki, N., Finegold, M. J., Haft, A., Vries, R. G., Grompe, M., & Clevers, H. (2013b). In vitro

expansion of single Lgr5 + liver stem cells induced by Wnt-driven regeneration. *Nature*, *494*(7436), 247–250. https://doi.org/10.1038/nature11826

Huch, M., Gehart, H., Van Boxtel, R., Hamer, K., Blokzijl, F., Verstegen, M. M. A., Ellis, E., Van Wenum, M., Fuchs, S. A., De Ligt, J., Van De Wetering, M., Sasaki, N., Boers, S. J., Kemperman, H., De Jonge, J., Ijzermans, J. N. M., Nieuwenhuis, E. E. S., Hoekstra, R., Strom, S., … Clevers, H. (2015). Long-term culture of genome-stable bipotent stem cells from adult human liver. *Cell*, *160*(1–2), 299–312. https://doi.org/10.1016/j.cell.2014.11.050

Huh, D., Fujioka, H., Tung, Y.-C., Futai, N., Paine, R., Grotberg, J. B., & Takayama, S. (2007). Acoustically detectable cellular-level lung injury induced by fluid mechanical stresses in microfluidic airway systems. *Proceedings of the National Academy of Sciences*, *104*(48), 18886–18891. https://doi.org/10.1073/pnas.0610868104

Iansante, V., Mitry, R. R., Filippi, C., Fitzpatrick, E., & Dhawan, A. (2018). Human hepatocyte transplantation for liver disease: current status and future perspectives. *Pediatric Research*, *83*(1–2), 232–240. https://doi.org/10.1038/pr.2017.284

Inoue, H., Nagata, N., Kurokawa, H., & Yamanaka, S. (2014). iPS cells: a game changer for future medicine. *The EMBO Journal*, *33*(5), 409–417. https://doi.org/10.1002/embj.201387098

Jang, K., Sato, K., Igawa, K., Chung, U., & Kitamori, T. (2008). Development of an osteoblast-based 3D continuous-perfusion microfluidic system for drug screening. *Analytical and Bioanalytical Chemistry*, *390*(3), 825–832. https://doi.org/10.1007/s00216-007-1752-7

Jang, K.-J., & Suh, K.-Y. (2010). A multi-layer microfluidic device for efficient culture and analysis of renal tubular cells. *Lab on a Chip*, *10*(1), 36–42. https://doi.org/10.1039/b907515a

Jing, R., Corbett, J. L., Cai, J., Beeson, G. C., Beeson, C. C., Chan, S. S., Dimmock, D. P., Lazcares, L., Geurts, A. M., Lemasters, J. J., & Duncan, S. A. (2018). A Screen Using iPSC-Derived Hepatocytes Reveals NAD+ as a Potential Treatment for mtDNA Depletion Syndrome. *Cell Reports*, *25*(6), 1469-1484.e5. https://doi.org/10.1016/j.celrep.2018.10.036

Julius, M. H., Masuda, T., & Herzenberg, L. A. (1972). Demonstration that antigen-binding cells are precursors of antibody-producing cells after purification with a fluorescence-activated cell sorter. *Proceedings of the National Academy of Sciences of the United States of America*, *69*(7), 1934–1938.

Kajiwara, M., Aoi, T., Okita, K., Takahashi, R., Inoue, H., Takayama, N., Endo, H., Eto, K., Toguchida, J., Uemoto, S., & Yamanaka, S. (2012). Donor-dependent variations in hepatic differentiation from human-induced pluripotent stem cells. *Proceedings of the National Academy of Sciences of the United States of America*, *109*(31), 12538–12543. https://doi.org/10.1073/pnas.1209979109

Kamiya, A. (1999). Fetal liver development requires a paracrine action of oncostatin M through the gp130 signal transducer. *The EMBO Journal*, *18*(8), 2127–2136. https://doi.org/10.1093/emboj/18.8.2127

Kamiya, A., Kinoshita, T., & Miyajima, A. (2001). Oncostatin M and hepatocyte growth factor induce hepatic maturation via distinct signaling pathways. *FEBS Letters*, *492*(1–2), 90–94. https://doi.org/10.1016/S0014-5793(01)02140-8

Kester, L., & van Oudenaarden, A. (2018). Single-Cell Transcriptomics Meets Lineage Tracing. *Cell Stem Cell*, *23*(2), 166–179. https://doi.org/10.1016/j.stem.2018.04.014

Kimbrel, E. a., & Lanza, R. (2015). Current status of pluripotent stem cells: moving the first therapies to the clinic. *Nature Reviews Drug Discovery*, *14*(September), 681–692. https://doi.org/10.1038/nrd4738

Kimura, H., Yamamoto, T., Sakai, H., Sakai, Y., & Fujii, T. (2008). An integrated microfluidic system for long-term perfusion culture and on-line monitoring of intestinal tissue models. *Lab on a Chip*, *8*(5), 741–746. https://doi.org/10.1039/b717091b

Kisseleva, T., & Brenner, D. A. (2019). The Crosstalk between Hepatocytes, Hepatic Macrophages, and Hepatic Stellate Cells Facilitates Alcoholic Liver Disease. *Cell Metabolism*, *30*(5), 850–852. https://doi.org/10.1016/j.cmet.2019.10.010

Knoblich, J. A. (2008). Mechanisms of Asymmetric Stem Cell Division. *Cell*, *132*(4), 583–597. https://doi.org/10.1016/j.cell.2008.02.007

Knowlton, S., & Tasoglu, S. (2016). A Bioprinted Liver-on-a-Chip for Drug Screening Applications. *Trends in Biotechnology*, *34*(9), 681–682. https://doi.org/10.1016/j.tibtech.2016.05.014

Koui, Y., Kido, T., Ito, T., Oyama, H., Chen, S. W., Katou, Y., Shirahige, K., & Miyajima, A. (2017). An In Vitro Human Liver Model by iPSC-Derived Parenchymal and Non-parenchymal Cells. *Stem Cell Reports*, *9*(2), 490–498. https://doi.org/10.1016/j.stemcr.2017.06.010

Kruitwagen, H. S., Oosterhoff, L. A., Vernooij, I. G. W. H., Schrall, I. M., van Wolferen, M. E., Bannink, F., Roesch, C., van Uden, L., Molenaar, M. R., Helms, J. B., Grinwis, G. C. M., Verstegen, M. M. A., van der Laan, L. J. W., Huch, M., Geijsen, N., Vries, R. G., Clevers, H., Rothuizen, J., Schotanus, B. A., … Spee, B. (2017). Long-Term Adult Feline Liver Organoid Cultures for Disease Modeling of Hepatic Steatosis. *Stem Cell Reports*, *8*(4), 822–830. https://doi.org/10.1016/j.stemcr.2017.02.015

Kubo, A., Shinozaki, K., Shannon, J. M., Kouskoff, V., Kennedy, M., Woo, S., Fehling, H. J., & Keller, G. (2004). Development of definitive endoderm from embryonic stem cells in culture. *Development*, *131*(7), 1651–1662. https://doi.org/10.1242/dev.01044

Kuijk, E. W., Rasmussen, S., Blokzijl, F., Huch, M., Gehart, H., Toonen, P., Begthel, H., Clevers, H., Geurts, A. M., & Cuppen, E. (2016). Generation and characterization of rat liver stem cell lines and their engraftment in a rat model of liver failure. *Scientific Reports*, *6*(February), 1–11. https://doi.org/10.1038/srep22154

Kumar, P., Tan, Y., & Cahan, P. (2017). Understanding development and stem cells using single cell-based analyses of gene expression. *Development*, *144*(1), 17–32. https://doi.org/10.1242/dev.133058

Kwon, G. S., Viotti, M., & Hadjantonakis, A. K. (2008). The Endoderm of the Mouse Embryo Arises by Dynamic Widespread Intercalation of Embryonic and Extraembryonic Lineages. *Developmental Cell*, *15*(4), 509–520. https://doi.org/10.1016/j.devcel.2008.07.017

Lam, M. T., Huang, Y. C., Birla, R. K., & Takayama, S. (2009). Microfeature guided skeletal muscle tissue engineering for highly organized 3-dimensional free-standing constructs. *Biomaterials*, *30*(6), 1150–1155. https://doi.org/10.1016/j.biomaterials.2008.11.014

Lamm, N., Ben-David, U., Golan-Lev, T., Storchová, Z., Benvenisty, N., & Kerem, B. (2016). Genomic Instability in Human Pluripotent Stem Cells Arises from Replicative Stress and Chromosome Condensation Defects. *Cell Stem Cell*, *18*(2), 253–261. https://doi.org/10.1016/j.stem.2015.11.003

Lancaster, M. A., & Knoblich, J. A. (2014a). Organogenesis in a dish: modeling development and disease using organoid technologies. *Science*, *345*(6194), 1247125. https://doi.org/10.1126/science.1247125

Lancaster, M. A., & Knoblich, J. A. (2014b). Organogenesis in a dish: modeling development and disease using organoid technologies. *Science*, *345*(6194), 1247125. https://doi.org/10.1126/science.1247125

Lancaster, M. A., Renner, M., Martin, C.-A., Wenzel, D., Bicknell, L. S., Hurles, M. E., Homfray, T., Penninger, J. M., Jackson, A. P., & Knoblich, J. A. (2013). Cerebral organoids model human brain development and microcephaly. *Nature*, *501*(7467), 373–379. https://doi.org/10.1038/nature12517

Langer-Safer, P. R., Levine, M., & Ward, D. C. (1982). Immunological method for mapping genes on Drosophila polytene chromosomes. *Proceedings of the National Academy of Sciences of the United States of America*, *79*(14), 4381–4385.

Lawson, K. A., Meneses, J. J., & Pedersen, R. A. (1991). Clonal analysis of epiblast fate during germ layer formation in the mouse embryo. *Development*, *113*(3), 891–911.

Le Douarin, N. M. (1964). Induction de l'endoderme pré-hépatique par le mésoderme de l'aire cardiaque chez l'embryon de poulet. *Development*, *12*(4), 651–664. https://doi.org/10.1242/dev.12.4.651

Le Douarin, N. M. (1975). An experimental analysis of liver development. *Medical Biology*, *53*(6), 427–455. http://www.ncbi.nlm.nih.gov/pubmed/765644

Lee, P. J., Hung, P. J., & Lee, L. P. (2007). An artificial liver sinusoid with a microfluidic endothelial-like barrier for primary hepatocyte culture. *Biotechnology and Bioengineering*, *97*(5), 1340–1346. https://doi.org/10.1002/bit.21360

Lee, T. T., García, J. R., Paez, J. I., Singh, A., Phelps, E. A., Weis, S., Shafiq, Z., Shekaran, A., Del Campo, A., & García, A. J. (2015). Light-triggered in vivo activation of adhesive peptides regulates cell adhesion, inflammation and vascularization of biomaterials. *Nature Materials*, *14*(3), 352–360. https://doi.org/10.1038/nmat4157

Lewis, F. T. (1912). Development of the Liver. In *Manual of Human Embryology* (Volume 2, pp. 403–428). J. B. Lippincott Company.

Li, M., & Belmonte, J. C. I. (2017). Ground rules of the pluripotency gene regulatory network. *Nature Reviews. Genetics*, *18*(3), 180–191. https://doi.org/10.1038/nrg.2016.156

Li, P., He, K., Li, J., Liu, Z., & Gong, J. (2017). The role of Kupffer cells in hepatic diseases. *Molecular Immunology*, *85*, 222–229. https://doi.org/10.1016/j.molimm.2017.02.018

Lindborg, B. A., Brekke, J. H., Vegoe, A. L., Ulrich, C. B., Haider, K. T., Subramaniam, S., Venhuizen, S. L., Eide, C. R., Orchard, P. J., Chen, W., Wang, Q., Pelaez, F., Scott, C. M., Kokkoli, E., Keirstead, S. A., Dutton, J. R., Tolar, J., & O'Brien, T. D. (2016). Rapid Induction of Cerebral Organoids From Human Induced Pluripotent Stem Cells Using a Chemically Defined Hydrogel and Defined Cell Culture Medium. *Stem Cells Translational Medicine*, *5*(7), 970–979. https://doi.org/10.5966/sctm.2015-0305

Loh, K. M., Chen, A., Koh, P. W., Deng, T. Z., Sinha, R., Tsai, J. M., Barkal, A. A., Shen, K. Y., Jain, R., Morganti, R. M., Shyh-Chang, N., Fernhoff, N. B., George, B. M., Wernig, G., Salomon, R. E. A., Chen, Z., Vogel, H., Epstein, J. A., Kundaje, A., … Weissman, I. L. (2016). Mapping the Pairwise Choices Leading from Pluripotency to Human Bone, Heart, and Other Mesoderm Cell Types. *Cell*, *166*(2), 451–467. https://doi.org/10.1016/j.cell.2016.06.011

Lorvellec, M., Scottoni, F., Crowley, C., Fiadeiro, R., Maghsoudlou, P., Pellegata, A. F., Mazzacuva, F., Gjinovci, A., Lyne, A. M., Zulini, J., Little, D., Mosaku, O., Kelly, D., De Coppi, P., & Gissen, P. (2017). Mouse decellularised liver scaffold improves human embryonic and induced pluripotent stem cells differentiation into hepatocyte-like cells. *PLoS ONE*, *12*(12), 1–23. https://doi.org/10.1371/journal.pone.0189586

Lowe, L. A., Yamada, S., & Kuehn, M. R. (2001). Genetic dissection of nodal function in patterning the mouse embryo. *Development*, *128*(10), 1831–1843.

Lüdtke, T. H. W., Christoffels, V. M., Petry, M., & Kispert, A. (2009). Tbx3 promotes liver bud expansion during mouse development by suppression of cholangiocyte differentiation. *Hepatology*, *49*(3), 969–978. https://doi.org/10.1002/hep.22700

Ma, X., Qu, X., Zhu, W., Li, Y.-S., Yuan, S., Zhang, H., Liu, J., Wang, P., Lai, C. S. E., Zanella, F., Feng, G.-S., Sheikh, F., Chien, S., & Chen, S. (2016). Deterministically patterned biomimetic human iPSC-derived hepatic model via rapid 3D bioprinting. *Proceedings of the National Academy of Sciences of the United States of America*, *113*(8), 2206–2211. https://doi.org/10.1073/pnas.1524510113

Maldonado, M., Wong, L. Y., Echeverria, C., Ico, G., Low, K., Fujimoto, T., Johnson, J. K., & Nam, J. (2015). Biomaterials The effects of electrospun substrate-mediated cell colony morphology on the self-renewal of human induced pluripotent stem cells. *Biomaterials*, *50*, 10–19. https://doi.org/10.1016/j.biomaterials.2015.01.037

Mandai, M., Watanabe, A., Kurimoto, Y., Hirami, Y., Morinaga, C., Daimon, T., Fujihara, M., Akimaru, H., Sakai, N., Shibata, Y., Terada, M., Nomiya, Y., Tanishima, S., Nakamura, M., Kamao, H., Sugita, S., Onishi, A., Ito, T., Fujita, K., … Takahashi, M. (2017). Autologous Induced Stem-Cell–Derived Retinal Cells for Macular Degeneration. *New England Journal of Medicine*, *376*(11), 1038–1046. https://doi.org/10.1056/NEJMoa1608368

Margagliotti, S., Clotman, F., Pierreux, C. E., Beaudry, J. B., Jacquemin, P., Rousseau, G. G., & Lemaigre, F. P. (2007). The Onecut transcription factors HNF-6/OC-1 and OC-2 regulate early liver expansion by controlling hepatoblast migration. *Developmental Biology*, *311*(2), 579–589. https://doi.org/10.1016/j.ydbio.2007.09.013

Margagliotti, S., Clotman, F., Pierreux, C. E., Lemoine, P., Rousseau, G. G., Henriet, P., & Lemaigre, F. P. (2008). Role of metalloproteinases at the onset of liver development. *Development Growth and Differentiation*, *50*(5), 331–338. https://doi.org/10.1111/j.1440-169X.2008.01031.x

Martin, G. R. (1981). Isolation of a pluripotent cell line from early mouse embryos cultured in medium conditioned by teratocarcinoma stem cells. *Proceedings of the National Academy of Sciences of the United States of America*, *78*(12), 7634–7638. https://doi.org/10.1073/pnas.78.12.7634

Matas, A. J., Sutherland, D. E. R., Steffes, M. W., Michael Mauer, S., Lowe, A., Simmons, R. L., & Najarian, J. S. (1976). Hepatocellular transplantation for metabolic deficiencies: Decrease of plasma bilirubin in Gunn rats. *Science*, *192*(4242), 892–894. https://doi.org/10.1126/science.818706

Matsui, Y., Zsebo, K., & Hogan, B. L. M. (1992). Derivation of pluripotential embryonic stem cells from murine primordial germ cells in culture. *Cell*, *70*(5), 841–847. https://doi.org/10.1016/0092-8674(92)90317-6

Matsumoto, K., Yoshitomi, H., Rossant, J., & Zaret, K. S. (2001). Liver organogenesis promoted by endothelial cells prior to vascular function. *Science*, *294*(5542), 559–563. https://doi.org/10.1126/science.1063889

McCracken, K. W., Catá, E. M., Crawford, C. M., Sinagoga, K. L., Schumacher, M., Rockich, B. E., Tsai, Y.-H., Mayhew, C. N., Spence, J. R., Zavros, Y., & Wells, J. M. (2014). Modelling human development and disease in pluripotent stem-cell-derived gastric organoids. *Nature*, *516*(7531), 400–404. https://doi.org/10.1038/nature13863

Medine, C. N., Lucendo-Villarin, B., Storck, C., Wang, F., Szkolnicka, D., Khan, F., Pernagallo, S., Black, J. R., Marriage, H. M., Ross, J. A., Bradley, M., Iredale, J. P., Flint, O., & Hay, D. C. (2013). Developing high-fidelity hepatotoxicity models from pluripotent stem cells. *Stem Cells Translational Medicine*, *2*(7), 505–509. https://doi.org/10.5966/sctm.2012-0138

Merrell, A. J., & Stanger, B. Z. (2016). Adult cell plasticity in vivo: de-differentiation and transdifferentiation are back in style. *Nature Reviews. Molecular Cell Biology*, *17*(7), 413–425. https://doi.org/10.1038/nrm.2016.24

Michalopoulos, G. K., Bowen, W. C., Mulè, K., & Stolz, D. B. (2001). Histological organization in hepatocyte organoid cultures. *American Journal of Pathology*, *159*(5), 1877–1887. https://doi.org/10.1016/S0002-9440(10)63034-9

Minami, T., Ishii, T., Yasuchika, K., Fukumitsu, K., Ogiso, S., Miyauchi, Y., Kojima, H., Kawai, T., Yamaoka, R., Oshima, Y., Kawamoto, H., Kotaka, M., Yasuda, K., Osafune, K., & Uemoto, S. (2019). Novel hybrid three-dimensional artificial liver using human induced pluripotent stem cells

and a rat decellularized liver scaffold. *Regenerative Therapy*, *10*, 127–133. https://doi.org/10.1016/j.reth.2019.03.002

Miranda, C. C., Fernandes, T. G., Diogo, M. M., & Cabral, J. M. S. (2018). Towards multi-organoid systems for drug screening applications. *Bioengineering*, *5*(3), 1–17. https://doi.org/10.3390/bioengineering5030049

Miranda, C. C., Fernandes, T. G., Pinto, S. N., Prieto, M., Diogo, M. M., & Cabral, J. M. S. (2018). A scale out approach towards neural induction of human induced pluripotent stem cells for neurodevelopmental toxicity studies. *Toxicology Letters*, *294*(December 2017), 51–60. https://doi.org/10.1016/j.toxlet.2018.05.018

Mito, M., & Kusano, M. (1993). Hepatocyte Transplantation in Man. *Cell Transplantation*, *2*(1), 65–74. https://doi.org/10.1177/096368979300200109

Miyajima, A., Tanaka, M., & Itoh, T. (2014). Stem/progenitor cells in liver development, homeostasis, regeneration, and reprogramming. *Cell Stem Cell*, *14*(5), 561–574. https://doi.org/10.1016/j.stem.2014.04.010

Morrison, S. J., & Kimble, J. (2006). Asymmetric and symmetric stem-cell divisions in development and cancer. *Nature*, *441*(7097), 1068–1074. https://doi.org/10.1038/nature04956

Muguruma, K., Nishiyama, A., Kawakami, H., Hashimoto, K., & Sasai, Y. (2015). Self-organization of polarized cerebellar tissue in 3D culture of human pluripotent stem cells. *Cell Reports*, *10*(4), 537–550. https://doi.org/10.1016/j.celrep.2014.12.051

Murphy, S. V., & Atala, A. (2014). 3D bioprinting of tissues and organs. *Nature Biotechnology*, *32*(8), 773–785. https://doi.org/10.1038/nbt.2958

Murrow, L. M., Weber, R. J., & Gartner, Z. J. (2017). Dissecting the stem cell niche with organoid models: an engineering-based approach. *Development (Cambridge, England)*, *144*(6), 998–1007. https://doi.org/10.1242/dev.140905

Nagamoto, Y., Takayama, K., Ohashi, K., Okamoto, R., Sakurai, F., Tachibana, M., Kawabata, K., & Mizuguchi, H. (2016). Transplantation of a human iPSC-derived hepatocyte sheet increases survival in mice with acute liver failure. *Journal of Hepatology*, *64*(5), 1068–1075. https://doi.org/10.1016/j.jhep.2016.01.004

Nakanishi, N., Sogabe, S., & Degnan, B. M. (2014). Evolutionary origin of gastrulation: Insights from sponge development. *BMC Biology*, *12*. https://doi.org/10.1186/1741-7007-12-26

Nantasanti, S., Spee, B., Kruitwagen, H. S., Chen, C., Geijsen, N., Oosterhoff, L. A., Van Wolferen, M. E., Pelaez, N., Fieten, H., Wubbolts, R. W., Grinwis, G. C., Chan, J., Huch, M., Vries, R. R. G., Clevers, H., De Bruin, A., Rothuizen, J., Penning, L. C., & Schotanus, B. A. (2015). Disease modeling and gene therapy of copper storage disease in canine hepatic organoids. *Stem Cell Reports*, *5*(5), 895–907. https://doi.org/10.1016/j.stemcr.2015.09.002

Nie, Y. Z., Zheng, Y. W., Miyakawa, K., Murata, S., Zhang, R. R., Sekine, K., Ueno, Y., Takebe, T., Wakita, T., Ryo, A., & Taniguchi, H. (2018). Recapitulation of hepatitis B virus–host interactions in liver organoids from human induced pluripotent stem cells. *EBioMedicine*, *35*, 114–123. https://doi.org/10.1016/j.ebiom.2018.08.014

Nie, Y. Z., Zheng, Y. W., Ogawa, M., Miyagi, E., & Taniguchi, H. (2018). Human liver organoids generated with single donor-derived multiple cells rescue mice from acute liver failure. *Stem Cell Research and Therapy*, *9*(1), 1–12. https://doi.org/10.1186/s13287-017-0749-1

Ober, E. A., & Lemaigre, F. P. (2018). Development of the liver: Insights into organ and tissue morphogenesis. *Journal of Hepatology*, *68*(5), 1049–1062. https://doi.org/10.1016/j.jhep.2018.01.005

Ogawa, M., Ogawa, S., Bear, C. E., Ahmadi, S., Chin, S., Li, B., Grompe, M., Keller, G., Kamath, B. M., & Ghanekar, A. (2015). Directed differentiation of cholangiocytes from human pluripotent stem cells. *Nature Biotechnology*, *33*(8), 853–861. https://doi.org/10.1038/nbt.3294

Ong, C. S., Yesantharao, P., Huang, C. Y., Mattson, G., Boktor, J., Fukunishi, T., Zhang, H., & Hibino, N. (2018). 3D bioprinting using stem cells. *Pediatric Research*, *83*(1–2), 223–231. https://doi.org/10.1038/pr.2017.252

Ouchi, R., Togo, S., Kimura, M., Shinozawa, T., Koido, M., Koike, H., Thompson, W., Karns, R. A., Mayhew, C. N., McGrath, P. S., McCauley, H. A., Zhang, R. R., Lewis, K., Hakozaki, S., Ferguson, A., Saiki, N., Yoneyama, Y., Takeuchi, I., Mabuchi, Y., … Takebe, T. (2019). Modeling Steatohepatitis in Humans with Pluripotent Stem Cell-Derived Organoids. *Cell Metabolism*, *30*(2), 374-384.e6. https://doi.org/10.1016/j.cmet.2019.05.007

Pander, C. H. (1817). *Beiträge zur Entwickelungsgeschichte des Hühnchens im Eye.* H. L. Brönner.

Papalexi, E., & Satija, R. (2018). Single-cell RNA sequencing to explore immune cell heterogeneity. *Nature Reviews Immunology*, *18*(1), 35–45. https://doi.org/10.1038/nri.2017.76

Parviz, F., Matullo, C., Garrison, W. D., Savatski, L., Adamson, J. W., Ning, G., Kaestner, K. H., Rossi, J. M., Zaret, K. S., & Duncan, S. A. (2003). Hepatocyte nuclear factor 4α controls the development of a hepatic epithelium and liver morphogenesis. *Nature Genetics*, *34*(3), 292–296. https://doi.org/10.1038/ng1175

Pettinato, G., Lehoux, S., Ramanathan, R., Salem, M. M., He, L. X., Muse, O., Flaumenhaft, R., Thompson, M. T., Rouse, E. A., Cummings, R. D., Wen, X., & Fisher, R. A. (2019). Generation of fully functional hepatocyte-like organoids from human induced pluripotent stem cells mixed with Endothelial Cells. *Scientific Reports*, *9*(1), 1–21. https://doi.org/10.1038/s41598-019-45514-3

Poisson, J., Lemoinne, S., Boulanger, C., Durand, F., Moreau, R., Valla, D., & Rautou, P. E. (2017). Liver sinusoidal endothelial cells: Physiology and role in liver diseases. *Journal of Hepatology*, *66*(1), 212–227. https://doi.org/10.1016/j.jhep.2016.07.009

Przybyla, L., Lakins, J. N., & Weaver, V. M. (2016). Tissue Mechanics Orchestrate Wnt-Dependent Human Embryonic Stem Cell Differentiation. *Cell Stem Cell*, *19*(4), 462–475. https://doi.org/10.1016/j.stem.2016.06.018

Ramalho-Santos, M., & Willenbring, H. (2007). On the Origin of the Term "Stem Cell." *Cell Stem Cell*, *1*(1), 35–38. https://doi.org/10.1016/j.stem.2007.05.013

Rambhatla, L., Chiu, C. P., Kundu, P., Peng, Y., & Carpenter, M. K. (2003). Generation of hepatocyte-like cells from human embryonic stem cells. *Cell Transplantation*, *12*(1), 1–11. https://doi.org/10.3727/000000003783985179

Ranga, A., Girgin, M., Meinhardt, A., Eberle, D., Caiazzo, M., Tanaka, E. M., & Lutolf, M. P. (2016). Neural tube morphogenesis in synthetic 3D microenvironments. *Proceedings of the National Academy of Sciences of the United States of America*, *113*(44), E6831–E6839. https://doi.org/10.1073/pnas.1603529113

Rashidi, H., Luu, N. T., Alwahsh, S. M., Ginai, M., Alhaque, S., Dong, H., Tomaz, R. A., Vernay, B., Vigneswara, V., Hallett, J. M., Chandrashekran, A., Dhawan, A., Vallier, L., Bradley, M., Callanan, A., Forbes, S. J., Newsome, P. N., & Hay, D. C. (2018). 3D human liver tissue from pluripotent stem cells displays stable phenotype in vitro and supports compromised liver function in vivo. *Archives of Toxicology*, *92*(10), 3117–3129. https://doi.org/10.1007/s00204-018-2280-2

Rheinwald, J. G., & Green, H. (1975). Serial cultivation of strains of human epidermal keratinocytes: the formation of keratinizing colonies from single cells. *Cell*, *6*(3), 331–343. https://doi.org/10.1016/S0092-8674(75)80001-8

Ronaldson-Bouchard, K., & Vunjak-Novakovic, G. (2018). Organs-on-a-Chip: A Fast Track for Engineered Human Tissues in Drug Development. *Cell Stem Cell*, *22*(3), 310–324. https://doi.org/10.1016/j.stem.2018.02.011

Rosenberg, A. B., Roco, C. M., Muscat, R. A., Kuchina, A., Sample, P., Yao, Z., Graybuck, L. T., Peeler, D. J., Mukherjee, S., Chen, W., Pun, S. H., Sellers, D. L., Tasic, B., & Seelig, G. (2018). Single-cell profiling of the developing mouse brain and spinal cord with split-pool barcoding. *Science*, *360*(6385), 176–182. https://doi.org/10.1126/science.aam8999

Rossi, G., Manfrin, A., & Lutolf, M. P. (2018a). Progress and potential in organoid research. *Nature Reviews Genetics*, *19*(11), 671–687. https://doi.org/10.1038/s41576-018-0051-9

Rossi, G., Manfrin, A., & Lutolf, M. P. (2018b). Progress and potential in organoid research. *Nature Reviews Genetics*, *19*(11), 671–687. https://doi.org/10.1038/s41576-018-0051-9

Rossi, J. M., Dunn, N. R., Hogan, B. L. M., & Zaret, K. S. (2001). Distinct mesodermal signals, including BMPs from the septum, transversum mesenchyme, are required in combination for hepatogenesis from the endoderm. *Genes and Development*, *15*(15), 1998–2009. https://doi.org/10.1101/gad.904601

Rowe, R. G., & Daley, G. Q. (2019a). Induced pluripotent stem cells in disease modelling and drug discovery. *Nature Reviews Genetics*, *1*. https://doi.org/10.1038/s41576-019-0100-z

Rowe, R. G., & Daley, G. Q. (2019b). Induced pluripotent stem cells in disease modelling and drug discovery. *Nature Reviews Genetics*, *1*. https://doi.org/10.1038/s41576-019-0100-z

Sakmann, B., & Neher, E. (1984). Patch clamp techniques for studying ionic channels in excitable membranes. *Annual Review of Physiology*, *46*, 455–472. https://doi.org/10.1146/annurev.ph.46.030184.002323

Sampaziotis, F., De Brito, M. C., Madrigal, P., Bertero, A., Saeb-Parsy, K., Soares, F. A. C., Schrumpf, E., Melum, E., Karlsen, T. H., Bradley, J. A., Gelson, W. T. H., Davies, S., Baker, A., Kaser, A., Alexander, G. J., Hannan, N. R. F., & Vallier, L. (2015). Cholangiocytes derived from human induced pluripotent stem cells for disease modeling and drug validation. *Nature Biotechnology*, *33*(8), 845–852. https://doi.org/10.1038/nbt.3275

Sánchez Alvarado, A., & Yamanaka, S. (2014). Rethinking differentiation: Stem cells, regeneration, and plasticity. *Cell*, *157*(1), 110–119. https://doi.org/10.1016/j.cell.2014.02.041

Sasai, Y. (2013a). Cytosystems dynamics in self-organization of tissue architecture. *Nature*, *493*(7432), 318–326. https://doi.org/10.1038/nature11859

Sasai, Y. (2013b). Next-generation regenerative medicine: organogenesis from stem cells in 3D culture. *Cell Stem Cell*, *12*(5), 520–530. https://doi.org/10.1016/j.stem.2013.04.009

Sato, T., Vries, R. G., Snippert, H. J., van de Wetering, M., Barker, N., Stange, D. E., van Es, J. H., Abo, A., Kujala, P., Peters, P. J., & Clevers, H. (2009a). Single Lgr5 stem cells build crypt-villus structures in vitro without a mesenchymal niche. *Nature*, *459*(7244), 262–265. https://doi.org/10.1038/nature07935

Sato, T., Vries, R. G., Snippert, H. J., van de Wetering, M., Barker, N., Stange, D. E., van Es, J. H., Abo, A., Kujala, P., Peters, P. J., & Clevers, H. (2009b). Single Lgr5 stem cells build crypt-villus structures in vitro without a mesenchymal niche. *Nature*, *459*(7244), 262–265. https://doi.org/10.1038/nature07935

Sayed, N., Liu, C., & Wu, J. C. (2016). Translation of Human-Induced Pluripotent Stem Cells from Clinical Trial in a Dish to Precision Medicine. *Journal of the American College of Cardiology*, *67*(18), 2161–2176. https://doi.org/10.1016/j.jacc.2016.01.083

Schwartz, R. E., Fleming, H. E., Khetani, S. R., & Bhatia, S. N. (2014). Pluripotent stem cell-derived hepatocyte-like cells. *Biotechnology Advances*, *32*(2), 504–513. https://doi.org/10.1016/j.biotechadv.2014.01.003

Serls, A. E., Doherty, S., Parvatiyar, P., Wells, J. M., & Deutsch, G. H. (2005). Different thresholds of fibroblast growth factors pattern the ventral foregut into liver and lung. *Development*, *132*(1), 35–47. https://doi.org/10.1242/dev.01570

Shamblott, M. J., Axelman, J., Wang, S., Bugg, E. M., Littlefield, J. W., Donovan, P. J., Blumenthal, P. D., Huggins, G. R., & Gearhart, J. D. (1998). Derivation of pluripotent stem cells from cultured human

primordial germ cells. *Proceedings of the National Academy of Sciences of the United States of America*, *95*(23), 13726–13731. https://doi.org/VL - 95

Shi, Y., Inoue, H., Wu, J. C., & Yamanaka, S. (2016). Induced pluripotent stem cell technology: a decade of progress. *Nature Reviews Drug Discovery*, *16*(2), 115–130. https://doi.org/10.1038/nrd.2016.245

Shiojiri, N., & Sugiyama, Y. (2004). Immunolocalization of extracellular matrix components and integrins during mouse liver development. *Hepatology*, *40*(2), 346–355. https://doi.org/10.1002/hep.20303

Siller, R., Greenhough, S., Naumovska, E., & Sullivan, G. J. (2015). Small-molecule-driven hepatocyte differentiation of human pluripotent stem cells. *Stem Cell Reports*, *4*(5), 939–952. https://doi.org/10.1016/j.stemcr.2015.04.001

Silva, T. P., Cotovio, J. P., Bekman, E., Carmo-Fonseca, M., Cabral, J. M. S., & Fernandes, T. G. (2019). Design Principles for Pluripotent Stem Cell-Derived Organoid Engineering. *Stem Cells International*, *2019*, 1–17. https://doi.org/10.1155/2019/4508470

Siramshetty, V. B., Nickel, J., Omieczynski, C., Gohlke, B. O., Drwal, M. N., & Preissner, R. (2016). WITHDRAWN - A resource for withdrawn and discontinued drugs. *Nucleic Acids Research*, *44*(D1), D1080–D1086. https://doi.org/10.1093/nar/gkv1192

Sirenko, O., Hancock, M. K., Hesley, J., Hong, D., Cohen, A., Gentry, J., Carlson, C. B., & Mann, D. A. (2016). Phenotypic characterization of toxic compound effects on liver spheroids derived from ipsc using confocal imaging and three-dimensional image analysis. *Assay and Drug Development Technologies*, *14*(7), 381–394. https://doi.org/10.1089/adt.2016.729

Si-Tayeb, K., Lemaigre, F. P., & Duncan, S. A. (2010). Organogenesis and Development of the Liver. *Developmental Cell*, *18*(2), 175–189. https://doi.org/10.1016/j.devcel.2010.01.011

Si-Tayeb, K., Noto, F. K., Nagaoka, M., Li, J., Battle, M. A., Duris, C., North, P. E., Dalton, S., & Duncan, S. A. (2010). Highly efficient generation of human hepatocyte-like cells from induced pluripotent stem cells. *Hepatology*, *51*(1), 297–305. https://doi.org/10.1002/hep.23354

Solter, D., & Solter, D. (2006). From teratocarcinomas to embryonic stem cells and beyond: a history of embryonic stem cell research. *Nature Reviews. Genetics*, *7*(4), 319–327. https://doi.org/10.1038/nrg1827

Song, J. W., Gu, W., Futai, N., Warner, K. A., Nor, J. E., & Takayama, S. (2005). Computer-controlled microcirculatory support system for endothelial cell culture and shearing. *Analytical Chemistry*, *77*(13), 3993–3999. https://doi.org/10.1021/ac050131o

Song, Z., Cai, J., Liu, Y., Zhao, D., Yong, J., Duo, S., Song, X., Guo, Y., Zhao, Y., Qin, H., Yin, X., Wu, C., Che, J., Lu, S., Ding, M., & Deng, H. (2009). Efficient generation of hepatocyte-like cells from human induced pluripotent stem cells. *Cell Research*, *19*(11), 1233–1242. https://doi.org/10.1038/cr.2009.107

Sørensen, K. K., Simon-Santamaria, J., McCuskey, R. S., & Smedsrød, B. (2015). Liver sinusoidal endothelial cells. *Comprehensive Physiology*, *5*(4), 1751–1774. https://doi.org/10.1002/cphy.c140078

Sosa-Pineda, B., Wigle, J. T., & Oliver, G. (2000). Hepatocyte migration during liver development requires Prox1. *Nature Genetics*, *25*(3), 254–255. https://doi.org/10.1038/76996

Sterneckert, J. L., Reinhardt, P., & Scholer, H. R. (2014). Investigating human disease using stem cell models. *Nat Rev Genet*, *15*(9), 625–639. https://doi.org/10.1038/nrg3764

Sterneckert, J. L., Reinhardt, P., & Schöler, H. R. (2014). Investigating human disease using stem cell models. *Nature Reviews Genetics*, *15*(9), 625–639. https://doi.org/10.1038/nrg3764

Sullivan, G. J., Hay, D. C., Park, I.-H., Fletcher, J., Hannoun, Z., Payne, C. M., Dalgetty, D., Black, J. R., Ross, J. A., Samuel, K., Wang, G., Daley, G. Q., Lee, J.-H., Church, G. M., Forbes, S. J., Iredale, J. P., & Wilmut, I. (2010). Generation of functional human hepatic endoderm from human induced pluripotent stem cells. *Hepatology*, *51*(1), 329–335. https://doi.org/10.1002/hep.23335

Tabar, V., & Studer, L. (2014). Pluripotent stem cells in regenerative medicine: challenges and recent progress. *Nat Rev Genet*, *15*(2), 82–92. https://doi.org/10.1038/nrg3563

Takahashi, K., Tanabe, K., Ohnuki, M., Narita, M., Ichisaka, T., Tomoda, K., & Yamanaka, S. (2007). Induction of Pluripotent Stem Cells from Adult Human Fibroblasts by Defined Factors. *Cell*, *131*(5), 861–872. https://doi.org/10.1016/j.cell.2007.11.019

Takahashi, K., & Yamanaka, S. (2006). Induction of pluripotent stem cells from mouse embryonic and adult fibroblast cultures by defined factors. *Cell*, *126*(4), 663–676. https://doi.org/10.1016/j.cell.2006.07.024

Takahashi, K., & Yamanaka, S. (2016). A decade of transcription factor-mediated reprogramming to pluripotency. *Nature Reviews. Molecular Cell Biology*, *17*(3), 183–193. https://doi.org/10.1038/nrm.2016.8

Takasato, M., Er, P. X., Chiu, H. S., Maier, B., Baillie, G. J., Ferguson, C., Parton, R. G., Wolvetang, E. J., Roost, M. S., Chuva de Sousa Lopes, S. M., & Little, M. H. (2015). Kidney organoids from human iPS cells contain multiple lineages and model human nephrogenesis. *Nature*, *526*(7574), 564–568. https://doi.org/10.1038/nature15695

Takayama, K., Akita, N., Mimura, N., Akahira, R., Taniguchi, Y., Ikeda, M., Sakurai, F., Ohara, O., Morio, T., Sekiguchi, K., & Mizuguchi, H. (2017). Generation of safe and therapeutically effective human induced pluripotent stem cell-derived hepatocyte-like cells for regenerative medicine. *Hepatology Communications*, *1*(10), 1058–1069. https://doi.org/10.1002/hep4.1111

Takebe, T., Sekine, K., Enomura, M., Koike, H., Kimura, M., Ogaeri, T., Zhang, R. R., Ueno, Y., Zheng, Y. W., Koike, N., Aoyama, S., Adachi, Y., & Taniguchi, H. (2013a). Vascularized and functional human liver from an iPSC-derived organ bud transplant. *Nature*, *499*(7459), 481–484. https://doi.org/10.1038/nature12271

Takebe, T., Sekine, K., Enomura, M., Koike, H., Kimura, M., Ogaeri, T., Zhang, R.-R., Ueno, Y., Zheng, Y.-W., Koike, N., Aoyama, S., Adachi, Y., & Taniguchi, H. (2013b). Takebe, T., Sekine, K., Enomura, M., Koike, H., Kimura, M., Ogaeri, T., Zhang, R.-R., Ueno, Y., Zheng, Y.-W., Koike, N.,

Aoyama, S., Adachi, Y., Taniguchi, H., 2013. Vascularized and functional human liver from an iPSC-derived organ bud transplant. Nature. *Nature*, *499*(7459), 481–484. https://doi.org/10.1038/nature12271

Takebe, T., Sekine, K., Kimura, M., Yoshizawa, E., Ayano, S., Koido, M., Funayama, S., Nakanishi, N., Hisai, T., Kobayashi, T., Kasai, T., Kitada, R., Mori, A., Ayabe, H., Ejiri, Y., Amimoto, N., Yamazaki, Y., Ogawa, S., Ishikawa, M., … Taniguchi, H. (2017a). Massive and Reproducible Production of Liver Buds Entirely from Human Pluripotent Stem Cells. *Cell Reports*, *21*(10), 2661–2670. https://doi.org/10.1016/j.celrep.2017.11.005

Takebe, T., Sekine, K., Kimura, M., Yoshizawa, E., Ayano, S., Koido, M., Funayama, S., Nakanishi, N., Hisai, T., Kobayashi, T., Kasai, T., Kitada, R., Mori, A., Ayabe, H., Ejiri, Y., Amimoto, N., Yamazaki, Y., Ogawa, S., Ishikawa, M., … Taniguchi, H. (2017b). Massive and Reproducible Production of Liver Buds Entirely from Human Pluripotent Stem Cells. *Cell Reports*, *21*(10), 2661–2670. https://doi.org/10.1016/j.celrep.2017.11.005

Tang, F., Barbacioru, C., Wang, Y., Nordman, E., Lee, C., Xu, N., Wang, X., Bodeau, J., Tuch, B. B., Siddiqui, A., Lao, K., & Surani, M. A. (2009). mRNA-Seq whole-transcriptome analysis of a single cell. *Nature Methods*, *6*(5), 377–382. https://doi.org/10.1038/nmeth.1315

Tasnim, F., Xing, J., Huang, X., Mo, S., Wei, X., Tan, M. H., & Yu, H. (2019). Generation of mature kupffer cells from human induced pluripotent stem cells. *Biomaterials*, *192*(November 2018), 377–391. https://doi.org/10.1016/j.biomaterials.2018.11.016

Tatsumi, N., Miki, R., Katsu, K., & Yokouchi, Y. (2007). Neurturin-GFRα2 signaling controls liver bud migration along the ductus venosus in the chick embryo. *Developmental Biology*, *307*(1), 14–28. https://doi.org/10.1016/j.ydbio.2007.03.519

Tesar, P. J., Chenoweth, J. G., Brook, F. a, Davies, T. J., Evans, E. P., Mack, D. L., Gardner, R. L., & McKay, R. D. (2007). New cell lines from mouse epiblast share defining features with human embryonic stem cells. *Nature*, *448*(7150), 196–199. https://doi.org/10.1038/nature05972

Tewary, M., Shakiba, N., & Zandstra, P. W. (2018). Stem cell bioengineering: building from stem cell biology. *Nature Reviews Genetics*, *19*(10), 595–614. https://doi.org/10.1038/s41576-018-0040-z

Thompson, P. (1908). A Note on the Development of the Septum Transversum and the Liver. *Journal of Anatomy and Physiology*, *42*(Pt 2), 170–175. http://www.ncbi.nlm.nih.gov/pubmed/17232762

Thomson, J. A. (1998). Embryonic Stem Cell Lines Derived from Human Blastocysts. *Science*, *282*(5391), 1145–1147. https://doi.org/10.1126/science.282.5391.1145

Tolosa, L., Caron, J., Hannoun, Z., Antoni, M., López, S., Burks, D., Castell, J. V., Weber, A., Gomez-Lechon, M. J., & Dubart-Kupperschmitt, A. (2015). Transplantation of hESC-derived hepatocytes protects mice from liver injury. *Stem Cell Research and Therapy*, *6*(1), 1–17. https://doi.org/10.1186/s13287-015-0227-6

Touboul, T., Hannan, N. R. F., Corbineau, S., Martinez, A., Martinet, C., Branchereau, S., Mainot, S., Strick-Marchand, H., Pedersen, R., Santo, J. Di, Weber, A., & Vallier, L. (2010). Generation of functional hepatocytes from human embryonic stem cells under chemically defined conditions that recapitulate liver development. In *Hepatology* (Vol. 51, Issue 5, pp. 1754–1765). https://doi.org/10.1002/hep.23506

Tremblay, K. D., & Zaret, K. S. (2005). Distinct populations of endoderm cells converge to generate the embryonic liver bud and ventral foregut tissues. *Developmental Biology*, *280*(1), 87–99. https://doi.org/10.1016/j.ydbio.2005.01.003

Tsuchida, T., & Friedman, S. L. (2017). Mechanisms of hepatic stellate cell activation. *Nature Reviews Gastroenterology and Hepatology*, *14*(7), 397–411. https://doi.org/10.1038/nrgastro.2017.38

Tumarkin, E., Tzadu, L., Csaszar, E., Seo, M., Zhang, H., Lee, A., Peerani, R., Purpura, K., Zandstra, P. W., & Kumacheva, E. (2011). High-throughput combinatorial cell co-culture using microfluidics. *Integrative Biology*, *3*(6), 653–662. https://doi.org/10.1039/c1ib00002k

Vincent, S. D., Dunn, N. R., Hayashi, S., Norris, D. P., & Robertson, E. J. (2003). Cell fate decisions within the mouse organizer are governed by graded Nodal signals. *Genes and Development*, *17*(13), 1646–1662. https://doi.org/10.1101/gad.1100503

Vining, K. H., & Mooney, D. J. (2017). Mechanical forces direct stem cell behaviour in development and regeneration. *Nature Reviews Molecular Cell Biology*, *18*(12), 728–742. https://doi.org/10.1038/nrm.2017.108

Viotti, M., Nowotschin, S., & Hadjantonakis, A. K. (2014). SOX17 links gut endoderm morphogenesis and germ layer segregation. *Nature Cell Biology*, *16*(12), 1146–1156. https://doi.org/10.1038/ncb3070

Vosough, M., Omidinia, E., Kadivar, M., Shokrgozar, M. A., Pournasr, B., Aghdami, N., & Baharvand, H. (2013). Generation of functional hepatocyte-like cells from human pluripotent stem cells in a scalable suspension culture. *Stem Cells and Development*, *22*(20), 2693–2705. https://doi.org/10.1089/scd.2013.0088

Waddington, C. H. (1957). *The Strategy of the Genes* (1st Editio). London : Allen & Unwin.

Wang, S., Wang, X., Tan, Z., Su, Y., Liu, J., Chang, M., Yan, F., Chen, J., Chen, T., Li, C., Hu, J., & Wang, Y. (2019). Human ESC-derived expandable hepatic organoids enable therapeutic liver repopulation and pathophysiological modeling of alcoholic liver injury. *Cell Research*, *29*(12), 1009–1026. https://doi.org/10.1038/s41422-019-0242-8

Wang, Y., Gunasekara, D. B., Reed, M. I., DiSalvo, M., Bultman, S. J., Sims, C. E., Magness, S. T., & Allbritton, N. L. (2017). A microengineered collagen scaffold for generating a polarized crypt-villus architecture of human small intestinal epithelium. *Biomaterials*, *128*, 44–55. https://doi.org/10.1016/j.biomaterials.2017.03.005

Wang, Y., Kim, R., Gunasekara, D. B., Reed, M. I., DiSalvo, M., Nguyen, D. L., Bultman, S. J., Sims, C. E., Magness, S. T., & Allbritton, N. L. (2018). Formation of Human Colonic Crypt Array by Application of Chemical Gradients Across a Shaped Epithelial Monolayer. *Cellular and Molecular Gastroenterology and Hepatology*, *5*(2), 113–130. https://doi.org/10.1016/j.jcmgh.2017.10.007

Wang, Y., Wang, H., Deng, P., Chen, W., Guo, Y., Tao, T., & Qin, J. (2018). In situ differentiation and generation of functional liver organoids from human iPSCs in a 3D perfusable chip system. *Lab on a Chip*, *18*(23), 3606–3616. https://doi.org/10.1039/c8lc00869h

Ware, B. R., Berger, D. R., & Khetani, S. R. (2015). Prediction of drug-induced liver injury in micropatterned co-cultures containing iPSC-derived human hepatocytes. *Toxicological Sciences*, *145*(2), 252–262. https://doi.org/10.1093/toxsci/kfv048

Weinberger, L., Ayyash, M., Novershtern, N., & Hanna, J. H. (2016). Dynamic stem cell states: naive to primed pluripotency in rodents and humans. *Nature Reviews Molecular Cell Biology*, *17*(3), 155–169. https://doi.org/10.1038/nrm.2015.28

Weissman, I. L. (2000). Stem cells: units of development, units of regeneration, and units in evolution. *Cell*, *100*(1), 157–168. https://doi.org/http://dx.doi.org/10.1016/S0092-8674(00)81692-X

Williams, I. M., & Wu, J. C. (2019). Generation of Endothelial Cells From Human Pluripotent Stem Cells. *Arteriosclerosis, Thrombosis, and Vascular Biology*, *39*(7), 1317–1329. https://doi.org/10.1161/ATVBAHA.119.312265

Wu, F., Wu, D., Ren, Y., Huang, Y., Feng, B., Zhao, N., Zhang, T., Chen, X., Chen, S., & Xu, A. (2019). Generation of hepatobiliary organoids from human induced pluripotent stem cells. *Journal of Hepatology*, *70*(6), 1145–1158. https://doi.org/10.1016/j.jhep.2018.12.028

Wu, J., & Izpisua Belmonte, J. C. (2016). Stem Cells: A Renaissance in Human Biology Research. *Cell*, *165*(7), 1572–1585. https://doi.org/10.1016/j.cell.2016.05.043

Wu, J., Yamauchi, T., & Izpisua Belmonte, J. C. (2016). An overview of mammalian pluripotency. *Development (Cambridge, England)*, *143*(10), 1644–1648. https://doi.org/10.1242/dev.132928

Xu, M., He, J., Zhang, C., Xu, J., & Wang, Y. (2019). Strategies for derivation of endothelial lineages from human stem cells. *Stem Cell Research and Therapy*, *10*(1), 1–14. https://doi.org/10.1186/s13287-019-1274-1

Yamanaka, Y., Lanner, F., & Rossant, J. (2010). FGF signal-dependent segregation of primitive endoderm and epiblast in the mouse blastocyst. *Development*, *137*(5), 715–724. https://doi.org/10.1242/dev.043471

Yamashita, T., Takayama, K., Sakurai, F., & Mizuguchi, H. (2018). Billion-scale production of hepatocyte-like cells from human induced pluripotent stem cells. *Biochemical and Biophysical Research Communications*, *496*(4), 1269–1275. https://doi.org/10.1016/j.bbrc.2018.01.186

Yin, X., Mead, B. E., Safaee, H., Langer, R., Karp, J. M., & Levy, O. (2016a). Engineering Stem Cell Organoids. *Cell Stem Cell*, *18*(1), 25–38. https://doi.org/10.1016/j.stem.2015.12.005

Yin, X., Mead, B. E., Safaee, H., Langer, R., Karp, J. M., & Levy, O. (2016b). Engineering Stem Cell Organoids. *Cell Stem Cell*, *18*(1), 25–38. https://doi.org/10.1016/j.stem.2015.12.005

Yu, J., Vodyanik, M., Smuga-Otto, K., Antosiewicz-Bourget, J., Frane, J., Tian, S., Nie, J., Jonsdottir, G., Ruotti, V., Stewart, R., Slukvin, I., & Thomson, J. (2007). Induced Pluripotent Stem Cell Lines Derived from Human Somatic Cells. *Science*, *318*(5858), 1917–1920. https://doi.org/10.1126/science.1151526

Yuan, G.-C., Cai, L., Elowitz, M., Enver, T., Fan, G., Guo, G., Irizarry, R., Kharchenko, P., Kim, J., Orkin, S., Quackenbush, J., Saadatpour, A., Schroeder, T., Shivdasani, R., & Tirosh, I. (2017). Challenges and emerging directions in single-cell analysis. *Genome Biology*, *18*(1), 84. https://doi.org/10.1186/s13059-017-1218-y

Zhang, B., Korolj, A., Lai, B. F. L., & Radisic, M. (2018a). Advances in organ-on-a-chip engineering. *Nature Reviews Materials*, *3*(8), 257–278. https://doi.org/10.1038/s41578-018-0034-7

Zhang, B., Korolj, A., Lai, B. F. L., & Radisic, M. (2018b). Advances in organ-on-a-chip engineering. *Nature Reviews Materials*, *3*(8), 257–278. https://doi.org/10.1038/s41578-018-0034-7

Zhang, L., Chen, K., Zhang, H., Pang, B., Choi, C.-H., Mao, A. S., Liao, H., Utech, S., Mooney, D. J., Wang, H., & Weitz, D. A. (2018). Microfluidic Templated Multicompartment Microgels for 3D Encapsulation and Pairing of Single Cells. *Small (Weinheim an Der Bergstrasse, Germany)*, *14*(9), 1–8. https://doi.org/10.1002/smll.201702955

Zhao, D., Chen, S., Cai, J., Guo, Y., Song, Z., Che, J., Liu, C., Wu, C., Ding, M., & Deng, H. (2009). Derivation and characterization of hepatic progenitor cells from human embryonic stem cells. *PLoS ONE*, *4*(7). https://doi.org/10.1371/journal.pone.0006468

2

HEPATIC DIFFERENTIATION

ABSTRACT

Optimizing the differentiation of hiPSCs into hepatocytes is crucial for advancing *in vitro* liver models. This study focused on refining differentiation protocols and integrating transcriptomic analysis to uncover novel regulatory genes. By combining Activin A with Wnt signaling activators, pluripotency markers were successfully downregulated, and definitive endoderm markers such as SOX17 were upregulated. Further differentiation yielded hepatocyte-like cells expressing key markers including HNF4a, AFP, ALB, and AAT. In addition, the impact of cell seeding procedures and adhesion substrates on cell survival during DE specification was investigated. Lastly, transcriptomic analysis at various differentiation stages identified novel putative regulators of endoderm specification, clustering genes based on their expression profiles. This analysis validated the differentiation protocol and revealed key insights into the gene networks driving hepatic lineage commitment. These findings not only enhance our understanding of liver development but also pave the way for improving hiPSC differentiation protocols, contributing to both basic research and potential therapeutic applications.

INTRODUCTION

The optimization of differentiation protocols of hiPSCs, particularly for generating hepatic lineages, holds significant promise for both fundamental research and therapeutic applications. These optimizations allow researchers to uncover the precise combinations and timings of signaling pathways to specify cell fate, since this level of detail is difficult to achieve *in vivo* due to the complexity and dynamic nature of the embryonic environment. By manipulating the differentiation process in a controlled *in vitro* setting, scientists can systematically explore how different pathways influence hepatic specification. For instance, studies have shown that the sequential activation and inhibition of pathways such as Wnt, BMP, and FGF are crucial for the proper differentiation of hiPSCs into hepatocytes (Hannan et al., 2013; Si-Tayeb et al., 2010).

Optimizing the differentiation protocols involves fine-tuning several key factors, including the morphogens used, their sequence and timing, concentrations, cell matrix, cell density, and pre-differentiation steps. All these factors can significantly affect the outcome of hiPSC differentiation. For instance, the early induction of definitive endoderm from hiPSCs typically requires the use of activin A, followed by factors such as BMP4 and FGF2 to promote hepatic specification (Cai et al., 2007). The ECM also plays a critical role in cell differentiation by providing structural support and influencing cell behavior through biochemical and mechanical cues. It is particularly known that optimizing the ECM composition can enhance the efficiency and fidelity of hepatic differentiation (Farhan et al., 2023). Similarly, the density of the cells during differentiation can affect cell-cell interactions and the availability of soluble factors, further impacting the differentiation outcome.

Moreover, transcriptomics has proved to be a crucial tool in understanding the gene networks underlying differentiation of hiPSCs. By analyzing the changes in gene expression during differentiation, researchers can identify novel putative regulators of hepatic specification. This information can be used to refine differentiation protocols, improving their efficiency and fidelity. For example, single-cell RNA sequencing has revealed heterogeneity within differentiating populations and identified key TFs involved in hepatic lineage commitment (Camp et al., 2017). These insights can lead to the development of more precise and effective protocols for generating hepatocytes from hiPSCs, advancing both our understanding of liver development and our ability to model liver diseases *in vitro*.

In this chapter, the complex but essential task of optimizing hepatic differentiation using hiPSCs is explored. The process follows a stepwise approach, beginning with the optimization of endoderm differentiation by testing several media and morphogen combinations. Subsequently, pre-differentiation settings such as cell matrix, cell density, and cell seeding methods are also refined, leading to a process of differentiation of hiPSCs into hepatocytes. Finally, a transcriptomic analysis is conducted to deepen the understanding of the gene networks involved in endoderm specification, identifying novel regulators that can be targeted to improve differentiation protocols in the future. This integrated approach holds significant potential for advancing hepatic differentiation.

METHODOLOGY

Maintenance of hiPSCs

In this work, experiments were performed using the hiPSC line iPS-DF6-9-9T.B, provided by WiCell Bank (Wisconsin, USA). This cell line was reprogramed from foreskin fibroblasts with a karyotype 46, XY that were collected from healthy donors using defined factors in the Laboratory of Dr. James Thomson, at University of Wisconsin. For hiPSC culture, mTeSR™1 (STEMCELL Technologies™, #85850) supplemented 1:200 (v/v) with penicillin/ streptomycin (Gibco™, #15140122) was used as culture medium in six-well plates coated with Matrigel® Growth Factor Reduced Matrix (Corning®, #354230). Culture medium was changed daily. Cell passaging was performed every three to four days when reaching a confluency ~70% using 0.5 mM EDTA (Invitrogen™, #15575020).

Pre-differentiation of hiPSCs in adherent culture

After hiPSC expansion, cells were dissociated using Accutase® solution (Sigma-Aldrich®, #A6964) for 7 min at 37°C or 0.5 mM EDTA solution (Invitrogen™, #15575020) for 5 min at room temperature (RT). Cells were seeded onto 12-well culture plates coated with Matrigel® Growth Factor Reduced Matrix (Corning®, #354230) or iMatrix-511 (Nippi/ Matrixome®, #NP892-011) at a cell density of $4x10^5$ cells/ well. mTeSR™1 (STEMCELL Technologies™, #85850) supplemented 1:200 (v/v) with penicillin/ streptomycin (Gibco™, #15140122) was used as culture medium, changed daily until a confluence of 90-95% was achieved. When Accutase® was used, culture medium was additionally supplemented 1:1000 (v/v) with Rho kinase inhibitor (ROCKi) Y-27632 (STEMCELL Technologies™, #72304) in the first 24 h.

Definitive endoderm differentiation in adherent culture

For hiPSC differentiation into definitive endoderm, Roswell Park Memorial Institute (RPMI) 1640 medium (Gibco™, #21875034) was used as basal medium. RPMI was supplemented with 1% (v/v) B-27™ minus insulin (Gibco™, #A1895601) and supplemented 1:200 (v/v) with penicillin/ streptomycin (Gibco™, #15140122). At day 0 (D0) of differentiation, basal medium was supplemented with 100 ng/mL of Activin A (PeproTech, #120-14P), 1 mM of sodium butyrate (NaB, Sigma-Aldrich®, #B5887) and 50 ng/mL of Wnt3a (R&D Systems™, #5036-WN) or 2 μM of CHIR99021 (CHIR, Stemgent™, #04-0004). At day 1 and 2, basal medium was again supplemented with 100 ng/mL of Activin A with or without 250 nM of LDN-193189 (StemMACS™, #130-103-925).

Hepatocyte differentiation in adherent culture

After hiPSC differentiation into definitive endoderm, cells continued to be cultured in RPMI 1640 medium supplemented with 1% (v/v) B-27™ minus insulin and 1:200 (v/v) with penicillin/ streptomycin, from D3 to D5 of differentiation. At D3, for hepatic induction, medium was additionally supplemented with 10 ng/mL of FGF2 (PeproTech, #100-18B) and 20 ng/mL of BMP4 (PeproTech, #120-05ET). From D6 to

D20, cells were refreshed every three days with hepatocyte culture medium (HCM) BulletKit™ (Lonza, #CC-3198) without the addition of human epidermal growth factor (hEGF). Medium was supplemented with 10 ng/mL of oncostatin M (OSM, R&D Systems™, #295-OM), 0.1 μM of dexametasone (Dex, Sigma-Aldrich®, #D4902) and 20 ng/mL of hepatic growth factor (HGF, Sigma-Aldrich®, #H1404). Working volume throughout differentiation was 1 mL per well.

Flow cytometry of intracellular markers

For sample collection at selected time points, culture medium was removed, and cells were washed with PBS followed by incubation with 0.25% (v/v) trypsin-EDTA (Gibco™, #R001100) in PBS at 37ºC for 7 min. Culture medium was added to inactivate enzymatic digestion and cells were homogenized and centrifuged at 200 xg for 3 min. The cell pellet was washed with PBS and centrifuged again at 200 xg for 3 min. After removing the PBS, cell pellet was fixed by incubation in 2% (v/v) paraformaldehyde (PFA) reagent (Sigma-Aldrich®) in PBS for 20 minutes at RT and stored at 4ºC until flow cytometry analysis. Fixed samples were centrifuged at 200 xg for 3 min. Cell pellet was resuspended and incubated in 90% (v/v) cold methanol in water at 4ºC for 15 min. Cells were then washed 3x with flow cytometry buffer 1 (FB1), constituted by 0.5% (v/v) bovine serum albumin (BSA) solution (Sigma-Aldrich®) in PBS, and centrifuged at 200 xg for 3 min, each time. Cell pellet was resuspended and incubated in primary antibody diluted in FB2, constituted by 0.1% (v/v) Triton X-100 (Sigma-Aldrich®) in FB1, at room temperature for 1 h. After incubation, cells were washed with FB2 and cell pellet was resuspended and incubated in the secondary antibody diluted in FB2, at room temperature for 30 min in the dark. Cells were washed twice with FB2 and centrifuged at 200 xg for 3 min, each time. Cell pellet were resuspended in FB1 for a final volume of 300 μL/FACS tube. Flow cytometry was performed using a FACSCalibur™ flow cytometer (Becton Dickinson) and data analysis using Flowing Software 2.0.

Immunocytochemestry of adherent culture

For sample preparation, after culture medium removal, cells were washed with PBS and then fixed in 4% (v/v) PFA (Sigma-Aldrich®) in PBS at 4ºC for 20 min. After PFA removal, cells were stored in PBS at 4ºC until further analysis. For cell staining, samples were incubated in 0.1 M glycine (Merck Millipore) for 10 min at RT to remove PFA residues, permeabilized with 0.1% (v/v) Triton X-100 (Sigma-Aldrich®) in PBS, at room temperature for 10 min and blocked with 10% (v/v) fetal goat serum (FGS, Gibco™) in TBST (20 mM Tris-HCl pH 8.0, 150 mM NaCl and 0.05% (v/v) Tween-20 (Sigma-Aldrich®) in PBS, at RT for 30 min. Cells were incubated in primary antibody diluted in blocking solution at 4ºC overnight followed by incubation with secondary antibody at RT for 30 min. Nuclear counterstaining was performed using 0.15% (v/v) 4',6-diamidino-2-phenylindole (DAPI) dye (Sigma-Aldrich®) in PBS, at RT for 5 min. Images were acquired with a LSM 710 Confocal Laser Point-Scanning Microscope (Zeiss) and data analysis was performed using ZEN Imaging Software (Zeiss) and ImageJ Software.

Quantitative real time (qRT)-PCR

For sample collection at selected time points, culture medium was removed, and cells were washed with PBS. Then cells were incubated with Accutase® solution (Sigma-Aldrich®, #A6964) in the case of hiPSCs or 0.25% (v/v) trypsin-EDTA (Gibco™, #R001100) in PBS for differentiated cells, both at 37ºC for 7 min. Culture medium was added to inactivate enzymatic digestion and cells were homogenized and centrifuged at 200 xg for 3 min. The cell pellet was washed with PBS and centrifuged again at 200 xg for 3 min. After removing the PBS, cell pellet was stored at -80ºC until further analysis. Total RNA was extracted from samples using the High Pure RNA Isolation Kit (Roche, #11828665001) following the provided instructions. RNA was quantified using a nanodrop and 1 μg of RNA was converted into cDNA with the High Capacity cDNA Reverse Transcription Kit (Applied Biosystems™, #4368814) also following the provided instructions. PCR reactions were run using SYBR Green Master Mix (Nzytech, #MB22303). Reactions were run in triplicate using ViiA™ 7 Real-Time PCR Systems (Applied Biosystems™) and data were analyzed using QuantStudio™ Real-Time PCR Software (Applied Biosystems™). The analysis was performed using the ΔΔCt method and values were normalized against the expression of the housekeeping gene glyceraldehyde-3-phosphate dehydrogenase (GAPDH).

Table 2.1. List of antibodies used in flow cytometry (FC) and immunocytochemistry (ICC).

Target	Brand	Reference	Host Specie	Isotype	Dilution
SOX17	Abcam	ab84990	Mouse	IgG1	1:100 (ICC), 1:500 (FC)
TBX3	Abcam	ab99302	Rabbit	IgG	1:100 (ICC)
AFP	Sigma-Aldrich	A8452	Mouse	IgG2a	1:500 (ICC)
ALB	Sigma-Aldrich	A6684	Mouse	IgG2a	1:500 (ICC)

Table 2.2. List of primers used in qRT-PCR analysis.

Gene	Primer (5´>3´)
GAPDH	FW: GAGTCAACGGATTTGGTCGT
	RV: TTGATTTTGGAGGGATCTCG
OCT4	FW: GAGAACCGAGTGAGAGGCAACC
	RV: CATAGTCGCTGCTTGATCGCTTG
T	FW: CTATTCTGACAACTCACCTGCAT
	RV: ACAGGCTGGGGTACTGACT
CER1	FW: TTCTCAGGGGGTCATCTTGC
	RV: ATGAACAGACCCGCATTTCC
FOXA2	FW: GGGAGCGGTGAAGATGGA
	RV: TCATGTTGCTCACGGAGGAGTA
SOX17	FW: CTCCGGTGTGAATCTCCCC
	RV: CACGTCAGGATAGTTGCAGTAAT
CXCR4	FW: CACCGCATCTGGAGAACCA
	RV: GCCCATTTCCTCGGTGTAGTT

RNA sequencing and transcriptomic analysis

Samples from different stages of differentiation were collected as described for qRT-PCR. Total RNA was extracted using the High Pure RNA Isolation Kit (Roche, #11828665001) following the provided instructions. RNA sequencing (RNA-seq) was performed using QuantSeq 3' mRNA-Seq Library Prep Kit FWD for Illumina (Lexogen) in a HiSeq™ Sequencing System (Illumina) by the Genomics Unit at Centre for Genomic Regulation (Barcelona, Spain). RNA-seq data analysis was performed using QuantSeq FWD analysis pipeline available on Bluebee® genomics analysis platform (Bluebee Holding BV). For each sample individually, the pipeline includes reads trimming using BBDuk, alignment against genomic sequence using STAR aligner, gene read counting using HTSeq and quality control using RSeQC. Based on these data, QuantSeq performed a transcriptomic analysis using DESeq2 and reported a list of differentially expressed genes (DEG). Transcriptomic results present a p-value according to Wald statistical test. p-values were corrected using the Benjamin-Hochberg method. Genes were considered up or downregulated when a one-fold or greater change was exhibited and whose expression values have statistically significance associated (p-value <0.05).

Gene ontology analysis

Gene ontology (GO) terms were identified using the PANTHER (protein annotation through evolutionary relationship) classification system (version 13.1) (Mi et al., 2013). GO terms were identified by analyzing differentially expressed genes using the following settings: GO Biological Process, test type FISHER, reference list Homo Sapiens and FDR<0.05.

RESULTS AND DISCUSSION

2.1. A dynamic play between TGF-β and Wnt initially establish the PS and DE

In this study, the initial focus was on systematically optimizing the differentiation of hiPSCs into DE with the aim of establishing a reliable and reproducible protocol for deriving hiPSC-derived hepatocytes. For that purpose, two promising protocols were taken into consideration: the one developed by Takebe and his team (Takebe et al., 2017) and the one developed by Loh and Ang team (Ang et al., 2018; Loh et al., 2014). These protocols were chosen due to their successful outcomes. As with the majority of protocols in this domain, the fundamental goal is to differentiate hiPSCs into a mesendodermal stage characteristic of the PS and, subsequently, into DE.

To accomplish these first steps, it essential to activate TGF-β/nodal/activin signaling since it plays a crucial role for mesendoderm induction. Additionally, Wnt signaling can also be activated to synergize with TGF-β signaling, enhancing the efficiency of differentiation. Taking this into account, six protocol combinations were designed (Figure 2.1A) starting with two distinct culture media, RPMI vs CDM2. Two strategies to PS induction were employed: one using CHIR and the other using Wnt3a both in combination with Activin A (denoted as 1 vs 2). Furthermore, for DE commitment, two approaches were tested: one using Activin A alone and the other using Activin A in combination with LDN-193189, a BMP inhibitor (denoted as A vs B). Sodium butyrate (NaB) was also used in this process as it has been proved to favor DE differentiation across the literature (Rambhatla et al., 2003).

To analyze the progression of gene expression throughout the sequential stages of differentiation, a comprehensive qRT-PCR analysis was performed up to day 3 (Figure 2.1B). This analysis focused on key regulatory genes that exhibit temporal expression patterns indicative of successful differentiation. At the beginning of differentiation, following induction with Activin A and Wnt signaling activators such as CHIR or Wnt3a, gene expression analysis demonstrated that the pluripotency gene *OCT4* started to be downregulated. This downregulation marks the initiation of differentiation as cells begin to lose their pluripotent characteristics and restrict their developmental potency. Notably, CHIR99021 and Wnt3a led to the similar outcomes, demonstrating their interchangeable utility in this context.

Simultaneously with the loss of pluripotency, the relative peak in mesendodermal gene expression, assessed by expression of *T* (Brachyury), was clearly perceptible at D1 of differentiation for all the conditions. This peak indicates the successful induction of the PS, one of the critical early steps in this differentiation. At this stage, with continuous addition of Activin A (with or without LDN-193189) cells activated several genes known to be expressed in DE, such as *CER1*, *FOXA2*, *SOX17* and *CXCR4*. The expression of these genes confirms the progression towards an endodermal fate. Additionally, the expression of MESP1, a gene usually associated to early mesoderm derivatives, was analyzed as a negative control to ensure specificity of DE induction. Results indicated that the conditions using LDN-193189 for DE specification at D1 and 2 of differentiation (RPMI-1B, RPMI-2B and CDM2-2B) presented similar or even lower performance when compared to the ones where only Activin A is used for DE commitment. The idea of supplementing the

medium with LDN-193189 is to neutralize endogenous BMP signaling that tend to favor mesodermal fate, but results suggest that inhibiting BMP do not improve DE differentiation. Moreover, both condition using CDM2 medium (CDM2-2A and CDM2-2B) had lower performance concerning the expression of DE genes. This suggests that RPMI medium is more conducive to efficient DE differentiation under the tested conditions.

A

Medium	PS	DE	
	d0 – d1	d1 – d2	d2 – d3
RPMI	1 Act A (100 ng) NaB 1mM Wnt3a (50 ng)	A Act A (100 ng)	A Act A (100 ng)
CDM2	2 Act A (100 ng) NaB 1mM CHIR (2 µM)	B Act A (100 ng) LDN (250 nm)	B Act A (100 ng) LDN (250 nm)

Tested Combinations

RPMI-1A / RPMI-1B / RPMI-2A / RPMI-2B / CDM2-2A / CDM2-2B

B

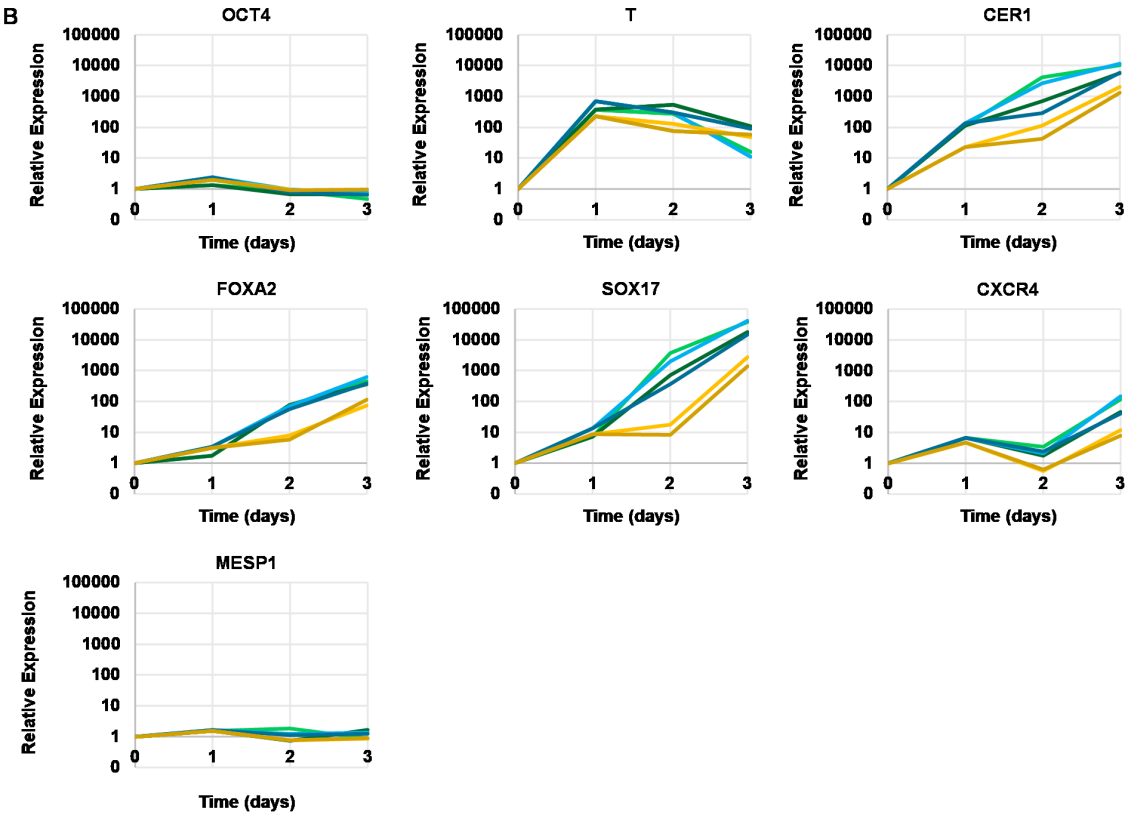

Figure 2.1. Relative expression profiles for pluripotency, PS and DE markers during hiPSCs differentiation. **(A)** Schematic outlining the media and morphogens combinations used to differentiate hiPSCs into definitive endoderm. **(B)** Gene expression was assessed by qRT-PCR at sequential stages for key genes that unveil the progression throughout DE differentiation with *OCT4* (pluripotency), *T* (PS/mesendoderm), *CER1, FOXA2, SOX17, CXCR4* (DE) and *MESP1* (mesoderm). Analysis was performed using the $^{\Delta\Delta}$Ct method with values being presented as relative expression taking day 0 as reference. The values were normalized against the expression of the housekeeping gene *GAPDH*. The Y axis has a $\log_{10}$ scale. n=1 experiment for each time point.

Overall, a dynamic interplay between TGF-β and Wnt signaling, through Activin A and CHIR or Wnt3a, is sufficient and optimal for initially establishing the PS and subsequent DE differentiation. Additionally, this optimized protocol provides a robust foundation for generating hiPSC-derived hepatocytes.

2.2. Cell survival during DE specification is dependent on cell seeding procedure and adhesion substrate

The optimal condition RPMI-1A is based on the methodology developed by Takebe (Kajiwara et al., 2012; Takebe et al., 2017) where hiPSCs are plated with ROCK inhibitor (ROCKi) Y-27632 at a cell density of $0.75x10^5$ cells/cm^2. In this study, various cell densities were tested, including 1.00, 0.75, 0.5 and $0.375x10^5$ cells/cm^2 using Accutase (ACC) as the cell detachment solution for single cell seeding, supplemented with ROCKi for single cell survival (data not shown). Besides that, the cell dissociation agent was also evaluated by comparing the use of ACC + ROCKi and EDTA (Figure 2.2), this last on being an enzyme-free colony seeding method (Beers et al., 2012). For further optimization of both cell seeding procedures, a comparative analysis between two different cell adhesion substrates was conducted (Figure 2.2). The selected substrates were Matrigel® Growth Factor Reduced Matrix, a complex but not defined protein mixture derived from mouse tumour cells (Hughes et al., 2010), and iMatrix 511, a recombinant laminin-511 E8 fragment product.

After culture of hiPSCs onto Matrigel and iMatrix 511 coated 12-well plates, cells were differentiated into DE using the optimized protocol. At D3 of differentiation, it was clear that iMatrix improved cell survival when compared to Matrigel®, particularly for cells treated with EDTA. The fact that EDTA led to higher cell viability shows that preserving the structural integrity of the colonies and consequently, minimizing cell damage and stress, can benefit hiPSC differentiation. On the cell matrix, it is also worth mentioning that iMatrix 511, being a recombinant laminin fragment, provides a more defined and consistent environment compared to the complex protein mixture of Matrigel®, thereby enhancing the reproducibility and efficiency of hiPSC differentiation.

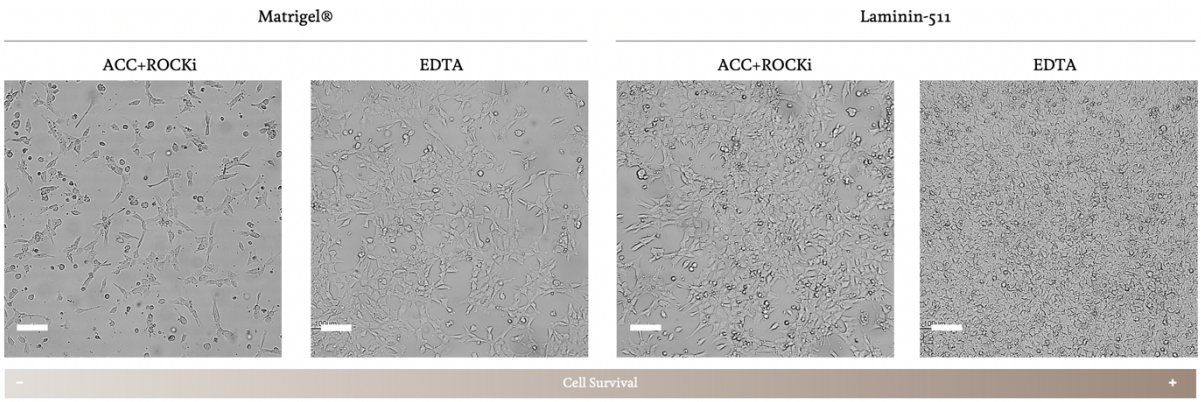

Figure 1.2. Cell seeding procedure and adhesion substrate optimization. (A) Bright-field images of the generated definitive endoderm on day 3 of differentiation using accutase (ACC) plus ROCK inhibitor (ROCKi) Y-27632 for single cell seeding and using EDTA for enzyme-free colony seeding. Both conditions were tested with two different cell adhesion substrates: Matrigel® and iMatrix 511. Scale bars represent 100 μm.

Therefore, the optimized protocol (Figure 2.3) involves colony cell seeding using EDTA in an iMatrix-coated 12-well plate at a cell density of $1x10^5$ cells/cm^2. When cells reach a confluence of 90-95% (normally 3 days after seeding), they are treated with Activin A from D0 to D3, with the adition of CHIR and NaB only on D0. This systematic approach to optimizing each step of the differentiation process highlights the importance of fine-tuning cell culture conditions to achieve the desired outcomes in stem cell research. This is particularly true for DE, as this preliminary stage is crucial for establishing a robust and reliable starting point for subsequent stages of differentiation, ensuring that cells are appropriately primed for further differentiation into hepatocytes.

2.3. Successful differentiation of hiPSCs into hepatocytes using optimized protocol

The optimized protocol for DE differentiation until D3 served as the foundation for developing a comprehensive protocol aimed at differentiating hiPSCs into hepatocytes. On D3, the differentiation protocol incorporated FGF2 and BMP4. These growth factors were selected based on their roles in mimicking the signals from cardiac mesoderm and STM, which are essential for guiding endoderm through the early stages of hepatic differentiation (Calmont et al., 2006; Rossi et al., 2001). The choice of FGF2 and BMP4 is supported by literature, though alternative factors such as FGF4 and BMP2 have also been used successfully in various studies to achieve similar outcomes (Song et al., 2009). From D6 onward, the differentiation protocol introduced a combination of OSM, DEX, and HGF, alongside hepatocyte culture medium. This stage is critical for promoting the maturation and functionality of the developing hepatocyte-like cells.

Throughout the differentiation process, several key markers were analyzed to monitor the progression and success of the protocol from D0 to D20. These markers include SOX17 and FOXA2, which are indicative of DE differentiation; TBX3, an early hepatic marker; and HNF4a, AFP, ALB, and AAT, which are associated with hepatoblasts and hepatocytes. The results of these analyses confirmed the successful differentiation of hiPSCs into hepatocytes, as evidenced by the appropriate expression patterns of these markers at various stages of differentiation. Additionally, to evaluate the efficiency of DE differentiation using the optimized protocol, the presence of SOX17 was assessed by flow cytometry. The results indicated that 74% of the cells expressed SOX17, demonstrating a high efficiency of DE differentiation under the optimized conditions. In addition to flow cytometry, immunofluorescence (ICC) staining was performed to further characterize the composition of the cell culture. This technique provided visual confirmation of the expression of key markers and allowed for the assessment of the morphology of differentiated cells. Markers tested during ICC staining included SOX17, TBX3, AFP, and ALB. The presence of these markers within the adherent monolayer confirmed the successful progression from DE to hepatic progenitors in a later stage to hepatocytes.

Overall, the comprehensive analysis of marker expression throughout the differentiation process underscored the effectiveness of the optimized protocol in guiding hiPSCs through the sequential stages of hepatic differentiation.

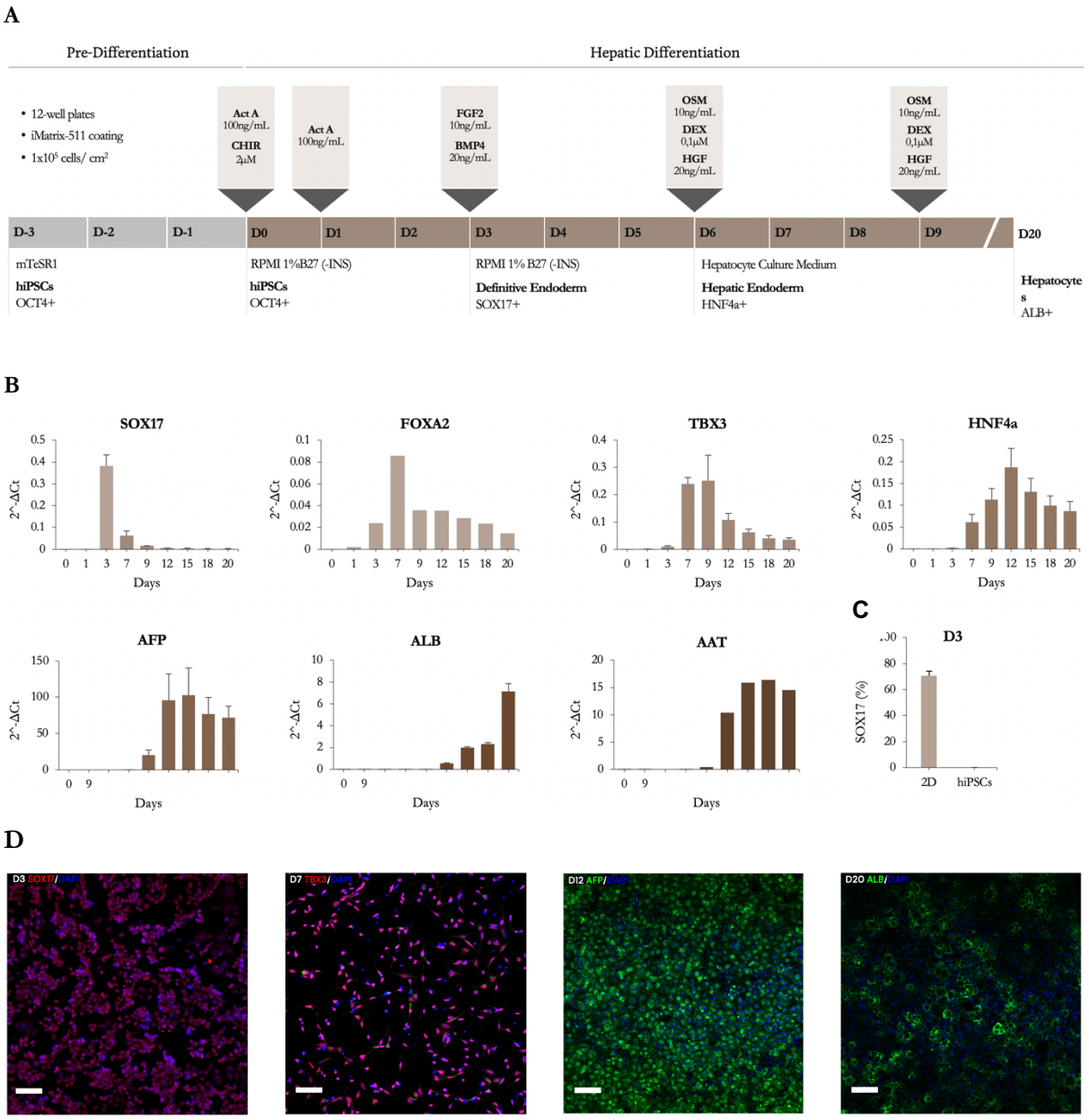

Figure 2.3. Characterization of hepatic differentiation from hiPSCs. (A) Schematic outlining of the procedures used to differentiate hiPSCs into definitive endoderm. **(B)** Gene expression was assessed by qRT-PCR at sequential stages for key genes that unveil the progression throughout hepatic differentiation with *SOX17* and *FOXA2* (definitive endoderm), *TBX3* (hepatic endoderm), *HNF4a* (hepatoblasts), *AFP* (fetal hepatocytes), *ALB* and *AAT* (mature hepatocytes). The analysis was performed using the ΔCt method. The values were normalized against the expression of the housekeeping gene *GAPDH*. n=3 for each time point (except n=1 for *FOXA2* and *AAT).* **(C)** Differentiation efficiency by flow-cytometry analysis for SOX17 on cells differentiated following the optimized protocol on day 3 of differentiation. n=3. **(D)** Immunofluorescent staining for SOX17 in red of differentiated cells on day 3 of differentiation. Nuclei in blue were stained with DAPI. Scale bars represent 50 μm.

2.4. Transcriptomic analysis unveils novel putative regulators of endoderm specification

After refining the differentiation protocol for hepatocytes from hiPSCs, the transcriptional events occurring during hepatic endoderm specification were comprehensively examined. The objective is to identify novel TFs, signaling mediators, surface markers, and metabolites that can be grouped into distinct clusters based on gene expression profiles during hepatic specification. For this analysis, 3 time points were selected: D3, D7, and D9. Four distinct clusters of genes were identified based on their transcriptional profiles throughout differentiation: cluster 1, for genes peeking in expression at D3; cluster 2, for genes that start to be upregulated from D7 onwards; cluster 3, for genes that start to be upregulated at D9; cluster 4, for genes that remain upregulated across all three timepoints. These sets of genes with similar expression profiles over time contain known endodermal and hepatic markers, validating the differentiation protocol and consequently the results extracted from it. Moreover, the data was also validated against a published dataset for hepatic differentiation (Touboul et al., 2016), making the results even more robust and universal, given that all genes mentioned from now on are not protocol-specific but shared by different protocols. A summary of the followed pipeline is depicted on Figure 2.3.

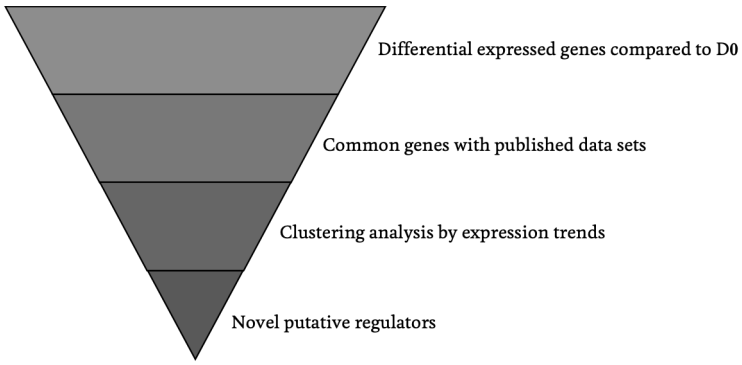

Figure 2.3. Transcriptomic analysis pipeline. This analysis started with identifying differentially expressed genes (DEGs) compared to D0. Common genes were then identified by comparing these DEGs with published datasets. This was followed by clustering analysis to observe expression trends. The final step involved identifying novel putative regulators from the clustered data.

Cluster 1 – Definitive Endoderm

Cluster 1 peaks at D3, with the expression of well-known endoderm/ mesendoderm TFs like *SOX17*, *MIXL1* and *GSC* (Figure 2.4), whose role in endoderm commitment has been known for a long time (Hart et al., 2002; Kanai-Azuma et al., 2002). Besides this, *NODAL* and other members of the TGF-β superfamily also peak at D3. In fact, Nodal signaling pathway plays a pivotal role in PS formation and definitive endoderm specification leading to the expression of key markers like *SOX17* but also *FOXA2* (Conlon et al., 1994; Faial et al., 2015). Corroborating the literature as well, a *CXCR4* (or *CD184*) expression peak was identified at D3, a gene that encodes a cell-surface cytokine receptor highly present in endoderm cells (D'Amour et al., 2005).

Two genes whose expression also peaks at D3 are *LHX1* (or *LIM1*) and *OTX2*. These genes encode TFs that are known to be present in visceral endoderm (Perea-Gómez et al., 1999; Perea-Gomez et al., 2001), but both protocols in analysis are expected to generate definitive endoderm through mesendoderm by using Activin A (Yasunaga et al., 2005). However, in a more recent study it is demonstrated that *EOMES*, acting downstream of Nodal signaling, activates *LHX1* in the epiblast contributing to the definitive endoderm lineage (Costello et al., 2015). Additionally, it is demonstrated that *LHX1* interacts with *OTX2* and *FOXA2* suggesting that this complex may activate gene regulatory networks required in both visceral and definitive endoderm. Thus, the presence of *LHX1* and *OTX2* in cluster 1 may support this idea.

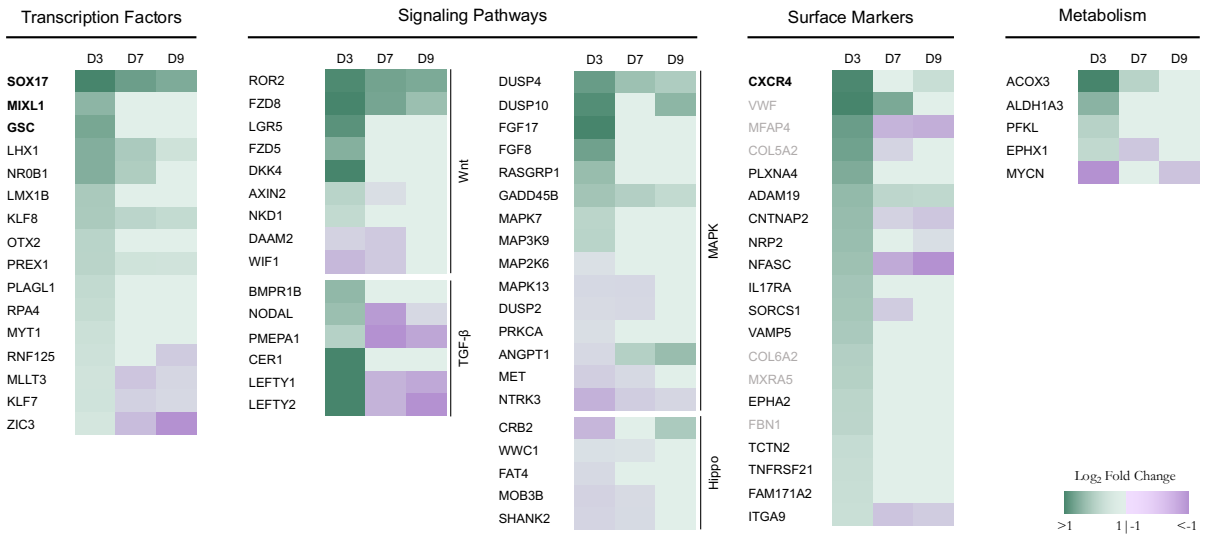

Figure 2.4. Cluster 1 with genes peaking expression at D3. This heat map displays the results for Cluster 1, highlighting genes that show peak expression at D3. Genes are categorized into transcription factors, signaling pathways, surface markers, and metabolism, with log2 fold change values greater than 1 or less than -1 (p-value <0.05).

Nevertheless, other TFs presented the same expression profile constituting novel putative regulators of endoderm specification. Other of these genes in cluster 1 is *PREX1*. In humans, this gene was never associated to endoderm, but in zebrafish *prex1* is a target of Nodal signaling, promoting *rac1* activity and regulating endodermal cell motility at early gastrulation stages (Woo et al., 2012). This *nodal/prex1* activated migration process seems to be required to maintain endoderm identity. The results may suggest that *PREX1* also play an important role in human endoderm commitment. Following the candidates list, zinc finger TFs of the Krüppel-like factors (KLF) family, in particular *KLF8* and *KLF7,* can also be found. In a study performed in frog embryos (Gao et al., 2015), gene expression changes were analyzed after overexpression or knockdown of KLF genes. In embryos with *klf7* knockdown it was possible to observe the downregulation of genes like *t*, *sox17a*, *cer1* and *nodal5*. In the case of *klf8* there was also downregulation of *t*, *sox17a*, *cer1*, *gsc* and *nodal5*. In fact, in embryos injected with *klf7* mRNA, *sox17a* was ectopically activated. This study showed that *klf7* and *klf8* play regulatory roles on endoderm formation, and that *klf8* also has a role in mesoderm specification. This is in agreement with the generated data since *KLF8* is expressed in both clusters from endoderm and mesoderm, but *KLF7* only peak at D3 during endoderm commitment. The

remaining TFs in cluster 1, *LMX1B*, *RPA4*, *MYT1*, *RNF125* and *MLLT3* are not yet described in the literature as regulators of endoderm commitment and they are not expressed in the mesoderm datasets under analysis, being of particular interest in future studies.

Regarding genes related to signaling pathways, *PMEPA1* (or *TMEPAI*, *STAG1*) deserves some attention. This gene encodes a transmembrane protein reported to be implicated in tumorigenesis, but it was also demonstrated in a previous study that PMEPA1 has an essential function in negative regulation of TGF-β signaling (Watanabe et al., 2010). PMEPA1 sequesters SMAD2/3 regulating the duration and intensity of TGF-β responses. Moreover, it was demonstrated that using this mechanism, PMEPA1 can also inhibit Activin signaling in frog embryogenesis perturbing mesoderm induction. It is therefore tempting to speculate that PMEPA1 also acts as a negative regulator of Nodal signaling during definitive endoderm commitment. Actually, other negative regulators of Nodal signaling, in particular nodal antagonists like CER1, LEFTY1 and LEFTY2, have also their gene expression peeking at D3. Their role in anterior visceral endoderm, important to establish the anterior-posterior axis, is related to the proper patterning of PS (Perea-Gomez et al., 2002) but little is known about their role in definitive endoderm. Still, CER1 has been regarded as a marker of definitive endoderm for some time (Iwashita et al., 2013).

Several other genes that encode surface markers were identified in cluster 1 besides *CXCR4*, and some of them have already been vaguely referenced as related to endoderm, like *EPHA2* (Moore-Scott et al., 2007), *CNTNAP* (Cuomo et al., 2020) and *ADAM19* (Scheibner et al., 2021). However, the majority of them have never been reported as related to endoderm and only *IL17RA*, *SORCS1*, *TNFRSF21* and *FAM171A2* are endoderm specific and not shared with mesoderm datasets. Not a membrane protein but an interesting extracellular matrix marker whose gene expression also peaks at D3 is *MFAP4*, which is involved in cell adhesion and intercellular interactions. This gene was also identified in a screening during definitive endoderm differentiation, and their data suggest that *MFAP4* is a direct target of EOMES and Nodal effector proteins SMAD2/3 during definitive endoderm commitment (Ong et al., 2020). In the future, it would be interesting to access in greater detail *MFAP4* role in endoderm commitment.

Lastly, genes involved in metabolic functions in cluster 1 were also investigated (Figure 2.4). During differentiation of hiPSCs into definitive endoderm, cells undergo a metabolic switch from glycolysis to oxidative phosphorylation. Additionally, a recent study shows that this switch coincides with a reduction in MYC/MYCN activity, working as developmental regulators that link metabolism to endoderm commitment (Cliff et al., 2017). In agreement with that, the present analysis revealed a downregulation of *MYCN* at D3. Recent evidence has shown that this metabolic switch is coupled with profound epigenetic changes (Fang & Li, 2022). In the present analysis, the expression levels of *ACOX3*, that encodes an enzyme capable to produce crotonyl-CoA during fatty acid oxidation, are particularly high at D3. This finding is in agreement with a very recent study that shows that crotonyl-CoA-producing enzymes are enriched in endodermal cells, increasing histone crotonylation and promoting endodermal gene expression (Fang et al., 2021). In fact, knocking out *ACOX3* in hESCs impairs *SOX17* gene expression during differentiation and the addition of crotonate, a short-chain fatty acid, increased endoderm differentiation efficiency. Therefore,

it is now known that during metabolic switch the pluripotent stem cells, with high glycolysis-mediated production of acetyl-CoA and histone acetylation, switch to oxidative phosphorylation and histone crotonylation enhancing endodermal differentiation. The obtained results clearly support this idea.

Cluster 2, 3 and 4 are not being analyzed under the scope of this thesis.

CONCLUSION

The optimization of differentiation protocols for hiPSCs uncover the precise combinations and timings of signaling pathways necessary for specifying cell fate, a level of detail that is difficult to achieve *in vivo* due to the complexity and dynamic nature of the embryonic environment. In this study, the stepwise optimization of hepatic differentiation using hiPSCs is thoroughly explored. It begins with the optimization of pre-differentiation settings such as cell matrix, cell density, and seeding methods, followed by refining endoderm differentiation through various media and morphogen combinations. Additionally, the optimized protocol for DE differentiation using TGF-β and Wnt signaling laid a solid foundation for the subsequent differentiation of hiPSCs into hepatocytes. Throughout the differentiation process, the expression of critical hepatic markers including HNF4a, AFP, ALB, and AAT confirmed the successful progression to hepatocyte-like cells. This sequential expression of markers not only validated the differentiation stages but also highlighted the efficiency of the protocol.

The comprehensive transcriptomic analysis conducted at multiple differentiation stages provided deep insights into the transcriptional dynamics behind endoderm specification. Identifying distinct gene clusters that peak at different stages of differentiation unveiled novel putative regulators, signaling mediators, and surface markers essential for hepatic development. This analysis highlighted the temporal expression patterns of key regulatory genes, validating the differentiation protocol and offering a broader understanding of the molecular mechanisms driving endoderm differentiation.

The findings of this study not only underscore the importance of optimizing differentiation protocols for generating hiPSC-derived hepatocytes but also set the stage for future research to refine these protocols further.

REFERENCES

Ang, L. T., Tan, A. K. Y., Autio, M. I., Goh, S. H., Choo, S. H., Lee, K. L., Tan, J., Pan, B., Lee, J. J. H., Lum, J. J., Lim, C. Y. Y., Yeo, I. K. X., Wong, C. J. Y., Liu, M., Oh, J. L. L., Chia, C. P. L., Loh, C. H., Chen, A., Chen, Q., … Lim, B. (2018). A Roadmap for Human Liver Differentiation from Pluripotent Stem Cells. *Cell Reports*, *22*(8), 2190–2205. https://doi.org/10.1016/j.celrep.2018.01.087

Beers, J., Gulbranson, D. R., George, N., Siniscalchi, L. I., Jones, J., Thomson, J. A., & Chen, G. (2012). Passaging and colony expansion of human pluripotent stem cells by enzyme-free dissociation in chemically defined culture conditions. *Nature Protocols*, *7*(11), 2029–2040. https://doi.org/10.1038/nprot.2012.130

Cai, J., Zhao, Y., Liu, Y., Ye, F., Song, Z., Qin, H., Meng, S., Chen, Y., Zhou, R., Song, X., Guo, Y., Ding, M., & Deng, H. (2007). Directed differentiation of human embryonic stem cells into functional hepatic cells. *Hepatology*, *45*(5), 1229–1239. https://doi.org/10.1002/hep.21582

Calmont, A., Wandzioch, E., Tremblay, K. D., Minowada, G., Kaestner, K. H., Martin, G. R., & Zaret, K. S. (2006). An FGF Response Pathway that Mediates Hepatic Gene Induction in Embryonic Endoderm Cells. *Developmental Cell*, *11*(3), 339–348. https://doi.org/10.1016/j.devcel.2006.06.015

Camp, J. G., Sekine, K., Gerber, T., Loeffler-Wirth, H., Binder, H., Gac, M., Kanton, S., Kageyama, J., Damm, G., Seehofer, D., Belicova, L., Bickle, M., Barsacchi, R., Okuda, R., Yoshizawa, E., Kimura, M., Ayabe, H., Taniguchi, H., Takebe, T., & Treutlein, B. (2017). Multilineage communication regulates human liver bud development from pluripotency. *Nature*, *546*(7659), 533–538. https://doi.org/10.1038/nature22796

Cliff, T. S., Wu, T., Boward, B. R., Yin, A., Yin, H., Glushka, J. N., Prestegaard, J. H., & Dalton, S. (2017). MYC Controls Human Pluripotent Stem Cell Fate Decisions through Regulation of Metabolic Flux. *Cell Stem Cell*, *21*(4), 502-516.e9. https://doi.org/10.1016/j.stem.2017.08.018

Conlon, F. L., Lyons, K. M., Takaesu, N., Barth, K. S., Kispert, A., Herrmann, B., & Robertson, E. J. (1994). A primary requirement for nodal in the formation and maintenance of the primitive streak in the mouse. *Development*, *120*(7), 1919–1928. https://doi.org/10.1242/dev.120.7.1919

Costello, I., Nowotschin, S., Sun, X., Mould, A. W., Hadjantonakis, A.-K., Bikoff, E. K., & Robertson, E. J. (2015). *Lhx1 functions together with Otx2, Foxa2, and Ldb1 to govern anterior mesendoderm, node, and midline development*. https://doi.org/10.1101/gad.268979

Cuomo, A. S. E., Seaton, D. D., McCarthy, D. J., Martinez, I., Bonder, M. J., Garcia-Bernardo, J., Amatya, S., Madrigal, P., Isaacson, A., Buettner, F., Knights, A., Natarajan, K. N., Agu, C. A., Alderton, A., Danecek, P., Denton, R., Durbin, R., Gaffney, D. J., Goncalves, A., … Stegle, O. (2020). Single-cell RNA-sequencing of differentiating iPS cells reveals dynamic genetic effects on gene expression. *Nature Communications*, *11*(1). https://doi.org/10.1038/s41467-020-14457-z

D'Amour, K. A., Agulnick, A. D., Eliazer, S., Kelly, O. G., Kroon, E., & Baetge, E. E. (2005). Efficient differentiation of human embryonic stem cells to definitive endoderm. *Nature Biotechnology*, *23*(12), 1534–1541. https://doi.org/10.1038/nbt1163

Faial, T., Bernardo, A. S., Mendjan, S., Diamanti, E., Ortmann, D., Gentsch, G. E., Mascetti, V. L., Trotter, M. W. B., Smith, J. C., & Pedersen, R. A. (2015). Brachyury and SMAD signalling collaboratively orchestrate distinct mesoderm and endoderm gene regulatory networks in differentiating human embryonic stem cells. *Development (Cambridge)*, *142*(12), 2121–2135. https://doi.org/10.1242/dev.117838

Fang, Y., & Li, X. (2022). Metabolic and epigenetic regulation of endoderm differentiation. In *Trends in Cell Biology* (Vol. 32, Issue 2, pp. 151–164). Elsevier Ltd. https://doi.org/10.1016/j.tcb.2021.09.002

Fang, Y., Xu, X., Ding, J., Yang, L., Doan, M. T., Karmaus, P. W. F., Snyder, N. W., Zhao, Y., Li, J. L., & Li, X. (2021). Histone crotonylation promotes mesoendodermal commitment of human embryonic stem cells. *Cell Stem Cell*, *28*(4), 748-763.e7. https://doi.org/10.1016/j.stem.2020.12.009

Farhan, F., Trivedi, M., Di Wu, P., & Cui, W. (2023). Extracellular matrix modulates the spatial hepatic features in hepatocyte-like cells derived from human embryonic stem cells. *Stem Cell Research and Therapy*, *14*(1). https://doi.org/10.1186/s13287-023-03542-x

Gao, Y., Cao, Q., Lu, L., Zhang, X., Zhang, Z., Dong, X., Jia, W., & Cao, Y. (2015). Kruppel-Like Factor Family Genes are Expressed During Xenopus Embryogenesis and Involved in Germ Layer Formation and Body Axis Patterning. *Developmental Dynamics*, *244*, 1328–1346. https://doi.org/10.1002/dvdy

Hannan, N. R. F., Segeritz, C. P., Touboul, T., & Vallier, L. (2013). Production of hepatocyte-like cells from human pluripotent stem cells. *Nature Protocols*, *8*(2), 430–437. https://doi.org/10.1038/nprot.2012.153

Hart, A. H., Hartley, L., Sourris, K., Stadler, E. S., Li, R., Stanley, E. G., Tam, P. P. L., Elefanty, A. G., & Robb, L. (2002). Mixl1 is required for axial mesendoderm morphogenesis and patterning in the murine embryo. *Development*, *129*(15), 3597–3608. https://doi.org/10.1242/dev.129.15.3597

Hughes, C. S., Postovit, L. M., & Lajoie, G. A. (2010). Matrigel: a complex protein mixture required for optimal growth of cell culture. *Proteomics*, *10*(9), 1886–1890. https://doi.org/10.1002/pmic.200900758

Iwashita, H., Shiraki, N., Sakano, D., Ikegami, T., Shiga, M., Kume, K., & Kume, S. (2013). Secreted Cerberus1 as a Marker for Quantification of Definitive Endoderm Differentiation of the Pluripotent Stem Cells. *PLoS ONE*, *8*(5). https://doi.org/10.1371/journal.pone.0064291

Kajiwara, M., Aoi, T., Okita, K., Takahashi, R., Inoue, H., & Takayama, N. (2012). Correction for Kajiwara et al., Donor-dependent variations in hepatic differentiation from human-induced pluripotent stem cells. *Proceedings of the National Academy of Sciences*, *109*(36), 14716–14716. https://doi.org/10.1073/pnas.1212710109

Kanai-Azuma, M., Kanai, Y., Gad, J. M., Tajima, Y., Taya, C., Kurohmaru, M., Sanai, Y., Yonekawa, H., Yazaki, K., Tam, P. P. L., & Hayashi, Y. (2002). Depletion of definitive gut endoderm in Sox17-null mutant mice. *Development*, *129*(10), 2367–2379. https://doi.org/10.1242/dev.129.10.2367

Loh, K. M., Ang, L. T., Zhang, J., Kumar, V., Ang, J., Auyeong, J. Q., Lee, K. L., Choo, S. H., Lim, C. Y. Y., Nichane, M., Tan, J., Noghabi, M. S., Azzola, L., Ng, E. S., Durruthy-Durruthy, J., Sebastiano, V., Poellinger, L., Elefanty, A. G., Stanley, E. G., … Lim, B. (2014). Efficient endoderm induction from human pluripotent stem cells by logically directing signals controlling lineage bifurcations. *Cell Stem Cell*, *14*(2), 237–252. https://doi.org/10.1016/j.stem.2013.12.007

Moore-Scott, B. A., Opoka, R., Lin, S. C. J., Kordich, J. J., & Wells, J. M. (2007). Identification of molecular markers that are expressed in discrete anterior-posterior domains of the endoderm from the gastrula stage to mid-gestation. *Developmental Dynamics*, *236*(7), 1997–2003. https://doi.org/10.1002/dvdy.21204

Ong, S. L. M., de Vos, I. J. H. M., Meroshini, M., Poobalan, Y., & Dunn, N. R. (2020). Microfibril-associated glycoprotein 4 (Mfap4) regulates haematopoiesis in zebrafish. *Scientific Reports*, *10*(1). https://doi.org/10.1038/s41598-020-68792-8

Perea-Gomez, A., Lawson, K. A., Rhinn, M., Zakin, L., Brûlet, P., Mazan, S., & Ang, S.-L. (2001). Otx2 is required for visceral endoderm movement and for the restriction of posterior signals in the epiblast of the mouse embryo. *Development*, *128*(5), 753–765. https://doi.org/10.1242/dev.128.5.753

Perea-Gómez, A., Shawlot, W., Sasaki, H., Behringer, R. R., & Ang, S.-L. (1999). HNF3β and Lim1 interact in the visceral endoderm to regulate primitive streak formation and anterior-posterior polarity in the mouse embryo. *Development*, *126*(20), 4499–4511. https://doi.org/10.1242/dev.126.20.4499

Perea-Gomez, A., Vella, F. D. J., Shawlot, W., Oulad-Abdelghani, M., Chazaud, C., Meno, C., Pfister, V., Chen, L., Robertson, E., Hamada, H., Behringer, R. R., & Ang, S.-L. (2002). Nodal Antagonists in the Anterior Visceral Endoderm Prevent the Formation of Multiple Primitive Streaks coordinates cell movements critical for the establish. In *Developmental Cell* (Vol. 3).

Rambhatla, L., Chiu, C.-P., Kundu, P., Peng, Y., & Carpenter, M. K. (2003). Generation of Hepatocyte-Like Cells From Human Embryonic Stem Cells. In *Cell Transplantation* (Vol. 12). www.cognizantcommunication.com

Rossi, J. M., Dunn, N. R., Hogan, B. L. M., & Zaret, K. S. (2001). Distinct mesodermal signals, including BMPs from the septum, transversum mesenchyme, are required in combination for hepatogenesis from the endoderm. *Genes and Development*, *15*(15), 1998–2009. https://doi.org/10.1101/gad.904601

Scheibner, K., Schirge, S., Burtscher, I., Büttner, M., Sterr, M., Yang, D., Böttcher, A., Ansarullah, Irmler, M., Beckers, J., Cernilogar, F. M., Schotta, G., Theis, F. J., & Lickert, H. (2021). Epithelial cell plasticity drives endoderm formation during gastrulation. *Nature Cell Biology*, *23*(7), 692–703. https://doi.org/10.1038/s41556-021-00694-x

Si-Tayeb, K., Noto, F. K., Nagaoka, M., Li, J., Battle, M. A., Duris, C., North, P. E., Dalton, S., & Duncan, S. A. (2010). Highly efficient generation of human hepatocyte-like cells from induced pluripotent stem cells. *Hepatology*, *51*(1), 297–305. https://doi.org/10.1002/hep.23354

Song, Z., Cai, J., Liu, Y., Zhao, D., Yong, J., Duo, S., Song, X., Guo, Y., Zhao, Y., Qin, H., Yin, X., Wu, C., Che, J., Lu, S., Ding, M., & Deng, H. (2009). Efficient generation of hepatocyte-like cells from human induced pluripotent stem cells. *Cell Research*, *19*(11), 1233–1242. https://doi.org/10.1038/cr.2009.107

Takebe, T., Sekine, K., Kimura, M., Yoshizawa, E., Ayano, S., Koido, M., Funayama, S., Nakanishi, N., Hisai, T., Kobayashi, T., Kasai, T., Kitada, R., Mori, A., Ayabe, H., Ejiri, Y., Amimoto, N., Yamazaki, Y., Ogawa, S., Ishikawa, M., … Taniguchi, H. (2017). Massive and Reproducible Production of Liver Buds Entirely from Human Pluripotent Stem Cells. *Cell Reports*, *21*(10), 2661–2670. https://doi.org/10.1016/j.celrep.2017.11.005

Touboul, T., Chen, S., To, C. C., Mora-Castilla, S., Sabatini, K., Tukey, R. H., & Laurent, L. C. (2016). Stage-specific regulation of the WNT/β-catenin pathway enhances differentiation of hESCs into hepatocytes. *Journal of Hepatology*, *64*(6), 1315–1326. https://doi.org/10.1016/j.jhep.2016.02.028

Watanabe, Y., Itoh, S., Goto, T., Ohnishi, E., Inamitsu, M., Itoh, F., Satoh, K., Wiercinska, E., Yang, W., Shi, L., Tanaka, A., Nakano, N., Mommaas, A. M., Shibuya, H., ten Dijke, P., & Kato, M. (2010). TMEPAI, a Transmembrane TGF-β-Inducible Protein, Sequesters Smad Proteins from Active Participation in TGF-β Signaling. *Molecular Cell*, *37*(1), 123–134. https://doi.org/10.1016/j.molcel.2009.10.028

Woo, S., Housley, M. P., Weiner, O. D., & Stainier, D. Y. R. (2012). Nodal signaling regulates endodermal cell motility and actin dynamics via Rac1 and Prex1. *Journal of Cell Biology*, *198*(5), 941–952. https://doi.org/10.1083/jcb.201203012

Yasunaga, M., Tada, S., Torikai-Nishikawa, S., Nakano, Y., Okada, M., Jakt, L. M., Nishikawa, S., Chiba, T., Era, T., & Nishikawa, S. I. (2005). Induction and monitoring of definitive and visceral endoderm differentiation of mouse ES cells. *Nature Biotechnology*, *23*(12), 1542–1550. https://doi.org/10.1038/nbt1167

3

LIVER ORGANOIDS

by Co-Culture

ABSTRACT

The need for reliable *in vitro* liver models is critical for studying liver biology, disease mechanisms, and drug toxicity. Liver organoids generated from hiPSCs present a promising solution by closely mimicking *in vivo* liver tissue. This study aimed to optimize differentiation protocols to generate hepatic endoderm, ECs, and STM cells from hiPSCs. The protocols were validated through marker analysis: ECs showed high expression of CD31 and CD34, while STM cells were confirmed by the gene expression of *GATA4*, *HLX1*, *FOXF1*, and *COL4A1*. Functionality of the ECs was confirmed through tube formation and Ac-LDL uptake assays. Liver bud organoids were generated by co-culturing the three differentiated cell types and were cultured until D20. Gene expression analysis confirmed the presence of critical hepatic markers, while ICC revealed AFP^+ hepatic cells predominantly at the periphery and $CD31^+$ ECs towards the core. Despite their composition, the organoids exhibited a lack of complexity compared to the human developing liver. While the generated liver organoids are vascularized, their inability to replicate key events of liver morphogenesis indicates a need for further refinement to enhance their application as reliable *in vitro* liver models.

INTRODUCTION

It has become evident that two-dimensional differentiation methods lack the ability to accurately mimic the intricate cell interactions that unfold during organogenesis. The emergence of 3D organoids has emerged as a promising approach for generating complex organ-like tissues. However, the comprehension on the impact of heterotypic interactions on lineage identity is only just beginning to take shape.

As previously mentioned, among the methodologies used for the generation of organoids, including those employed for liver organoids, is the co-culture technique (Takebe et al., 2013). Researchers have understood that hiPSC-derived hepatic cells, within these microenvironments, are able to diverge from the typical two-dimensional setting expressing signature genes characteristic of liver budding (Camp et al., 2017). Moreover, single-cell RNA sequencing not only reveled a significant similarity between the gene expression profiles of liver organoids and fetal liver cells, but also shed light on the intricate interplay between the different cell lineages of the organoid.

For the co-culture approach, it is necessary to bring together the cell lineages that play crucial roles in liver development and become integral parts of the final liver structure. One of those strategies is to bring together hepatic endoderm, ECs, and STM. This approach requires parallel differentiation of these three cell types and their co-culture at a specific stage of differentiation. Current published work on co-culture for liver bud organoid generation often focuses on analyzing gene expression for hepatic markers and highlighting the functionality of the organoids. However, these studies do not explore how these three cell types evolve over time or how they organize themselves within the organoid, thereby not demonstrating the self-organization capability of the distinct components.

To address this, in this work the differentiation of these three cell types from hiPSCs was established, followed by co-culture to form liver bud organoids. The differentiation process was monitored until day 20, allowing for a detailed investigation into the dynamic interactions and spatial organization within the organoid. This comprehensive approach aimed to shed light on the mechanisms of self-organization and the developmental processes involved in liver formation.

METHODOLOGY

Maintenance of hiPSCs

In this In this work, experiments were performed using the hiPSC line iPS-DF6-9-9T.B, provided by WiCell Bank (Wisconsin, USA). This cell line was reprogramed from foreskin fibroblasts with a karyotype 46, XY that were collected from healthy donors using defined factors in the Laboratory of Dr. James Thomson, at University of Wisconsin. For hiPSC culture, mTeSR™1 (STEMCELL Technologies™, #85850) supplemented 1:200 (v/v) with penicillin/ streptomycin (Gibco™, #15140122) was used as culture medium in six-well plates coated with Matrigel® Growth Factor Reduced Matrix (Corning®, #354230). Culture medium was changed daily. Cell passaging was performed every three to four days when reaching a confluency ~70% using 0.5 mM EDTA (Invitrogen™, #15575020).

Pre-differentiation of hiPSCs in adherent culture

After hiPSC expansion, cells were dissociated using 0.5 mM EDTA solution (Invitrogen™, #15575020) for 5 min at room temperature (RT). Cells were seeded onto 12-well culture plates coated with iMatrix-511 (Nippi/ Matrixome®, #NP892-011) at a cell density of $4x10^5$ cells/ well. mTeSR™1 (STEMCELL Technologies™, #85850) supplemented 1:200 (v/v) with penicillin/ streptomycin (Gibco™, #15140122) was used as culture medium, changed daily until a confluence of 90-95% was achieved. This procedure was followed for hepatic endoderm, ECs and STM differentiation.

Hepatic endoderm differentiation in adherent culture

For hiPSC differentiation into hepatic endoderm, Roswell Park Memorial Institute (RPMI) 1640 medium (Gibco™, #21875034) was used as basal medium. RPMI was supplemented with 1% (v/v) B-27™ minus insulin (Gibco™, #A1895601) and supplemented 1:200 (v/v) with penicillin/ streptomycin (Gibco™, #15140122). At D0, basal medium was supplemented with 100 ng/mL of Activin A (PeproTech, #120-14P) and 2 μM of CHIR (Stemgent™, #04-0004). At D1, medium was again supplemented with 100 ng/mL of Activin A. After hiPSC differentiation into definitive endoderm, at D3, cells were refreshed with basal medium supplemented with 10 ng/mL of FGF2 (PeproTech, #100-18B) and 20 ng/mL of BMP4 (PeproTech, #120-05ET). Cells were cultured until D6 or D7 of differentiation. Working volume throughout differentiation was 1 mL per well.

Endothelial cell differentiation in adherent culture

For hiPSC differentiation into mesoderm, DMEM/F12 GlutaMAX™ (Gibco™, #31331028) was used as basal medium supplemented with 1% (v/v) B-27™ minus insulin (Gibco™, #A1895601), from D0 to D2 of differentiation. At D0 medium was supplemented with 6 μM of CHIR (Stemgent™, #04-0004) and 25 ng/mL of BMP4 (PeproTech, #120-05ET). At D2, cells were refreshed with basal medium. After hiPSC differention into mesoderme, at D3, cells were refreshed with StemPro-34 SFM medium (Gibco™, #10639011) supplemented with 100 ng/mL of VEGF (PeproTech, #100-20) and 2 μM of forskolin

(Sigma-Aldrich®, #F3917). Next day, cells were refreshed with same combination. At D5, cells were replated in 12-well culture plates coated with iMatrix-511 (Nippi/ Matrixome®, #NP892-011) at a cell density of $1x10^5$ cells/well ($2.5x10^4$ cells/cm^2). From D5, cells were refreshed every other day with StemPro-34 SFM medium supplemented with 50 ng/mL of VEGF. Working volume throughout differentiation was 1 mL per well.

Septum transversum mesenchyme differentiation in adherent culture

For hiPSC differentiation into mesoderm, see steps from D0 to D2 of endothelial cell differentiation. After hiPSC differention into mesoderme, at D3, cells were refreshed with DMEM/F12 GlutaMAX™ supplemented with 1% (v/v) B-27™ minus insulin. Medium was supplemented with 2 ng/mL activin A (PeproTech, #120-14P) and 10 ng/ml PDGF-BB (PeproTech, #120-14B). At D6, medium was replaced for StemPro-34 SFM medium (Gibco™, #10639011) supplemented with 10 ng/mL of FGF2 (PeproTech, #100-18B) and 10 ng/ml PDGF-BB. Cells were kept in culture until D8 or D9 of differentiation. Working volume throughout differentiation was 1 mL per well.

Immunocytochemistry

For sample preparation, aggregates were fixed in 4% (v/v) PFA (Sigma-Aldrich®) at 4ºC for 30 minutes. After PFA removal, cells were stored in PBS at 4ºC until further analysis. Aggregates were then incubated in 15% (m/v) sucrose in PBS at 4ºC overnight, embedded in a 7.5%/15% gelatin/sucrose mixture, and frozen in isopentane at -80ºC. Aggregates were sectioned at 12 μm using a cryostat-microtome (Leica CM3050S, Leica Microsystems), collected on Superfrost™ Microscope Slides (Thermo Scientific), and stored at -20ºC. Before staining, sections were de-gelatinized in PBS at 37ºC for 45 minutes. The sections were then incubated in 0.1 M glycine (Merck Millipore) for 10 minutes at room temperature (RT) to remove PFA residues, permeabilized with 0.1% (v/v) Triton X-100 (Sigma-Aldrich®) in PBS at RT for 10 minutes, and blocked with 10% (v/v) fetal goat serum (FGS, Gibco™) in TBST (20 mM Tris-HCl pH 8.0, 150 mM NaCl, and 0.05% (v/v) Tween-20, Sigma-Aldrich®) at RT for 30 minutes. The sections were then incubated with primary antibodies diluted in 10% FBS in TBST solution at 4ºC overnight (Table 3.1). Following primary antibody incubation, secondary antibodies were applied for 30 minutes at RT, and nuclear counterstaining was performed using 1.5 μg/mL 4',6-diamidino-2-phenylindole (DAPI, Sigma-Aldrich®) in PBS at RT for 5 minutes. Images were acquired using a LSM 710 Confocal Laser Point-Scanning Microscope (Zeiss), and data analysis was conducted using ZEN Imaging Software (Zeiss) and ImageJ Software.

Table 3.1 – List of antibodies used in flow cytometry (FC) and immunocytochemistry (ICC).

Target	Brand	Reference	Host Specie	Isotype	Dilution
AFP	Sigma-Aldrich	A8452	Mouse	IgG2a	1:500 (ICC)
CD31	Dako	M0823	Mouse	IgG1	1:50 (ICC), 1:50 (FC)
CD34 PerCP-Cy™5.5.	BD	347222	Mouse	IgG1	1:50 (FC)

Flow cytometry of extracellular markers

Cells were washed twice with PBS and re-suspended in primary antibody (Table 3.1) diluted in FACS buffer, and incubated for 30 minutes at RT. After incubation, cells were washed with PBS and re-suspended in secondary antibody diluted in FACS buffer for another 15 minutes, at RT in the dark. For conjugated antibodies, a single incubation period of 20 minutes at RT in the dark was performed. Finally, cells were washed twice with PBS and re-suspended to a final volume of 300 µL per FACS tube.

Quantitative real time (qRT)-PCR

For sample collection at selected time points, culture medium was removed and cells were washed with PBS. Then cells were incubated with Accutase® solution (Sigma-Aldrich®, #A6964) in the case of hiPSCs or 0.25% (v/v) trypsin-EDTA (Gibco™, #R001100) in PBS for differentiated cells, both at 37ºC for 7 min. Culture medium was added to inactivate enzymatic digestion and cells were homogenized and centrifuged at 200 xg for 3 min. The cell pellet was washed with PBS and centrifuged again at 200 xg for 3 min. After removing the PBS, cell pellet was stored at -80ºC until further analysis. Total RNA was extracted from samples using the High Pure RNA Isolation Kit (Roche, #11828665001) following the provided instructions. RNA was quantified using a nanodrop and 1 µg of RNA was converted into cDNA with the High Capacity cDNA Reverse Transcription Kit (Applied Biosystems™, #4368814) also following the provided instructions. PCR reactions were run using SYBR Green Master Mix (Nzytech, #MB22303). Reactions were run in triplicate using ViiA™ 7 Real-Time PCR Systems (Applied Biosystems™) and data were analysed using QuantStudio™ Real-Time PCR Software (Applied Biosystems™). The analysis was performed using the ΔΔCt method and values were normalized against the expression of the housekeeping gene glyceraldehyde-3-phosphate dehydrogenase (GAPDH).

Table 3.2 – List of primers used in qRT-PCR analysis.

Gene	Primer (5´>3´)
GAPDH	FW: GAGTCAACGGATTTGGTCGT
	RV: TTGATTTTGGAGGGATCTCG
COL4A1	FW: GGCAGATTCGGACCACTAGG
	RV: GCGTCTGTGGCAATACTAGC
GATA4	FW: CGGAAGCCCAAGAACCTGAATAAAT
	RV: ACTGAGAACGTCTGGGACACG
FOXF1	FW: AGCGAGTTCATGTTCGAGGAG
	RV: TGAAGCCGAGCCCGTTCAT
HLX1	FW: CGGAAGCCCAAGAACCTGAATAAAT
	RV: ACTGAGAACGTCTGGGACACG

Tube formation assay

For tube formation assay, 2x10^4 hiPSC-ECs were cultured on 96-wells coated with Matrigel standard formulation 356234 (50uL/well). Cells were cultured in StemPro-34 SFM medium (Gibco™, #10639011). The observation of the tube formation was compared with hiPSCs as a negative control. After incubation for 4 h at 37°C, imaging was performed using an optical microscope DMI 3000B (Leica) with a digital camera DXM 1200F (Nikon).

Liver bud organoid co-culture

To generate liver bud organoids, a co-culture of hiPSC-derived hepatic endoderm, hiPSC-ECs, and hiPSC-STM was performed at a ratio of 10:7:2, targeting 1140 cells per aggregate. The cells were resuspended in a mixture 1:1 of endothelial cell growth medium (EGM) BulletKit™ (Lonza, #CC-3124) and hepatocyte culture medium (HCM) BulletKit™ (Lonza, #CC-3198) without the addition of human epidermal growth factor (hEGF). Medium was supplemented with 10 ng/mL of oncostatin M (OSM, R&D Systems™, #295-OM), 0.1 μM of dexametasone (Dex, Sigma-Aldrich®, #D4902) and 20 ng/mL of hepatic growth factor (HGF, Sigma-Aldrich®, #H1404). The suspension was plated in AggreWell™ 800 wells (STEMCELL Technologies, #34815). To prevent cell adhesion, wells were treated with anti-adherence rinsing solution (STEMCELL Technologies, #07010) prior to cell culture and according to manufacturer instructions. The medium was refreshed every 3 days with the same composition as the seeding day.

RESULTS AND DISCUSSION

3.1. Successful establishment of differentiation protocols for endothelial and septum transversum mesenchyme cells from hiPSCs

Similarly to the DE protocol optimization, a protocol was developed to generate ECs from hiPSCs, drawing inspiration from previous studies (Patsch et al., 2015; Takebe et al., 2017). This protocol aimed to differentiate hiPSCs through a series of stages: PS, mesoderm, and finally, an EC-like state (Figure 3.1A). The differentiation procedure started with the induction of PS and mesoderm using CHIR99021 and BMP4. Adjustments were made to the concentrations of these factors to improve differentiation efficiency, specifically the concentration of CHIR99021 for mesoderm induction and VEGF for endothelial specification. Particularly, VEGF concentrations were lowered from 200 to 100 ng/mL at days 3 and 4, maintaining efficiency in terms of CD31 expression. The hiPSCs subjected to the full differentiation program were assessed by FC analysis and ICC staining (Figure 3.1C, 3.1D), revealing high expression of EC markers like CD31 and CD34, with 81% co-expression at D8. This high level of co-expression indicates successful differentiation into ECs, validating the adjustments made to the protocol.

To evaluate the functionality of the derived ECs, two key assays were performed: tube formation and uptake of acetylated low-density lipoprotein (Ac-LDL). Tube formation assays assess the ability of ECs to form capillary-like structures *in vitro*, a critical feature of functional ECs. The positive results in the tube formation assay (Figure 3.1E) demonstrated that the differentiated cells could organize into vascular structures, indicating their functional capability. Similarly, the Ac-LDL uptake by the differentiated ECs further confirmed the functionality of the ECs by demonstrating their capacity to endocytose modified LDL, a characteristic trait of endothelial cells (Figure 3.1F).

To differentiate hiPSCs into STM cells, the protocol followed by Takebe was reproduced in this work (Takebe et al., 2017). This approach mirrors the initial steps used in differentiating hiPSCs into ECs, as it also progresses through the PS and mesoderm stages (Figure 3.2A). This protocol was adapted by Takebe from a method originally designed for the differentiation of hiPSCs into smooth muscle cells (Patsch et al., 2015). From the mesoderm stage, the protocol employed platelet-derived growth factor-BB (PDGF-BB) and Activin A were used to guide cells into a smooth muscle fate. These morphogens have shown to promote this phenotype (Chan et al., 2010). The differentiation was carried out until D8 or D9 of differentiation. To assess the efficiency of differentiation into STM-like cells, the expression of specific genes associated with STM was analyzed using qRT-PCR (Figure 3.2C). The expression levels of *GATA4*, *HLX1*, *FOXF1*, and *COL4A1* were confirmed, indicating successful differentiation.

Finally, the hepatic endoderm was differentiated from hiPSCs following the protocol previously optimized but only until D6 of differentiation (Figure 3.3). Previous studies identified by transcriptomic analysis cells that optimal generation of liver organoids by co-culture was obtained when the hepatic component expressed *TBX3* and *ADRA1B*. In the differentiation process optimized in this work, *TBX3* already presents heigh levels of expression at D7 (Figure 2.3B).

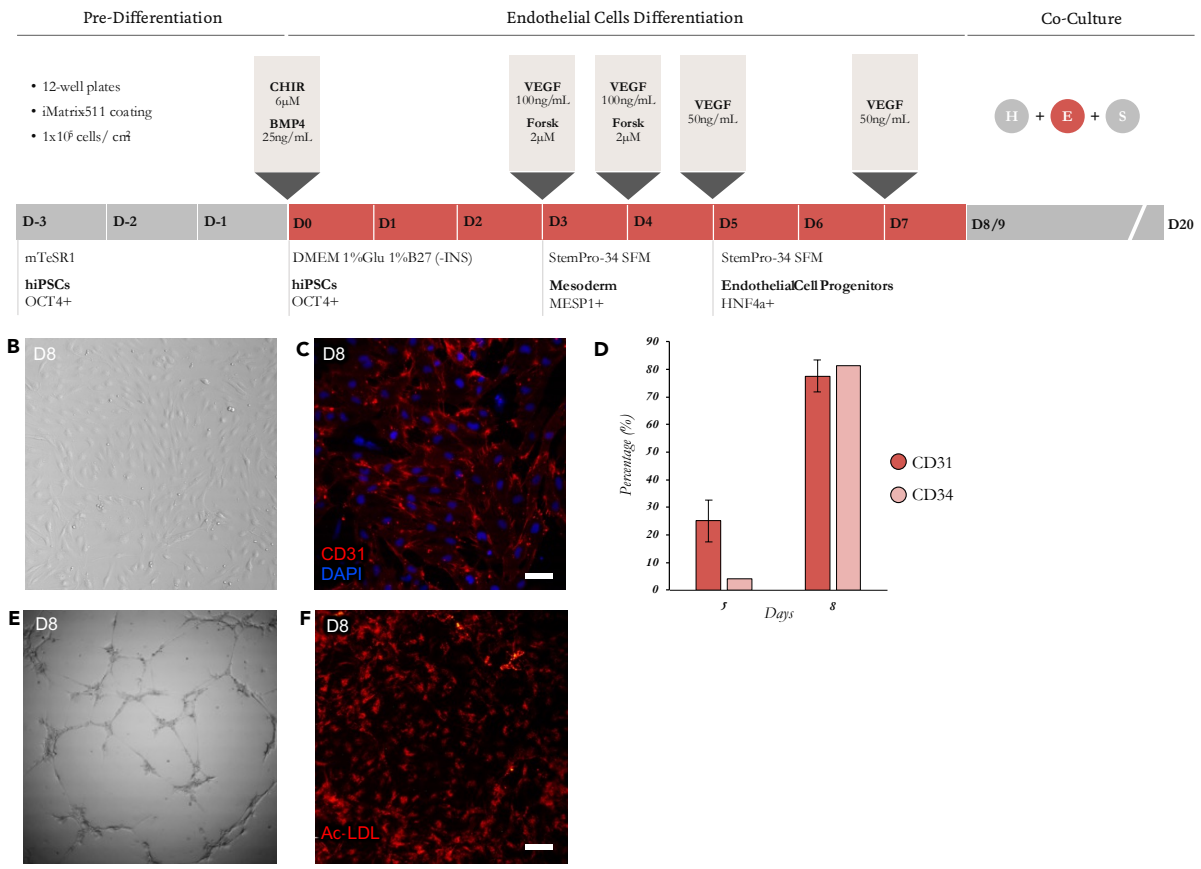

Figure 3.1. Differentiation of hiPSCs into ECs. (A) Schematic representation of the established differentiation protocol for ECs. **(B)** Bright-field image of hiPSC-ECs at D8 of differentiation. **(C)** ICC for CD31 at D8 of differentiation. **(D)** Differentiation efficiency at D5 and D8 by flow-cytometry analysis for CD31 and CD34. **(E)** ECs functionality assessment by tube formation assay at D8. Image after 4h of incubation at 37°C in Matrigel®. **(F)** Assay for uptake of Ac-LDL. Scale bars = 50 µm.

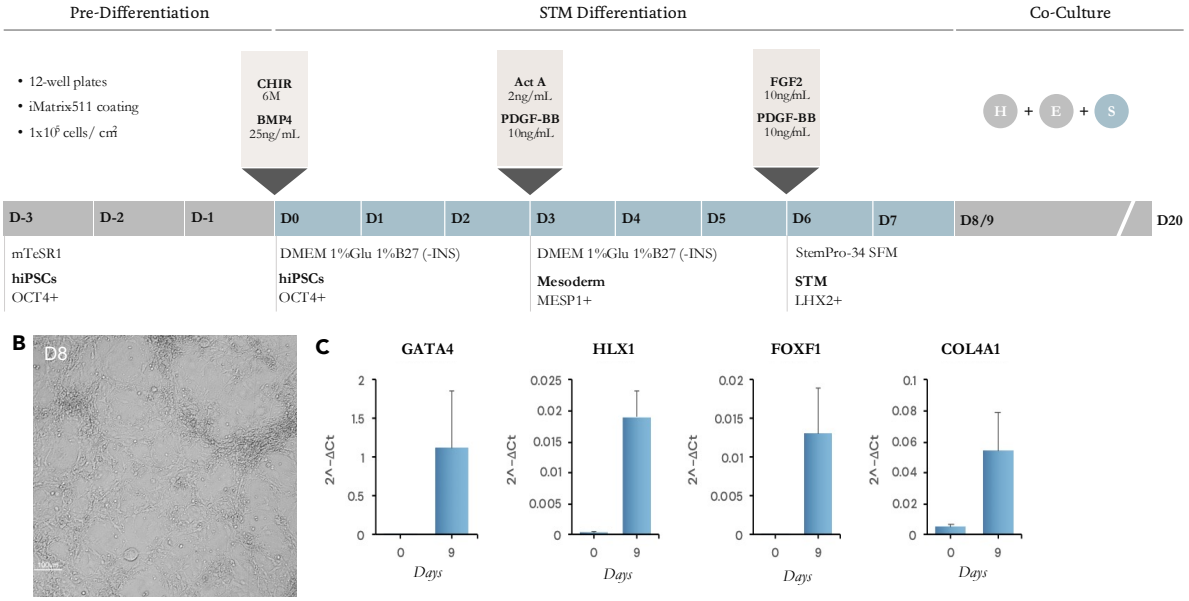

Figure 3.1. Differentiation of hiPSCs into STM cells. (A) Schematic representation of the established differentiation protocol for STM. **(B)** Bright-field image of hiPSC-STM at D8 of differentiation. **(C)** Gene expression assessed by qRT-PCR at D0 and D9 for STM genes *GATA4*, *HLX1*, *FOXF1*, *COL4A1*. The analysis was performed using the ΔCt method. The values were normalized against the expression of the housekeeping gene GAPDH. n=3.

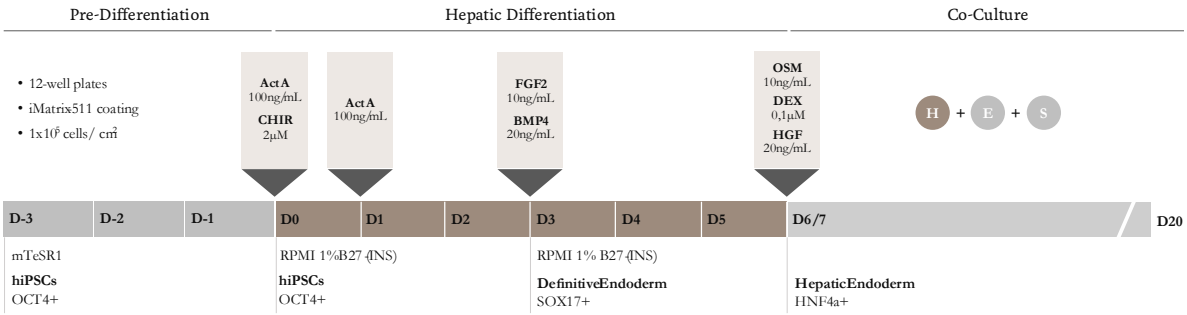

Figure 3.3. Differentiation of hiPSCs into hepatic endoderm. (A) Schematic representation of the established differentiation protocol for hepatic endoderm, based on previously optimized method for differentiation of hepatocytes.

3.1. Generation of liver bud organoids by co-culture demonstrates lack of complexity when compared to *in vivo* liver bud structure

After establishing the three distinct differentiation protocols for hepatic endoderm, ECs, and STM, the generation of liver bud organoids was initiated through co-culture. This process involved mixing the three cell types in a specific ratio of 10:7:2 using microwells, with the organoids being cultured until D20.

To characterize the generated liver bud organoids, gene expression analysis of key hepatic markers was performed, confirming the expression of important later-stage hepatic genes. These findings indicate successful differentiation and maturation of hepatic cells within the organoids, underscoring their hepatic identity. Additionally, ICC on D20 cryosections of the organoids revealed AFP^+ and ALB^+ hepatic cells primarily situated at the periphery of the organoids, while $CD31^+$ ECs were concentrated towards the core (Figure 3.4). This spatial organization contrasts with observations from Takebe's work, where ICC images of the whole organoid suggested a more intermixed arrangement of hepatic cells and ECs (Takebe et al., 2017), although the specific day of differentiation was not specified.

While the generated organoids are obviously vascularized, they exhibit a lack of refined spatial organization when compared to the *in vivo* liver bud morphology. Furthermore, the process of generating liver bud organoids through co-culture is inherently laborious and time-consuming. It necessitates the simultaneous differentiation of three distinct cell types, which must be coordinated to reach specific developmental stages suitable for co-culture. This complexity requires precise timing and extensive optimization to ensure all cell types are prepared concurrently.

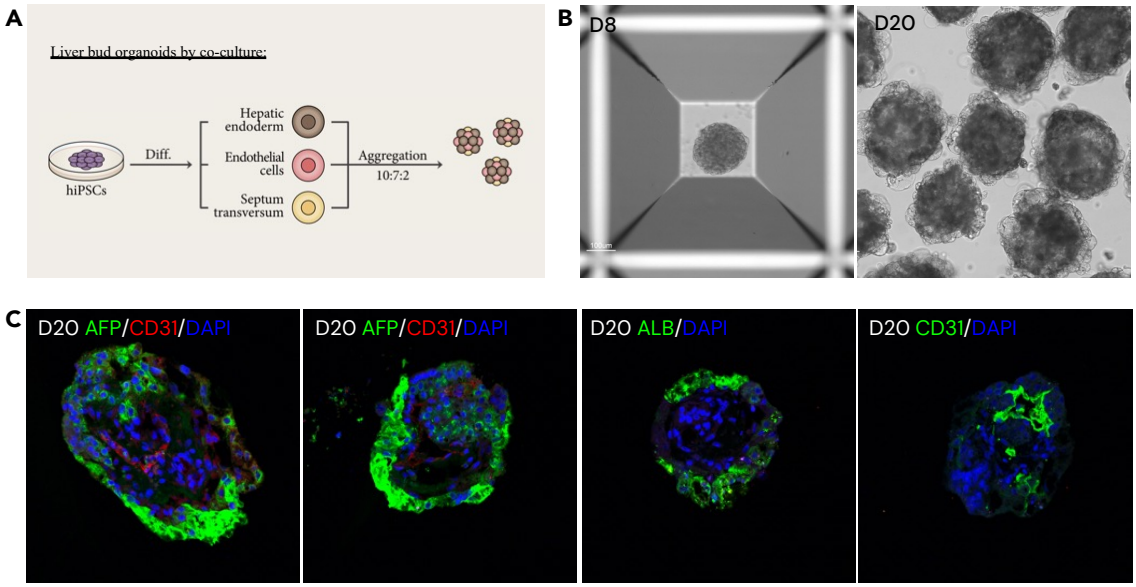

Figure 3.2 – Liver bud organoids generated by co-culturing different cell types of the developing liver. **(A)** Schematic representation of the co-culture of hepatic endoderm, ECs and STM to generate liver bud organoids. **(B)** Bright-field image of liver bud organoids at D8 and D20 of differentiation. (C) ICC for AFP, ALB and CD31 of aggregate cryosections at D20. Different organoids are depicted.

CONCLUSION

The establishment of three distinct differentiation protocols for hepatic endoderm, ECs, and STM cells enabled the generation of liver bud organoids through co-culture. This method involved precise mixing ratios and culture conditions to maintain organoid viability and functionality. The characterization of these organoids revealed successful expression of key hepatic markers and distinct spatial organization, with AFP^+ and ALB^+ hepatic cells at the periphery and $CD31^+$ ECs in the core. Despite these achievements, the generated organoids exhibited a lack of refined spatial organization compared to *in vivo* liver buds. This highlights the need for further optimization in the generation process. Additionally, the labor-intensive and time-consuming nature of co-culturing three cell types simultaneously presents challenges that must be addressed to streamline and enhance the reproducibility of liver organoid production. Although the current organoids present vascularization, their inability to replicate key events of liver morphogenesis underscores a critical area for improvement in future studies, aiming to better mimic the intricate architecture and functionality of native liver tissue.

REFERENCES

Camp, J. G., Sekine, K., Gerber, T., Loeffler-Wirth, H., Binder, H., Gac, M., Kanton, S., Kageyama, J., Damm, G., Seehofer, D., Belicova, L., Bickle, M., Barsacchi, R., Okuda, R., Yoshizawa, E., Kimura, M., Ayabe, H., Taniguchi, H., Takebe, T., & Treutlein, B. (2017). Multilineage communication regulates human liver bud development from pluripotency. *Nature*, *546*(7659), 533–538. https://doi.org/10.1038/nature22796

Chan, M. C., Hilyard, A. C., Wu, C., Davis, B. N., Hill, N. S., Lal, A., Lieberman, J., Lagna, G., & Hata, A. (2010). Molecular basis for antagonism between PDGF and the TGFB family of signalling pathways by control of miR-24 expression. *EMBO Journal*, *29*(3), 559–573. https://doi.org/10.1038/emboj.2009.370

Patsch, C., Challet-Meylan, L., Thoma, E. C., Urich, E., Heckel, T., O'Sullivan, J. F., Grainger, S. J., Kapp, F. G., Sun, L., Christensen, K., Xia, Y., Florido, M. H. C., He, W., Pan, W., Prummer, M., Warren, C. R., Jakob-Roetne, R., Certa, U., Jagasia, R., … Cowan, C. A. (2015). Generation of vascular endothelial and smooth muscle cells from human pluripotent stem cells. *Nature Cell Biology*, *17*(8), 994–1003. https://doi.org/10.1038/ncb3205

Takebe, T., Sekine, K., Enomura, M., Koike, H., Kimura, M., Ogaeri, T., Zhang, R.-R., Ueno, Y., Zheng, Y.-W., Koike, N., Aoyama, S., Adachi, Y., & Taniguchi, H. (2013). Takebe, T., Sekine, K., Enomura, M., Koike, H., Kimura, M., Ogaeri, T., Zhang, R.-R., Ueno, Y., Zheng, Y.-W., Koike, N., Aoyama, S., Adachi, Y., Taniguchi, H., 2013. Vascularized and functional human liver from an iPSC-derived organ bud transplant. Nature. *Nature*, *499*(7459), 481–484. https://doi.org/10.1038/nature12271

Takebe, T., Sekine, K., Kimura, M., Yoshizawa, E., Ayano, S., Koido, M., Funayama, S., Nakanishi, N., Hisai, T., Kobayashi, T., Kasai, T., Kitada, R., Mori, A., Ayabe, H., Ejiri, Y., Amimoto, N., Yamazaki, Y., Ogawa, S., Ishikawa, M., … Taniguchi, H. (2017). Massive and Reproducible Production of Liver Buds Entirely from Human Pluripotent Stem Cells. *Cell Reports*, *21*(10), 2661–2670. https://doi.org/10.1016/j.celrep.2017.11.005

4

LIVER ORGANOIDS

by Co-Emergence

ABSTRACT

This study introduced a co-emergence strategy for recreating liver morphogenesis, producing liver bud organoids with unprecedented complexity in a dynamic suspension culture. This approach contrasts with traditional co-culture methods. By varying activin A concentrations, differential morphological and differentiation outcomes were achieved: the 10 ng/mL condition fostered posterior foregut-like structures, while the 100 ng/mL condition promoted extensive endodermal differentiation. Extended cultures up to D40 revealed advanced hepatic structures, including pseudostratified epithelia with HNF4a$^+$ hepatoblasts, LHX2$^+$ STM, and WT1$^+$ hepatic mesothelium, generating liver bud organoids and effectively mimicking *in vivo* liver development. Vascularization was confirmed by CD31$^+$ ECs and the emergence of gene expression markers characteristic of hepatic-specific ECs. Balancing nutrient supply and paracrine factor retention proved critical, as frequent medium refreshes reduced hepatic marker expression. This research successfully demonstrates *in vitro* liver morphogenesis, creating complex liver bud organoids with significant potential for tissue engineering and biomedical applications.

INTRODUCTION

As discussed in the previous chapter, liver organoids generated through co-culture methods still lack structural organization and their production is quite labor-intensive. An emerging strategy in the literature is the generation of organoids from a homogeneous starting cell population of hiPSCs, referred to here as the co-emergence strategy. In the context of liver organoids, the idea is that within a single hiPSC aggregate the different cell types that constitute the developing liver will co-emerge and self-organize between themselves to form a liver organoid. This strategy enables the replication of *in vivo* morphogenesis where cell differentiation and spatial organization occur in a coordinated manner. As a result, it leads to the formation of a liver organoid that more accurately reflects the cellular composition and structural intricacy of the developing liver. Additionally, by enabling the spontaneous and synchronized emergence of various liver cell types within a controlled environment, the co-emergence strategy can potentially produce organoids that are more physiologically relevant. Such organoids can provide valuable models for studying liver development, disease mechanisms, and drug responses. Moreover, the streamlined nature of this approach may enhance reproducibility and scalability, making it more feasible for large-scale applications.

Although there are already some examples in the literature of liver organoids generated through this method (Ouchi et al., 2019; Wu et al., 2019), the full potential of the co-emergence strategy remains to be thoroughly explored. Further investigation is needed to optimize the conditions that promote effective differentiation and organization of multiple cell lineages within hiPSC aggregates. Investigating the signaling pathways and environmental factors that influence these processes will be crucial for refining the co-emergence strategy.

It is now a central dogma in modern developmental biology that one of the most important mechanisms in cell fate specification involves gradients of morphogens regulating gene expression (Rogers & Schier, 2011). This idea can be traced back to the so-called reaction-diffusion model published by Alan Turing in his work *'The Chemical Basis of Morphogenesis'* in 1952 (Turing, 1952), which provided a mathematical explanation for how patterns can naturally emerge through the interaction of diffusible chemicals. This theoretical framework was pivotal in understanding spatial patterning in developing tissues. Subsequently, in 1969, Lewis Wolpert's French flag model expanded on this concept (Wolpert, 1969), using the analogy of the French tricolor flag to explain how cells interpret positional information from morphogen gradients to differentiate into specific cell types, depending on the morphogen concentrations they are exposed to (Figure 4.1). Building on these foundational models, John Gurdon's work in 1994 demonstrated practical applications of morphogen gradients using *Xenopus* as model organisms (Gurdon et al., 1994). Gurdon showed that the selection of genes activated in a cell is determined by its distance from a source of a certain inducer, and hence, the concentration of the inducer. He also demonstrated that this signal is transmitted by passive diffusion rather than by cell-to-cell amplification. Specifically, his experiments with activin-secreting beads revealed that high concentrations of activin induced the expression of the *goosecoid* gene, while lower concentrations activated the *Xbra* gene, the equivalent to the human gene T (Figure 4.2). These studies

collectively highlight the critical role of morphogen gradients in regulating gene expression and determining cell fate during development.

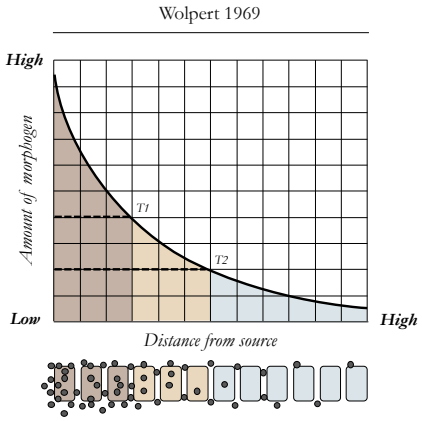

Figure 4.1. French flag model by Lewis Wolpert. The model created by Wolpert in 1969 describes the formation of three cell types in response to a morphogen gradient: a paracrine morphogen (black dots) is secreted by some given source cells, creating a concentration gradient across an adjacent tissue. Cells exposed to high morphogen levels (above threshold 1) activate specific genes (brown). Intermediate morphogen levels (between thresholds 1 and 2) lead to activation of different genes (yellow). Cells in low morphogen areas (below threshold 2) activate another distinct set of genes (blue). This gradient establishes multiple cell fates and positional information in the tissue. Image after Rogers and Schier 2011.

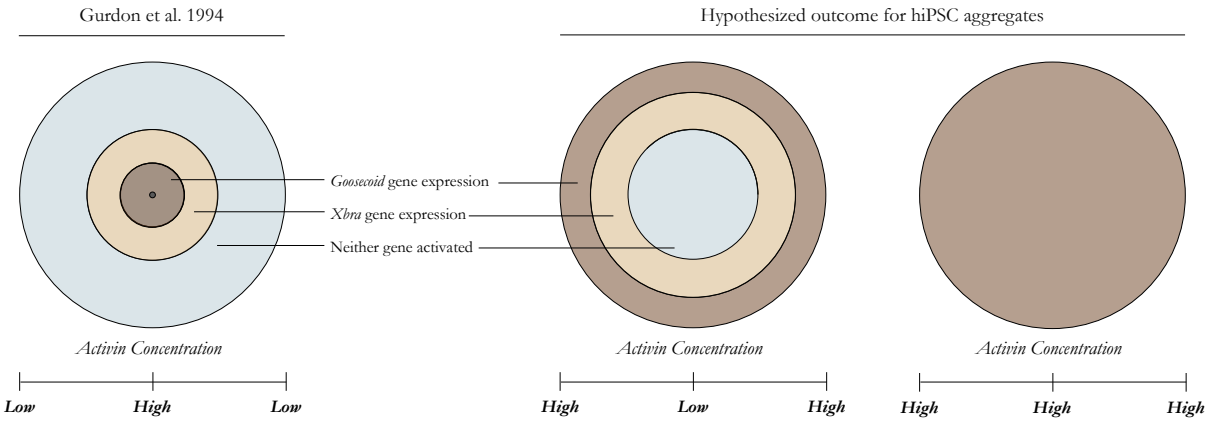

Figure 4.2. Concentration-dependent gene expression in *Xenopus* by Gurdon. A gradient of the paracrine factor activin A, a morphogen, induces concentration-dependent expression of two genes in unspecified amphibian cells (*Xenopus*). Beads containing activin A led to *goosecoid* expression in the cells proximal to the source, while cells further away expressed *Xbra*. This suggests that high concentrations of activin A activate *goosecoid*, whereas lower concentrations activate *Xbra*. A threshold concentration determines whether a cell will express *goosecoid*, *Xbra*, or neither gene (left diagram after Gurdon et al, 1994). Based on this information, it can be hypothesized that a reverse pattern can be observed in hiPSCs aggregates exposed to an external source of activin A. Additionally, if the concentration is sufficiently high, the entire aggregate is expected to express *goosecoid*.

Within this framework, exploring the significance of TGF-β signaling could be an interesting approach, since it plays a pivotal role in endoderm differentiation. As mentioned above, Activin A, a member of the TGF-β superfamily, has been utilized to create gradients that induce different cell types from pluripotent cells. For instance, high concentrations of activin A tend to induce endodermal differentiation, while lower concentrations favor mesodermal outcomes. As a reverse model from Gurdon's experiments, it is here hypothesized that hiPSCs aggregates exposed to different concentrations of activin A will be differently patterned into endodermal and mesodermal fate. This can be of particular interest for liver organoid

generation, since the liver is a complex organ derived primarily from the endoderm, but with critical contributions from the mesoderm during its developmental path. Achieving a realistic mimicry of the liver architecture requires a balanced differentiation of hepatoblasts (from the endoderm) and the simultaneous development of vascularization and stromal components (from the mesoderm). Modulating the concentration of activin A can potentially demonstrate how to achieve this balance, supporting the co-emergence of parenchymal and non-parenchymal cell types and fine-tuning the final organoid composition. Ultimately, this approach has the intention to manipulate the processes of organogenesis in a controlled yet complex environment. This idea of generating liver organoids through co-emergence by modulating initial activin A concentrations will be the focus of this chapter.

METHODOLOGY

Maintenance of hiPSCs

In this work, experiments were performed using the hiPSC line iPS-DF6-9-9T.B, provided by WiCell Bank (Wisconsin, USA). This cell line was reprogramed from foreskin fibroblasts with a karyotype 46, XY that were collected from healthy donors using defined factors in the Laboratory of Dr. James Thomson, at University of Wisconsin. An additional hiPSC line was used for results validation, the hiPSC line F002.1A.13, derived from a healthy female donor and provided by TCLab (Tecnologias Celulares para Aplicação Médica, Unipessoal, Lda.). For hiPSC culture, mTeSR™1 (STEMCELL Technologies™, #85850) supplemented 1:200 (v/v) with penicillin/streptomycin (Gibco™, Thermo Fisher Scientific, #15140122) was used as culture medium in six-well plates coated with Matrigel® Growth Factor Reduced Matrix (Corning®, #354230). Culture medium was changed daily. Cell passaging was performed every three to four days when reaching a confluency ~70% using 0.5 mM EDTA (Invitrogen™, Thermo Fisher Scientific, #15575020).

Liver Organoid Generation

Before inoculation, cells were incubated with 10μM ROCKi Y-27632 (STEMCELL Technologies™, #72304) for 1h at 37ºC and then treated with Accutase® solution (Sigma-Aldrich®, #A6964) for 7 min at 37ºC. After dissociation, cells were added to the vertical-wheel bioreactor PBS Mini 0.1L (PBS Biotech, USA) at a density of 250 000 cells/mL in 60 mL of mTeSR™1 supplemented with 10μM ROCKi. To promote cell aggregation an agitation speed of 27 rotations per minute (rpm) was used. After 24h and 48h, full volume of the medium was replaced and aggregates were maintained in mTeSR™1 without ROCKi at an agitation speed of 25 rpm. For hiPSC differentiation into definitive endoderm, Roswell Park Memorial Institute (RPMI) 1640 medium (Gibco™, #21875034) was used as basal medium. RPMI was supplemented with 1% (v/v) B-27™ minus insulin (Gibco™, #A1895601) and supplemented 1:200 (v/v) with penicillin/ streptomycin (Gibco™, #15140122). At D0 of differentiation, basal medium was supplemented with 10 ng/mL or 100 ng/mL of Activin A (PeproTech, #120-14P) and 6 μM of CHIR99021 (CHIR, Stemgent™, #04-0004). Agitation speed was changed to 30 rpm. At day 1 basal medium was again supplemented with 10 ng/mL or 100 ng/mL of Activin A. Agitation speed was changed to 33 rpm. After hiPSC differentiation into definitive endoderm, cells continued to be cultured in RPMI 1640 medium supplemented with 1% (v/v) B-27™ minus insulin and 1:200 (v/v) with penicillin/ streptomycin, from D3 to D5 of differentiation. At D3, for hepatic induction, medium was additionally supplemented with 10 ng/mL of FGF2 (PeproTech, #100-18B) and 20 ng/mL of BMP4 (PeproTech, #120-05ET). From D6 to D20, cells were refreshed every three days with hepatocyte culture medium (HCM) BulletKit™ (Lonza, #CC-3198) without the addition of human epidermal growth factor (hEGF). Medium was supplemented with 10 ng/mL of oncostatin M (OSM, R&D Systems™, #295-OM), 0.1 μM of dexametasone (Dex, Sigma-Aldrich®, #D4902) and 20 ng/mL of hepatic growth factor (HGF, Sigma-Aldrich®, #H1404).

Immunocytochemistry

For sample preparation, aggregates were fixed in 4% (v/v) PFA (Sigma-Aldrich®) at 4ºC for 30 minutes. After PFA removal, cells were stored in PBS at 4ºC until further analysis. Aggregates were then incubated in 15% (m/v) sucrose in PBS at 4ºC overnight, embedded in a 7.5%/15% gelatin/sucrose mixture, and frozen in isopentane at -80ºC. Aggregates were sectioned at 12 μm using a cryostat-microtome (Leica CM3050S, Leica Microsystems), collected on Superfrost™ Microscope Slides (Thermo Scientific), and stored at -20ºC. Before staining, sections were de-gelatinized in PBS at 37ºC for 45 minutes. The sections were then incubated in 0.1 M glycine (Merck Millipore) for 10 minutes at room temperature (RT) to remove PFA residues, permeabilized with 0.1% (v/v) Triton X-100 (Sigma-Aldrich®) in PBS at RT for 10 minutes, and blocked with 10% (v/v) fetal goat serum (FGS, Gibco™) in TBST (20 mM Tris-HCl pH 8.0, 150 mM NaCl, and 0.05% (v/v) Tween-20, Sigma-Aldrich®) at RT for 30 minutes. The sections were then incubated with primary antibodies diluted in 10% FBS in TBST solution at 4ºC overnight (Table 4.1). Following primary antibody incubation, secondary antibodies were applied for 30 minutes at RT, and nuclear counterstaining was performed using 1.5 μg/mL 4',6-diamidino-2-phenylindole (DAPI, Sigma-Aldrich®) in PBS at RT for 5 minutes. Images were acquired using a LSM 710 Confocal Laser Point-Scanning Microscope (Zeiss), and data analysis was conducted using ZEN Imaging Software (Zeiss) and ImageJ Software.

Quantitative real time (qRT)-PCR

Total RNA from cells of dissociated liver organoids was extracted using High Pure RNA Isolation Kit following the provided instructions. RNA was quantified using a nanodrop and 1 μg of RNA was converted into cDNA with High Capacity cDNA Reverse Transcription Kit (Applied Biosystems™/ Thermo Fisher Scientific) also following the provided instructions. PCR reactions were run using SYBR Green Master Mix (Nzytech). Reactions were run in triplicate using ViiA™ 7 Real-Time PCR Systems (Applied Biosystems™/ Thermo Fisher Scientific) and data were analysed using QuantStudio™ Real-Time PCR Software (Applied Biosystems™/ Thermo Fisher Scientific). The analysis was performed using the ΔΔCt method and values were normalized against the expression of the housekeeping gene glyceraldehyde-3-phosphate dehydrogenase (GAPDH). List of primers on Table 4.2.

Metabolite Analysis

The concentrations of glucose and lactate were analyzed before and after each medium change in. Samples were centrifuged for 10 min to remove dead cells and debris. Glucose and lactate levels were then measured using a multi-parameter analyzer (YSI 7100MBS, Yellow Springs Instruments).

Table 4.1. List of antibodies used in ICC.

Target	Brand	Reference	Host Specie	Isotype	Dilution
SOX17	Abcam	ab84990	Mouse	IgG1	1:100
TBX3	Abcam	ab99302	Rabbit	IgG	1:100
HNF4a	Santa Cruz Biotech.	sc-374229	Mouse	IgG1	1:50
AFP	Sigma-Aldrich	A8452	Mouse	IgG2a	1:500
CK19	Abcam	ab52625	Rabbit	IgG	1:200
LHX2	Abcam	ab184337	Rabbit	IgG	1:200
WT1	Abcam	ab89901	Rabbit	IgG	1:50
Laminin	Abcam	ab11575	Rabbit	IgG	1:400
CD31	Dako	M0823	Mouse	IgG	1:50
Desmin	Santa Cruz Biotech.	sc-271677	Mouse	IgG2a	1:50

Table 4.2. List of primers used in qRT-PCR analysis.

Gene	Primer (5´>3´)
GAPDH	FW: GAGTCAACGGATTTGGTCGT
	RV: TTGATTTTGGAGGGATCTCG
SOX17	FW: CTCCGGTGTGAATCTCCCC
	RV: CACGTCAGGATAGTTGCAGTAAT
TBX3	FW: TTACCAAGTCGGGAAGGCGAAT
	RV: CATCCTCTTTGGCATTTCGGGG
CK19	FW: GATCCTGAGTGACATGCGAAGC
	RV: GTAACCTCGGACCTGCTCATCT
PROX1	FW: GGGCTCTCCTTGTCGCTCATAAA
	RV: GGTAATGCATCTGTTGAACTTTACGTC
HNF4a	FW: GAGCGATCCAGGGAAGATCA
	RV: CATACTGGCGGTCGTTGATG
AFP	FW: CTTTGGGCTGCTCGCTATGA
	RV: GCATGTTGATTTAACAAGCTGCT
ALB	FW: ACCCCACACGCCTTTGGCACAA
	RV: CACACCCCTGGAATAAGCCGAGCT
CYP3A4	FW: AAGTGTGGGGCTTTTATGATGGT
	RV: GGTGAAGGTTGGAGACAGCAATG

RESULTS AND DISCUSSION

4.1. Varying activin A concentrations differentially influence hiPSC aggregate morphology during hepatic differentiation

To delve deeper into the effect of exposing hiPSC aggregates to varying concentrations of activin A, the selection of a platform able to generate aggregates with homogeneous sizes and homogenous activin distribution is a critical parameter. In fact, even the aggregation method can create a lineage bias (Xie et al., 2017). Taking that into consideration, a vertical-wheel bioreactor from PBS Biotech, particularly the PBS Mini 0.1L (hereinafter referred to as PBS Mini), was selected for its ability to create a controlled and consistent culture environment. Vertical-wheel bioreactors are ideal for generating uniform cell aggregates due to their gentle and efficient stirring mechanism (Nogueira et al., 2019). The large vertical wheel ensures thorough radial and axial mixing, while the U-shaped bottom design minimizes dead zones and cell settling, thereby providing a uniform exposure to nutrients and signaling molecules (Figure 4.3).

Figure 4.3. Vertical-wheel bioreactor PBS Mini 0.1L by PBS Biotech. Vertical-wheel bioreactors are designed for single use and ensure a consistent culture environment through gentle and efficient stirring. These bioreactors employ a large vertical wheel to achieve radial and axial mixing, while the U-shaped bottom prevents dead zones and limits cell settling. This design allows for lower agitation speeds, reducing shear stress on cells. Magnetic coupling between the impeller's magnets and the base unit drives the agitation, resulting in effective and gentle mixing.

In this study, the PBS mini was used as a starting point for the liver organoid culture, where hiPSC aggregation was promoted to generate 3D aggregates. The process began with a single-cell inoculation density of 250,000 cells per mL in a final volume of 60 mL of mTeSR1 medium, agitated at 27 rpm. At 24h, homogeneous aggregates were formed. Achieving a specific aggregate diameter is crucial for creating a spatial gradient of morphogen concentrations within the aggregates. For instance, a previous study suggested that a diameter of around 280-300 μm would be optimal for mesendoderm induction (Branco et al., 2019). Therefore, the aim was to produce aggregates with a diameter close to this range, typically achieved by the third day of pre-differentiation.

The differentiation protocol followed for liver organoid generation was adapted from the previously optimized protocol applied in the adherent culture (Figure 4.4A). However, to explore the differential patterning within the aggregates, two concentrations of activin A were selected, 10 ng/mL and 100 ng/mL,

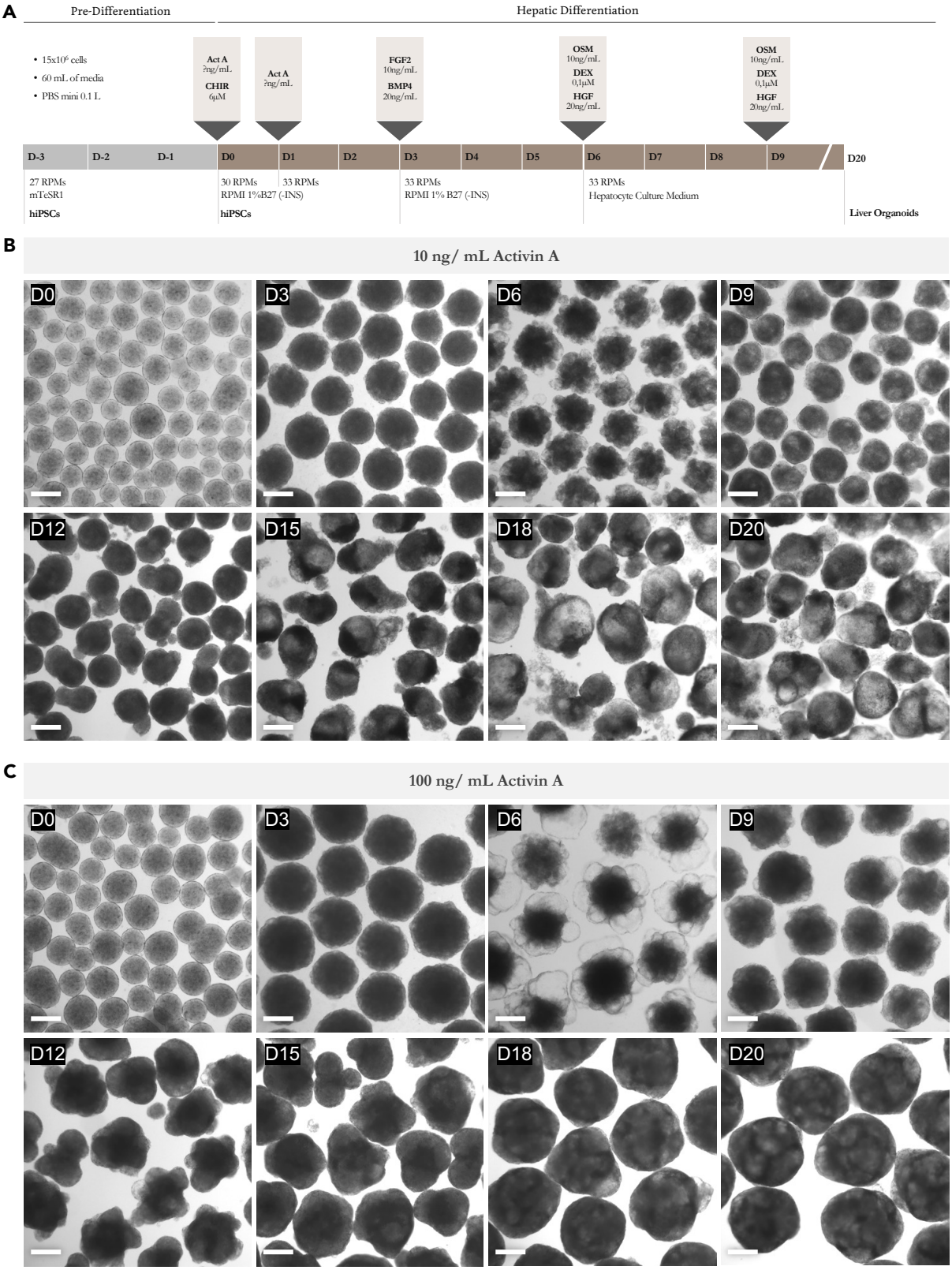

Figure 4.4. hiPSC aggregate morphology during hepatic differentiation. (A) Schematic representation of the established hepatic differentiation for liver organoid generation. Activin A concentration tested: 10 ng/mL and 100 ng/mL. **(B),(C)** Bright-field images demonstrating aggregate morphology at selected timepoints of differentiation from D0 to D20. Scale bars represent 300 µm.

each one being applied at D0 and D1 of differentiation in separate bioreactors. By systematically varying activin A concentrations, the aim was to observe the resulting differentiation patterns and the spatial organization of the cell types within the aggregate. The differentiation was carried out for 20 days in the PBS Mini and samples were collected at selected timepoints. When starting to compare the differences between 10 ng/mL and 100 ng/mL of activin A, the morphology of the aggregates during the differentiation process was the first sign that these different concentrations were leading to different cell products (Figure 4.4B and 4.4C). It was observed that cell aggregates treated with 10 ng/mL of activin A began to increasingly develop cystic regions, particularly noticeable in the last stages of differentiation. These cystic regions, or cavities, were typically spherical or oval in shape and most likely lined by a layer of epithelial cells. In contrast, aggregates treated with 100 ng/mL of activin A exhibited a denser morphology overall. However, around D18-D20, these aggregates reveled a reticulated organization within their interior.

4.2. Activin A concentration gradients drive spatial patterning and endodermal differentiation within hiPSC aggregates

To determine whether varying activin concentrations resulted in distinct patterning within the aggregates, ICC was performed on cryosections of the aggregates at D3 of differentiation (Figure 4.5A). The images depict the results for SOX17 staining, a well described endodermal marker. With a higher concentration of 100 ng/mL activin A, the image showed more extensive and intense SOX17 staining across the aggregate. This indicates a stronger and more widespread induction of endodermal differentiation. With a lower concentration of 10 ng/mL activin A, it was possible to notice that only the peripheral cells of the aggregate stain for SOX17. This indicates that fewer cells had undergone endodermal differentiation compared to the higher concentration. In the context of Lewis Wolpert's theory, activin A diffusion can be seen as creating a gradient of positional information where cells differentiate accordingly. With a concentration of 100 ng/mL the entire hiPSC aggregate is exposed to high concentrations of activin A, differentiating a significant part of the cells into the endoderm lineage. Conversely, with a concentration of 10 ng/ mL, only the cells in the outer region were exposed to a given morphogen level capable of surpassing the necessary threshold for a cell to be induced into an endodermal fate. Cells in the interior of the aggregate wwhere ere most likely experiencing lower concentrations of activin A and might become mesodermal cells. This spatial

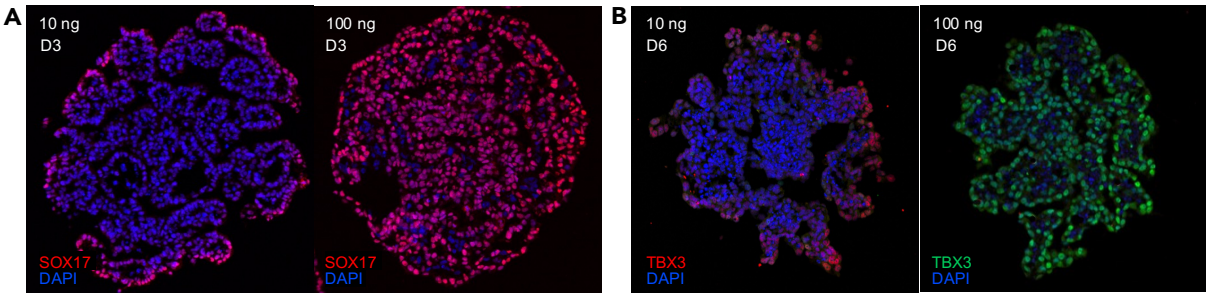

Figure 4.5. Activin A concentration-dependent spatial patterning. (A) ICC for SOX17 (endoderm marker) and **(B)** for TBX3 (hepatic endoderm marker) of aggregate cryosections at D3 and D6 of differentiation, respectively. For both markers 10 ng/mL nd 100 ng/mL of activin A conditions are represented.

patterning is crucial for the correct formation of tissues that require interactions between different cell types, such as the liver. In fact, this approach can validate both Lewis Wolpert's theory of positional information and Alan Turing's reaction-diffusion theory in a 3D culture system, just like Gurdon did using a *Xenopus* model. The observation that cells within the aggregate differentiate in distinct patterns, influenced by the concentration gradients of activin A, clearly supports the idea that reaction-diffusion mechanisms are at play. Moreover, it was possible to understand that this patterning was preserved in the following days of differentiation by accessing the presence of TBX3 at D6, an early hepatic marker (Figure 4.5B). After the addition of FGF2 and BMP4, only the regions initially patterned for endoderm proceed the differentiation into a hepatic fate, resulting in an aggregate mostly composed of hepatic endoderm for the 100 ng/mL condition, versus an aggregate here only the peripheral cells constituted hepatic endoderm for the 10 ng/mL condition.

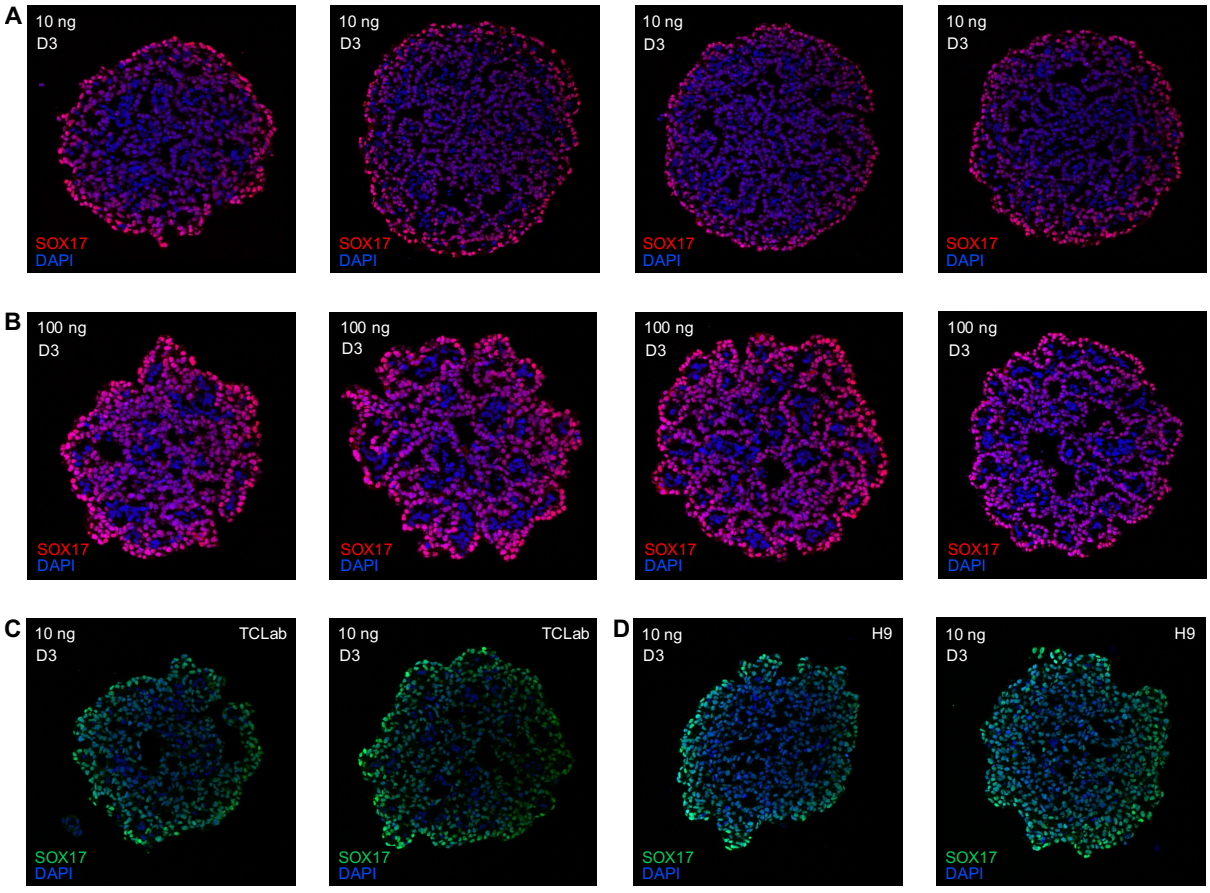

Figure 4.6. Reproducibility of the Activin A concentration gradients. ICC for SOX17 (endoderm marker) of aggregate cryosections at D3 of differentiation, for both **(A)** 10 ng/mL and **(B)** 100 ng/mL of activin A. SOX17 staining also analyzed at D3 for 10 ng/mL activin A condition for **(C)** TCLab hiPSC line and **(D)** H9 ESC line.

It is also important to mention that the results for SOX17 were remarkably reproducible, as the pattern was consistently observed across all analyzed cryosections from both the same experiment and different experiments (Figure 4.6A and 4.6B). This consistency was maintained regardless of the cell lines used, whether it was the hiPSC line DF6 under analysis or different cell line tested, the hiPSC line TCLab and

the ESC line H9 (Figure 4.6C and 4.6D). Such reproducibility highlights the robustness of the experimental setup and the reliability of the activin A concentration gradients in directing endodermal differentiation within the aggregates.

4.3. Initial low activin A concentrations facilitate liver morphogenesis by promoting the emergence of posterior foregut-like structures

To assess the fate of the hepatic endoderm detected at day 6 in both conditions, ICC for cryosections of day 12 was performed. For this purpose, the hepatic marker HNF4a and the marker LHX2, characteristic of the STM, were assessed (Figure 4.7A and 4.7B). The images for the 10 ng/mL condition revealed HNF4a$^+$ cells still located near the peripheral region but already attempting to reorganize, indicating active cell movements. This reorganization suggests that the cells are beginning to establish the structural foundation necessary for liver morphogenesis. The interior of these aggregates stained prominently for LHX2, confirming that the cells in the interior were not only primed for a mesodermal fate but were also being specified into lateral plate mesoderm derivatives like the STM. This observation is consistent with the role of STM in providing critical signals for hepatic differentiation. In contrast, the images for the 100 ng/mL condition revealed a different pattern of cellular organization. The hepatic cells were observed to reorganize into bubble-shaped structures around the aggregate, also visible in the bright-field images from day 6 to day 12. The presence of LHX2$^+$ cells in this condition was minimal compared to the 10 ng/mL condition, indicating a reduced presence of mesodermal derivatives and a more pronounced hepatic differentiation pathway.

Furthermore, cryosections from D20 were also analyzed by ICC. The analysis revealed significant insights into the organization and differentiation status of the different lineages at this later stage. For the aggregates exposed to low concentrations of activin A, the resultant structures interestingly resembled the initial steps of liver bud formation seen during embryonic development (Figure 4.7C). The cryosections exhibited an epithelium composed of HNF4a$^+$ cells arranged in a posterior foregut tube-like structure, surrounded by a laminin (LAM$^+$) basal lamina. Furthermore, in close contact with the HNF4a$^+$ cells but separated by the basal lamina, it was possible to distinguish the LHX2$^+$ population, that similarly to what happens *in vivo*, was surrounding the posterior foregut tube. LHX2 is expressed in the STM that not only play a crucial role in hepatoblast differentiation and migration, but will latter contribute for non-parenchymal cells in the liver (Kolterud et al., 2004; Lotto et al., 2020). Finally, it was still possible to distinguish WT1$^+$ cells on the edge of the organoid. Based on the literature, it is hypothesized that these WT1$^+$ cells are forming a hepatic mesothelium (Asahina et al., 2011). Altogether, the ICC results revealed a well-organized and developmentally relevant liver bud morphology within the aggregates exposed to low concentrations of activin A.

In contrast, organoids exposed to high concentrations of activin A displayed a different organizational pattern (Figure 4.7D). These organoids lacked the distinct gut tube-like structures observed in the low activin A condition. Instead, cells in the peripheral region as wells as clusters in the cells appeared more

dispersed and less organized into a cohesive structure, highlighting the impact of higher activin A concentrations on the spatial arrangement and differentiation pathways within the organoids.

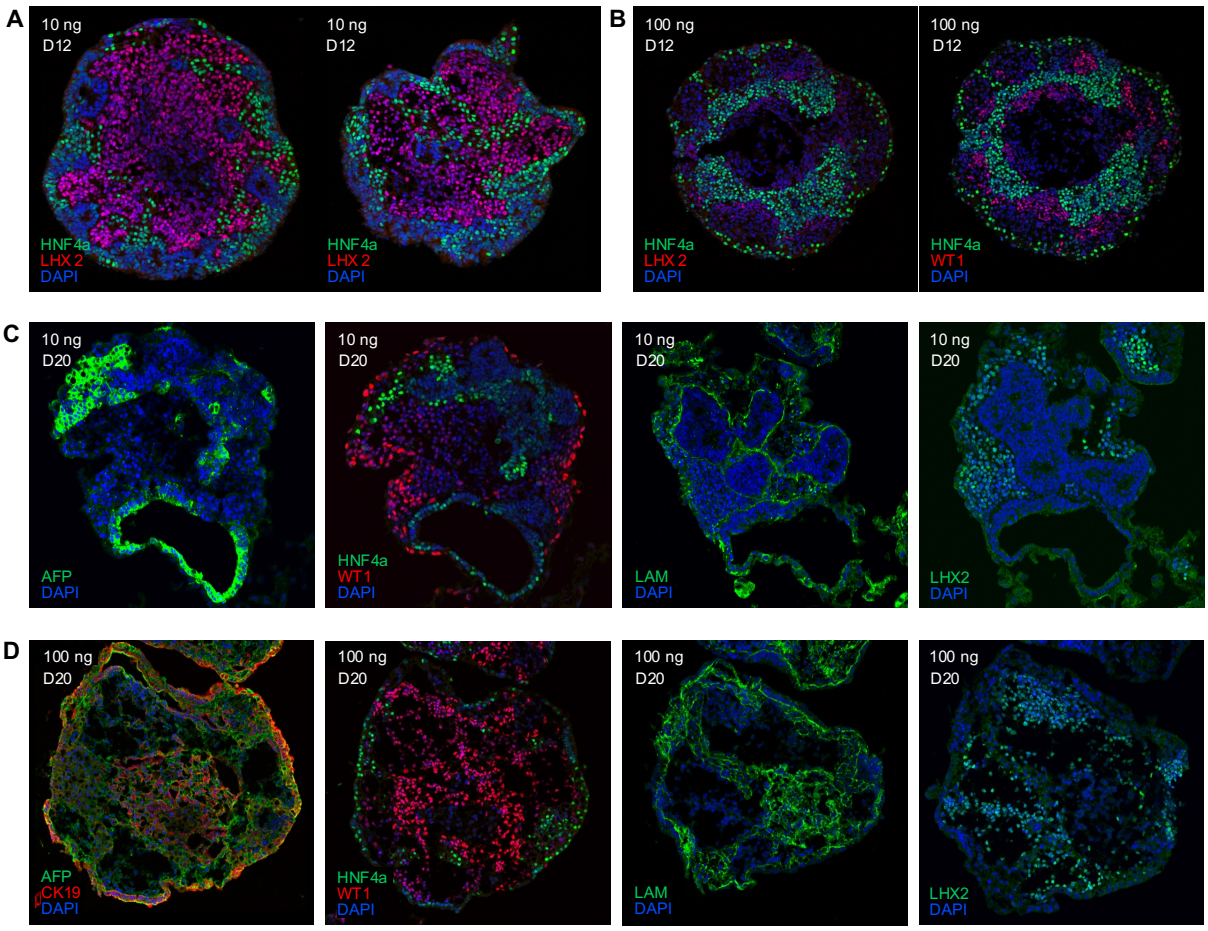

Figure 4.7. Distinct differentiation and spatial organization between conditions as differentiation progresses. (A) ICC for HNF4a and LHX2 of aggregate cryosections at D12, for 10 ng/mL of activin A. Different aggregates are depicted. **(B)** ICC for HNF4a, LHX2 and WT1 of aggregate cryosections at D12, for 100 ng/mL of activin A. Cryosections of the same aggregate are depicted. **(C)** ICC for AFP, HNF4a, WT1, Laminin (LAM) and LHX2 of aggregate cryosections at D20, for 10 ng/mL of activin A. Cryosections of the same aggregate are depicted. **(D)** ICC for AFP, CK19, HNF4a, WT1, Laminin (LAM) and LHX2 of aggregate cryosections at D20, for 100 ng/mL of activin A. Cryosections of the same aggregate are depicted.

4.4. Extended cell culture unveils liver bud organoid formation under low activin A concentrations

To further investigate the long-term development of the hepatic structures, the differentiation process was extended until D40. At this stage, the aggregates were transferred from the PBS Mini bioreactor to ultra-low attachment plates to better support long-term culture conditions. The analysis of these extended cultures provided additional insights into the maturation and self-organization of the different cell lineages.

By analyzing the morphology of the aggregates based on bright-field images, it was possible to identify clear tube-like structures for the 10 ng/mL condition (Figure 4.8A). In contrast, these structures were not present in aggregates from the 100 ng/mL condition and in fact, they exhibited a remarkable transparency (Figure 4.8B).

When analyzing the ICC results for cryosections of the aggregates treated with 10 ng/mL activin A, the resemblance to the liver budding process became clearly pronounced over the extended culture period (Figure 4.8C). It was evident that the hepatic endoderm has thickened by transitioning from a columnar to a pseudostratified epithelium composed of HNF4a$^+$ hepatoblasts. Moreover, it was still possible to observe the laminin layer surrounding the HNF4a$^+$ hepatoblasts, as well as the LHX2$^+$ STM and WT1$^+$ hepatic mesothelium. This self-organization effectively mimics the proximal-distal outgrowth of the hepatoblasts into the STM, characteristic of liver bud formation in the human embryo. Therefore, the exposure of hiPSC aggregates to low activin concentrations at initial stages of differentiation, establishes the precise spatial patterning that leads to liver bud organoid generation.

It can be argued that by D40 of differentiation, the basal lamina was expected to have already disintegrated, allowing the hepatoblasts to migrate and integrate into the surrounding STM cells. In most of the organoids, the basal lamina was still intact delineating the hepatic structure, but there were cases where HNF4a$^+$ cells were spotted out of the pseudostratified epithelium, suggesting the beginning of hepatoblast migration (Figure 4.8D). The persistence of the basal lamina in a great number of organoids suggests that additional factors or conditions may be necessary to stimulate this migration and further maturation of the hepatoblasts into fully differentiated hepatocytes and cholangiocytes. To stimulate hepatoblast migration, the addition of SDF1 to the culture medium was tested (300 ng/mL, n=1). This chemokine is known for its chemotactic effect on several types of cells, being a common player in cell migration processes. Accordingly, it was hypothesized that SDF1 would facilitate hepatoblast migration into the STM, however, its addition did not produce the desired effect (data not shown).

An interesting observation in this cryosections was the fact that in all the organoids it was possible to stain AFP in the lumen of the liver bud (Figure 4.8E). This protein is secreted by hepatoblasts in the human embryo and in this context, it makes sense that in developing liver bud AFP can be secreted into the extracellular space, including luminal areas.

It is also important to note that in some of the cryosections of liver bud organoids, more than one liver bud structure was observed (Figure 4.9). These structures indicate that hepatic endoderm can organize into more than one posterior foregut tube within the same aggregate, and at D20 this multi-tube organization is already noticeable in some aggregates. Subsequently, at D40 multiple liver bud structures can be identified in the same organoid. This phenomenon, although not exactly replicating *in vivo* conditions, it can be compared to what is observed in neural differentiation processes using 3D aggregates, where multiple neural rosettes often form, modeling several neural tubes *in vitro*. Interestingly, neural rosette morphogenesis shares common themes of self-organization and collective behavior and has been shown to rely on complex interactions between cell differentiation, migration, and mechanical forces. It is possible that these principles might also apply to liver organoids, where cells exhibit collective behaviors driven by local interactions and signaling gradients, guiding the differentiation and organization of the cells into functional tissue structures. This phenomenon is not directed by a single leader cell but emerges from the interactions among individual cells responding to chemical and mechanical cues in their environment (Miotto et al., 2023).

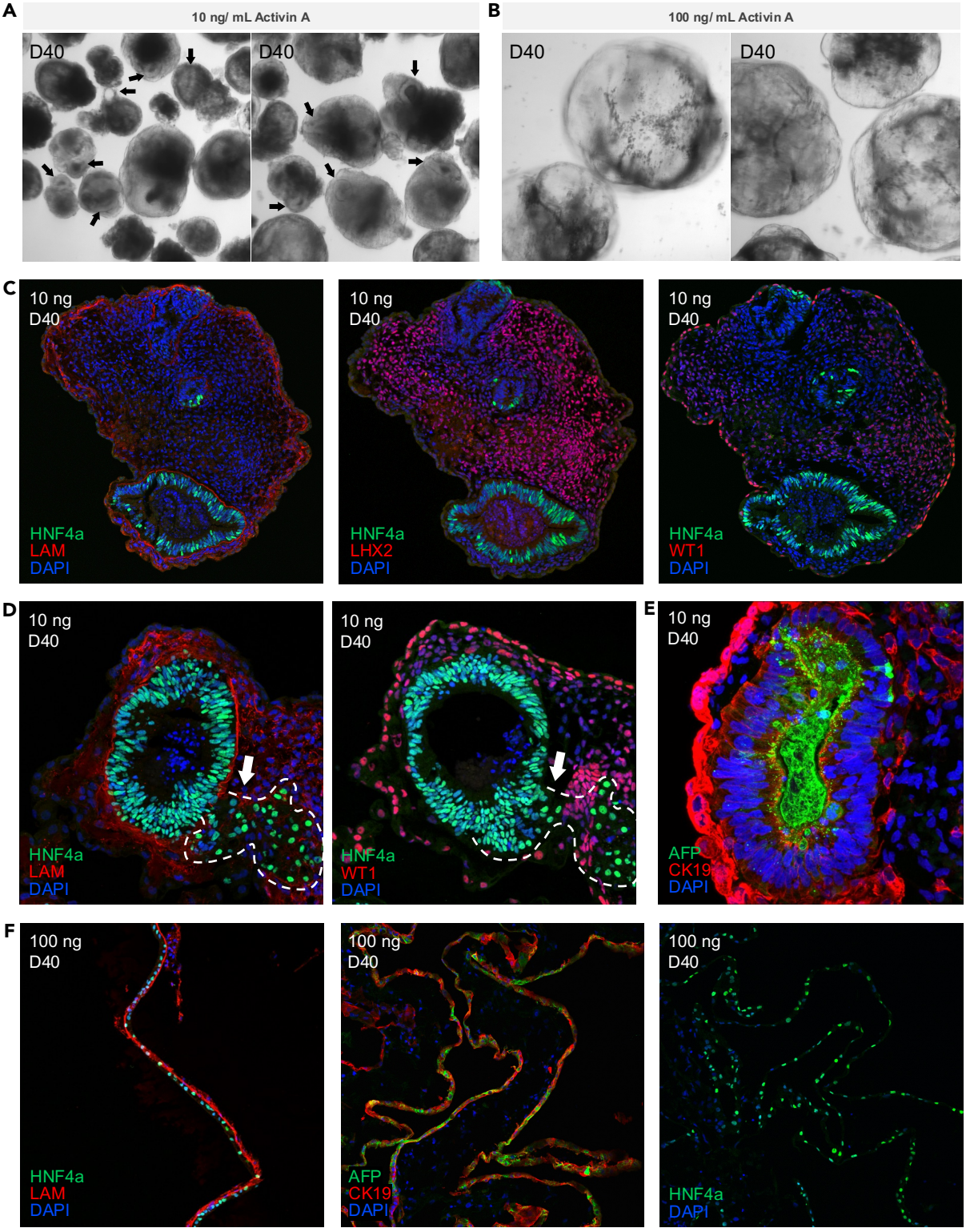

Figure 4.8. Liver bud organoids generated under low activin A condition and extended hepatic differentiation for high activin A condition. (A),(B) Brightfield images of generated organoids at D40. Arrows highlight visible tube-like structures. **(C)** Liver bud organoid by ICC for HNF4a, LAM, LHX2 and WT1 of aggregate cryosections at D40, for 10 ng/mL of activin A. Cryosections of the same organoid are depicted. **(D)** Closer look into the hepatoblasts and potential cell migration. ICC for HNF4a, LAM and WT1 at D20, for 10 ng/mL of activin A. Cryosections of the same aggregate are depicted. **(E)** Secretion of AFP into the luminal space by ICC at D40, for 10 ng/mL of activin A. **(F)** ICC for HNF4a, LAM, AFP and CK19 of aggregate cryosections at D40, for 100 ng/mL of activin A. Cryosections of different organoids are depicted.

When the same strategy was followed using the hiPSC line TCLab, the generation of liver bud organoids was also clear (Figure 4.10), validating the reproducibility of this approach.

In the case of aggregates treated with 100 ng/mL activin A, the cryosections revealed to be predominantly composed of epithelial cells expressing AFP, CK19, HNF4α, and laminin (Figure 4.8F). These results indicate a robust epithelialization process, with cells differentiating extensively into hepatic lineages. The high levels of AFP, a marker for fetal liver cells, suggest that these organoids are progressing towards a more mature hepatic state, although the exact degree of maturation and functional equivalence to *in vivo* liver tissue remains to be fully characterized.

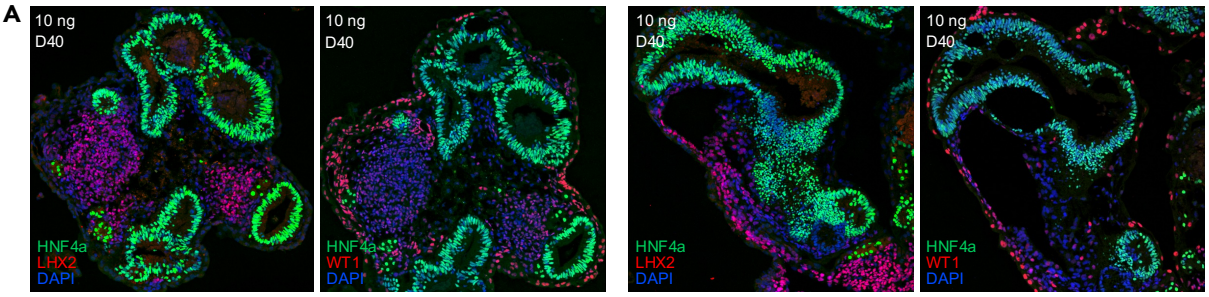

Figure 4.9. Multiple liver bud structures within the organoid. (A) ICC for HNF4a, LHX2 and WT1 of aggregate cryosections at D40, for 10 ng/mL of activin A. In each group of images, cryosections of the same organoid are depicted.

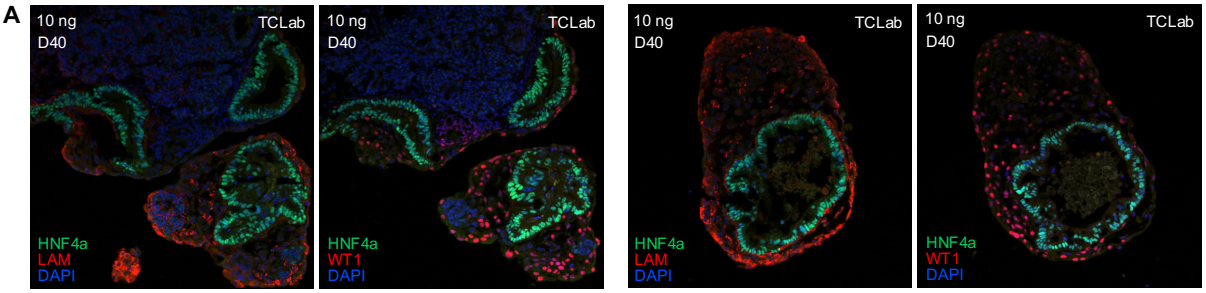

Figure 4.10. Liver bud organoid generation using a different hiPSC line. (A) ICC for HNF4a, LAM, and WT1 of aggregate cryosections at D40, for 10 ng/mL of activin A using the hiPSC line TCLab. In each group of images, cryosections of the same organoid are depicted.

4.4. Gene expression profiles via qRT-PCR validate differentiation patterns observed by ICC

qRT-PCR provided further confirmation of the differentiation patterns observed via ICC (Figure 4.11). The expression of the endoderm marker SOX17 was markedly higher in organoids treated with 100 ng/mL activin A, aligning seamlessly with the ICC data that showed extensive SOX17 staining across these aggregates. By its turn, TBX3 expression exhibited a sustained increase from D6 to D9 in the 100 ng/mL condition, contrasting with a peak only at D6 in the 10 ng/mL condition. This pattern suggests a prolonged and sustained activation of early hepatic differentiation markers under higher activin A concentrations, corresponding to the more pronounced and persistent endodermal and early hepatic markers seen in ICC.

The hepatoblast marker CK19 showed nearly double the expression in the higher activin condition, and PROX1 levels followed a similar trend, peaking at D9 in both conditions but at higher levels in the 100 ng/mL condition. Remarkably, HNF4a expression remained consistently high until day 20 in the 100 ng/mL condition, whereas it began to decrease from D6 in the 10 ng/mL condition. This data is once more aligned with the idea of a more advanced state of hepatic differentiation when hiPSC aggregates are exposed to high concentrations of activin A. Moreover, markers indicative of mature liver functions, such as AFP, ALB, and CYP3A4, were significantly amplified in the 100 ng/mL condition, with ALB and CYP3A4 being nearly absent in the 10 ng/mL condition. Overall, the qRT-PCR data corroborates the ICC findings, providing a molecular confirmation of the spatial and temporal patterns of differentiation induced by varying activin A concentrations.

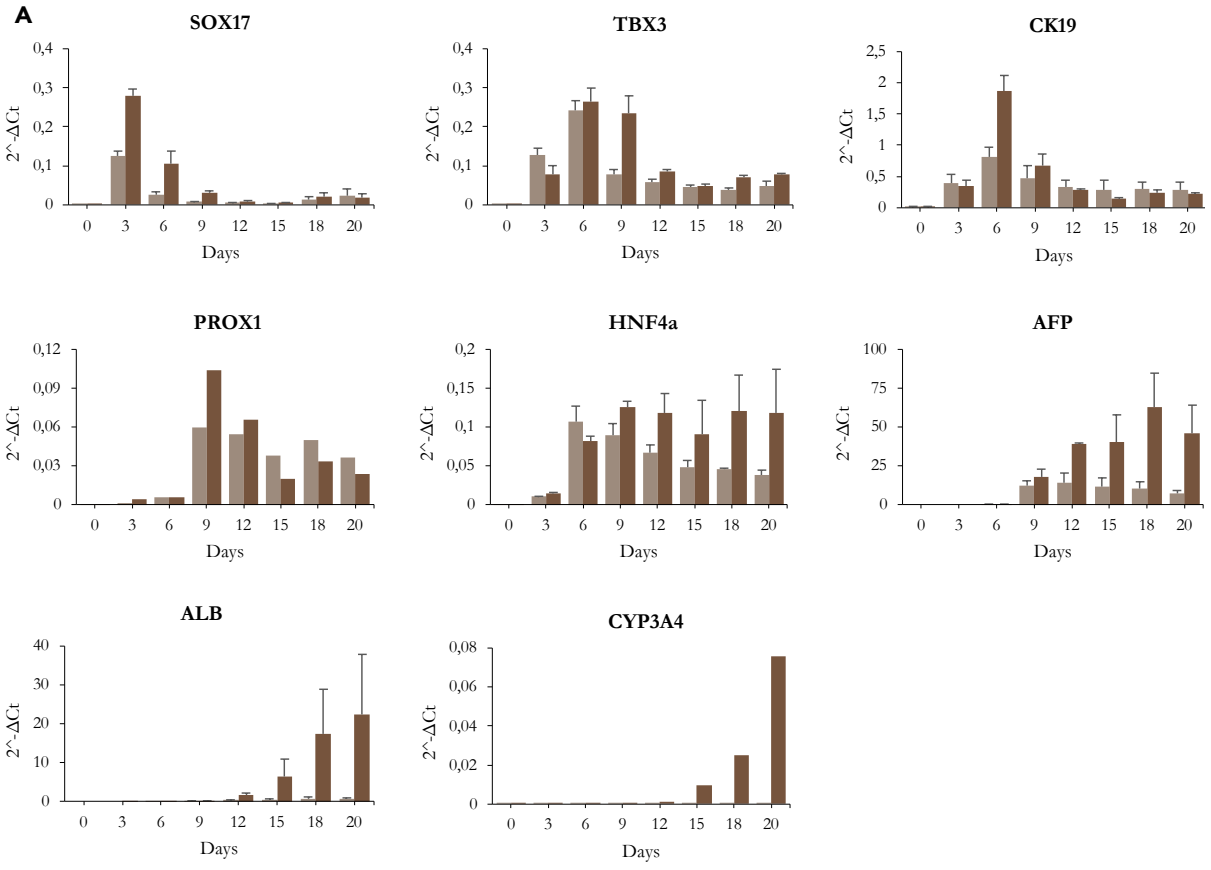

Figure 4.11. Generated liver organoids recapitulate gene expression profiles of *in vivo* hepatic development. (A) Gene expression was assessed by qRT-PCR at sequential stages for key genes that unveil the progression throughout hepatic differentiation with *OCT4* (pluripotency), *SOX17* (definitive endoderm), *TBX3* (hepatic endoderm), *CK19, PROX1, HNF4a* (hepatoblasts), *AFP* (fetal hepatocytes), *ALB, CYP3A4* and *TTR* (mature hepatocytes). The analysis was performed using the ΔCt method. The values were normalized against the expression of the housekeeping gene *GAPDH*. n=4 for 10 ng/mL and n=3 for 100 ng/mL for each time point (except n=1 for PROX1 and *CYP3A4).*

4.5. Liver bud organoids exhibit vascularization and other non-parenchymal cells with origin in the STM

The next step in this study was to investigate whether liver bud organoids generated under the 10 ng/mL activin A condition were vascularized. Vascularization is crucial not only for liver development, as ECs secrete important signaling molecules that facilitate this process (Matsumoto et al., 2001), but also for providing essential nutrients and oxygen. This enhances the viability and functionality of the organoids, ensuring they mimic the physiological conditions when compared to *in vivo* liver tissue.

To assess this, ICC images for cryosections of D40 organoids were analyzed. The presence of CD31$^+$ endothelial cells was confirmed, indicating vascularization within these organoids (Figure 4.12A). This finding was further substantiated by qRT-PCR gene expression analysis (Figure 4.12B), which confirmed the expression of the endothelial marker CD31. Interestingly, from D12 onwards, the expression of CD31 was reduced, coinciding with the emergence of LYVE1, a marker specific to hepatic endothelial cells, already referred in this work as LSECs (Poisson et al., 2017). This transition highlights the dynamic changes in endothelial cell populations within the developing liver bud organoids, reflecting a maturation process that aligns with *in vivo* liver development.

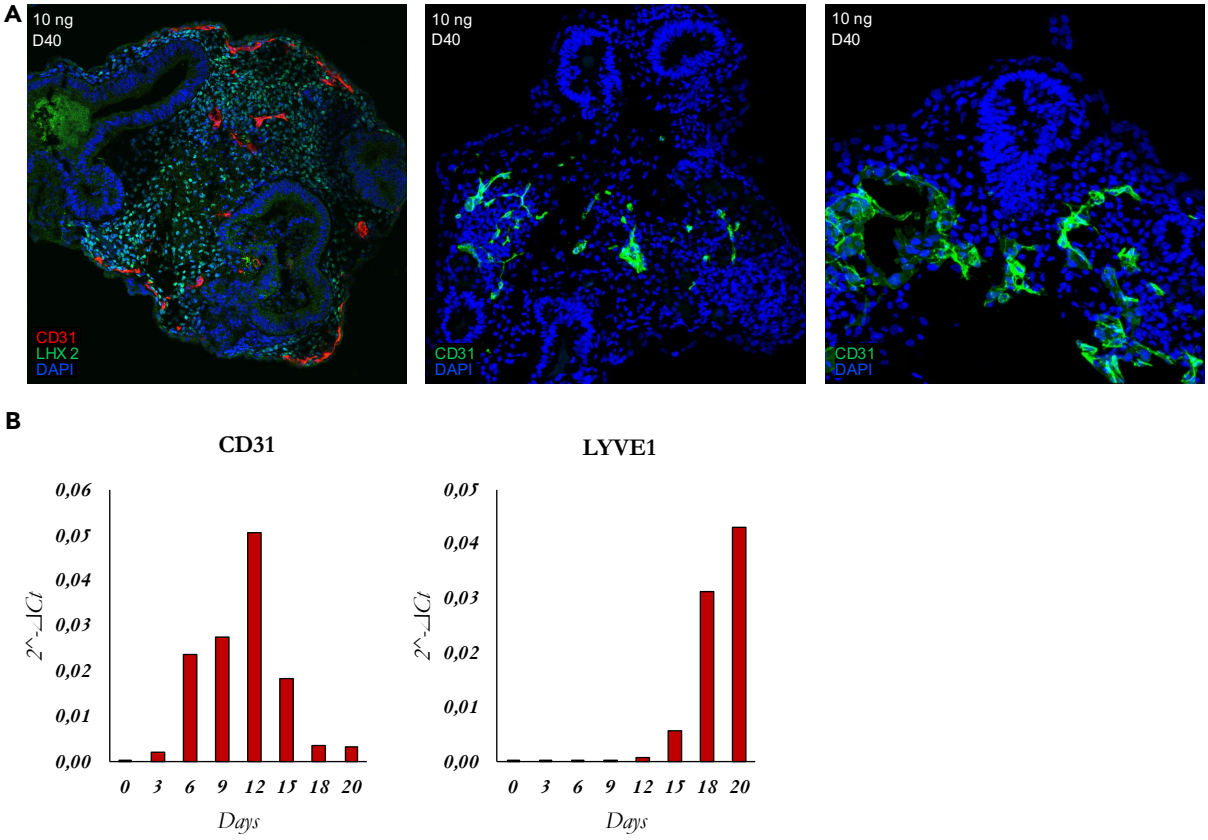

Figure 4.12 Liver bud organoids are vascularized. (A) ICC for CD31 and LHX2 of aggregate cryosections at D40, for 10 ng/mL of activin A. Different organoids are depicted. **(B)** Gene expression profiles throughout differentiation for *CD31* (endothelial cells) and and *LYVE1* (liver sinusoidal endothelial cells) suggesting the organoid vascularization. Analysis performed by qRT-PCR, ΔCt method; the values were normalized to GAPDH). n=1 experiment for each time point.

As mentioned above, the liver bud organoids generated under the 10 ng/mL activin A condition were composed of LHX2+ STM cells and WT1+ hepatic mesothelial cells (MCs). To further characterize these cells, ICC and gene expression analyses were performed. It is known that in mice, STM gives rise to hepatic MCs, submesothelial cells (SubMCs) as well as HSCs (Asahina et al., 2011). Both MCs and SubMCs, separated by a basal lamina, express Alcam, Desmin and WT1. These SubMCs will then migrate inwards and differentiate into HSCs (Asahina et al., 2011; Ijpenberg et al., 2007). The complete mechanisms for HSCs origin are still not entirely know and the lack of specific markers make them difficult to identify. Desmin keeps being expressed by HSCs but is also expressed in STM, MCs and SubMCs. Nevertheless, these markers were analyzed in this study. It is possible to see that a clear WT1+ cell population delineates the organoid and that these cells also co-express Desmin (Figure 4.13A). Additionally, a LAM+ basal lamina was also evident around the aggregate (Figure 4.8C). All these results reinforce the idea that the liver bud organoid is also constituted by MCs and possibly SubMCs. Interestingly, these cells also expressed CK19 (Figure 4.13B), something that is not described in the literature. When performing ICC for Desmin, not only the surface of the organoid had positive staining, as it was also possible to identify positive cells in the interior organoid (Figure 4.13C). Further investigation is needed to understand if HSCs can already be present on the organoid or if these are just unspecified STM progenitors. When gene expression analysis was performed by qRT-PCR, it was confirmed that all these markers were increasing their expression, *LHX2*, *WTI*, *DES* and *Alcam* (Figure 4.13D), also supporting the presence and differentiation of these cell types within the liver bud organoid.

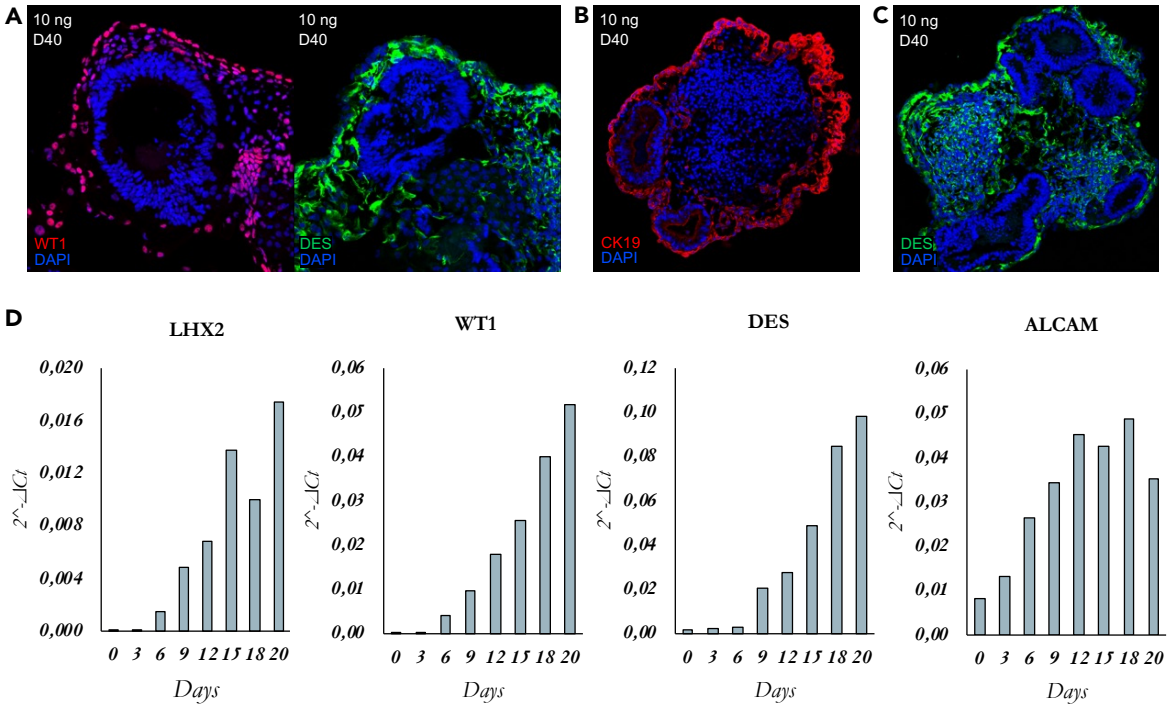

Figure 4.13 Liver bud organoids constituted by others non-parenchymal cells. (A),(B),(C) ICC for WT1, Desmin (DES) and CK19 of aggregate cryosections at D40, for 10 ng/mL of activin A. Different organoids are depicted, except in A. **(B)** Gene expression profiles throughout differentiation for markers of STM, MCs, SubMCs and HSCs: *LHX2*, *WT1*, *DES*, *ALCAM*. Analysis performed by qRT-PCR, ΔCt method; the values were normalized to GAPDH). n=1 experiment for each time point.

4.6. Medium refresh frequency affects paracrine signaling and hepatic differentiation

Additionally, the concentration of metabolites such as glucose and lactate was analyzed for both the 10 ng/mL and 100 ng/mL activin A conditions (Figure 4.14A). Predictably, in both conditions, glucose levels diminished with each medium refresh, whereas lactate levels conversely increased. However, it was observed that in the 10 ng/mL condition, glucose levels dropped to nearly zero g/L, particularly from D9 onwards, while lactate levels were elevated between 1 to 1.5 g/L. This lactate concentration is relatively high and suggests an increased reliance on glycolysis for energy production, which can occur when glucose is depleted and cells shift towards anaerobic metabolism. This can impact cell viability and function. In contrast, the 100 ng/mL condition did not exhibit these issues.

Initially, the bioreactor's medium refresh scheme was set to every three days from D6 onwards. To address the glucose depletion and lactate accumulation observed in the 10 ng/mL condition, a more frequent refresh scheme of every other day was tested. Nonetheless, this adjustment led to significantly lower gene expression levels of hepatic markers such as HNF4α, AFP, and ALB, as confirmed by qRT-PCR (Figure 4.14B). It is hypothesized that the frequent medium refreshment might have discarded essential secreted signaling molecules, including crucial paracrine factors, necessary for proper hepatic differentiation and maturation. Further investigation is needed to understand the importance of the secretome in this context, as well as the optimal balance between nutrient supply and retention of critical signaling factors. As a future alternative, supplementing the medium with additional glucose could be tested to mitigate the depletion while maintaining the necessary signaling environment for optimal liver organoid development.

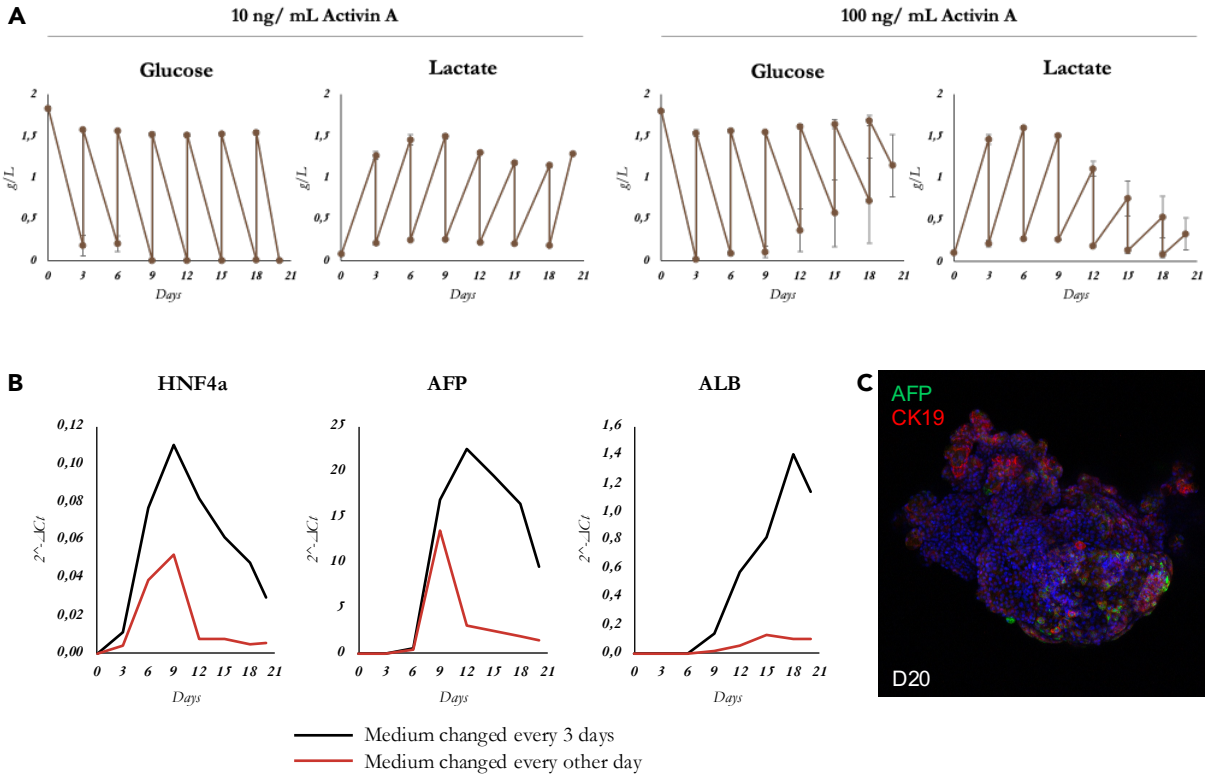

4.6. Developed approach as an instrument to improve organoid technology

An important contribution of this study on the development and optimization of liver organoid culture is that its insights can also be applied to other organ systems, particularly those derived from the gut tube, where similar principles of endoderm-mesoderm interactions and signaling gradients are crucial. Interestingly, several organs derived from the gut tube, such as the pancreas, gallbladder, thyroid gland, and lungs, also develop as buds surrounded by mesodermal derivatives. In all these cases, the surrounding mesodermal tissues play a vital role by providing structural support, essential signaling molecules, and contributing to the formation of connective tissues and vascularization. Therefore, diverging at D3 of differentiation from the 10 ng/mL model to different organoid protocols could be a valuable strategy for modeling these interactions *in vitro*. This approach would enable researchers to study the critical signaling pathways and cellular dynamics involved in the development of various organs derived from the gut tube. By refining these protocols, it may be possible to generate more accurate and functional organoids. The generation of a ventral pancreatic organoid would be the most straightforward way to test this approach in a different organ, given its close developmental relationship with the liver. Both hepatoblasts and ventral pancreatic progenitors share a common origin in the ventral foregut and receive crucial signals from the STM (Li et al., 2018). In this context, the gradients of activin A and the balance between endodermal and mesodermal components would also play a significant role. Properly managing these gradients and interactions would be essential to replicate the complex signaling environment necessary for accurate pancreatic organoid development.

Besides that, the mathematical modeling of activin A diffusion within a spheroid would be interesting to explore. This provides a quantitative framework to predict and analyze how cells at different positions respond based on their exposure to the growth factor and consequently, it can predict the formation of distinct zones of differentiation within the spheroid. This helps in designing organoid cultures where all cells have access to the necessary signals for proper differentiation, regardless of the differentiation platform used, such as microwells, suspension plates, bioreactors, or variations in aggregate size. By accurately controlling the signaling environments, particularly through activin A gradients, organoids can become even more effective tools in biomedical research. However, the complexity of biological systems often leads to unpredictable outcomes, requiring extensive calibration and validation of models against experimental data. This iterative process of model validation and refinement leads to a deeper understanding of the underlying biological processes and improves the predictive accuracy of the models.

Figure 4.14. More frequent medium changes lead to a reduction in hepatic markers. (A) Metabolic profile of the culture media with the evolution of glucose and lactate concentrations for both conditions under test. n=2 experiment for each time point. **(B)** Gene expression profiles throughout differentiation for *HNF4a*, *AFP* and *ALB*, hepatoblasts and hepatocytes specific genes, for the 2 medium change settings. n=1 experiment for each time point. **(C)** Immunofluorescent staining for AFP and CK19 at D20.

CONCLUSION

The investigation into varying activin A concentrations has revealed significant insights into the morphological and differentiation patterns of hiPSC aggregates during hepatic differentiation. Utilizing the PBS Mini bioreactor, which provides a controlled and uniform culture environment, has allowed for the generation of homogeneous cell aggregates, crucial for studying the effects of activin A gradients.

Further analysis through ICC confirmed that higher concentrations of activin A induced more extensive and widespread endodermal differentiation, as evidenced by SOX17 staining. This aligns with theoretical models suggesting that morphogen gradients drive spatial patterning within the aggregates. The 100 ng/mL condition consistently produced aggregates with a significant proportion of endodermal cells, whereas the 10 ng/mL condition resulted in more peripheral differentiation, highlighting the role of activin A diffusion in cellular differentiation.

The study also demonstrated that low activin A concentrations facilitate the emergence of foregut-like structures, essential for liver morphogenesis. The presence of HNF4a$^+$ cells in the 10 ng/mL condition indicated active cell reorganization and structural foundation establishment for liver development. In contrast, the 100 ng/mL condition exhibited different organizational patterns, emphasizing the concentration-dependent effects on cellular arrangement and differentiation pathways.

Extending the differentiation process to D40 provided deeper insights into the maturation of liver bud organoids. The persistence of the basal lamina and the emergence of HNF4a+ hepatoblasts suggest a well-organized and developmentally relevant liver bud morphology under low activin A conditions.

The presence of vascularization in liver bud organoids, especially under the 10 ng/mL condition, was confirmed through ICC and qRT-PCR, highlighting the emergence of CD31$^+$ ECs and the transition to LYVE1$^+$ LSECs. This finding underscores the importance of endothelial cells in liver development and the need for proper vascularization in organoid cultures to mimic *in vivo* conditions effectively.

Lastly, the analysis of metabolite concentrations revealed challenges associated with glucose depletion and lactate accumulation in the 10 ng/mL condition. Adjusting the medium refresh scheme impacted the gene expression levels of hepatic markers, suggesting that frequent refreshes may discard crucial paracrine factors. This study emphasizes the need for a balanced nutrient supply and retention of essential signaling molecules to optimize hepatic differentiation and organoid functionality.

REFERENCES

Asahina, K., Zhou, B., Pu, W. T., & Tsukamoto, H. (2011). Septum transversum-derived mesothelium gives rise to hepatic stellate cells and perivascular mesenchymal cells in developing mouse liver. *Hepatology*, *53*(3), 983–995. https://doi.org/10.1002/hep.24119

Branco, M. A., Cotovio, J. P., Rodrigues, C. A. V., Vaz, S. H., Fernandes, T. G., Moreira, L. M., Cabral, J. M. S., & Diogo, M. M. (2019). Transcriptomic analysis of 3D Cardiac Differentiation of Human Induced Pluripotent Stem Cells Reveals Faster Cardiomyocyte Maturation Compared to 2D Culture. *Scientific Reports*, *9*(1), 1–13. https://doi.org/10.1038/s41598-019-45047-9

Gurdon, J. B., Harger, P., Mitchell, A., & Lemaire, P. (1994). Activin signalling and response to a morphogen gradient. *Nature*, *371*(6497), 487–492. https://doi.org/10.1038/371487a0

Ijpenberg, A., Pérez-Pomares, J. M., Guadix, J. A., Carmona, R., Portillo-Sánchez, V., Macías, D., Hohenstein, P., Miles, C. M., Hastie, N. D., & Muñoz-Chápuli, R. (2007). Wt1 and retinoic acid signaling are essential for stellate cell development and liver morphogenesis. *Developmental Biology*, *312*(1), 157–170. https://doi.org/10.1016/j.ydbio.2007.09.014

Kolterud, Å., Wandzioch, E., & Carlsson, L. (2004). Lhx2 is expressed in the septum transversum mesenchyme that becomes an integral part of the liver and the formation of these cells is independent of functional Lhx2. *Gene Expression Patterns*, *4*(5), 521–528. https://doi.org/10.1016/j.modgep.2004.03.001

Li, L., Qiu, W., Zhang, Y., Xu, Z., Xiao, Y., Hou, C., Lamaoqiezhong, Yu, P., Cheng, X., & Xu, C. (2018). Single-cell transcriptomic analyses reveal distinct dorsal/ventral pancreatic programs. *EMBO Reports*, *19*(10). https://doi.org/10.15252/embr.201846148

Lotto, J., Drissler, S., Cullum, R., Wei, W., Setty, M., Bell, E. M., Boutet, S. C., Nowotschin, S., Kuo, Y. Y., Garg, V., Pe'er, D., Church, D. M., Hadjantonakis, A. K., & Hoodless, P. A. (2020). Single-Cell Transcriptomics Reveals Early Emergence of Liver Parenchymal and Non-parenchymal Cell Lineages. *Cell*, *183*(3), 702-716.e14. https://doi.org/10.1016/j.cell.2020.09.012

Matsumoto, K., Yoshitomi, H., Rossant, J., & Zaret, K. S. (2001). Liver organogenesis promoted by endothelial cells prior to vascular function. *Science*, *294*(5542), 559–563. https://doi.org/10.1126/science.1063889

Miotto, M., Rosito, M., Paoluzzi, M., de Turris, V., Folli, V., Leonetti, M., Ruocco, G., Rosa, A., & Gosti, G. (2023). Collective behavior and self-organization in neural rosette morphogenesis. In *Frontiers in Cell and Developmental Biology* (Vol. 11). Frontiers Media SA. https://doi.org/10.3389/fcell.2023.1134091

Nogueira, D. E. S., Rodrigues, C. A. V., Carvalho, M. S., Miranda, C. C., Hashimura, Y., Jung, S., Lee, B., & Cabral, J. M. S. (2019). Strategies for the expansion of human induced pluripotent stem cells as aggregates in single-use Vertical-Wheel™ bioreactors. *Journal of Biological Engineering*, *13*(1). https://doi.org/10.1186/s13036-019-0204-1

Ouchi, R., Togo, S., Kimura, M., Shinozawa, T., Koido, M., Koike, H., Thompson, W., Karns, R. A., Mayhew, C. N., McGrath, P. S., McCauley, H. A., Zhang, R. R., Lewis, K., Hakozaki, S., Ferguson, A., Saiki, N., Yoneyama, Y., Takeuchi, I., Mabuchi, Y., … Takebe, T. (2019). Modeling Steatohepatitis in Humans with Pluripotent Stem Cell-Derived Organoids. *Cell Metabolism*, *30*(2), 374-384.e6. https://doi.org/10.1016/j.cmet.2019.05.007

Poisson, J., Lemoinne, S., Boulanger, C., Durand, F., Moreau, R., Valla, D., & Rautou, P. E. (2017). Liver sinusoidal endothelial cells: Physiology and role in liver diseases. *Journal of Hepatology*, *66*(1), 212–227. https://doi.org/10.1016/j.jhep.2016.07.009

Rogers, K. W., & Schier, A. F. (2011). Morphogen gradients: From generation to interpretation. *Annual Review of Cell and Developmental Biology*, *27*, 377–407. https://doi.org/10.1146/annurev-cellbio-092910-154148

Turing, A. (1952). The chemical basis of morphogenesis. *Philosophical Transactions of the Royal Society of London. Series B, Biological Sciences*, *237*(641), 37–72. https://doi.org/10.1098/rstb.1952.0012

Wolpert, L. (1969). Positional information and the spatial pattern of cellular differentiation. *Journal of Theoretical Biology*, *25*(1), 1–47. https://doi.org/10.1016/S0022-5193(69)80016-0

Wu, F., Wu, D., Ren, Y., Huang, Y., Feng, B., Zhao, N., Zhang, T., Chen, X., Chen, S., & Xu, A. (2019). Generation of hepatobiliary organoids from human induced pluripotent stem cells. *Journal of Hepatology*, *70*(6), 1145–1158. https://doi.org/10.1016/j.jhep.2018.12.028

Xie, A. W., Binder, B. Y. K., Khalil, A. S., Schmitt, S. K., Johnson, H. J., Zacharias, N. A., & Murphy, W. L. (2017). Controlled Self-assembly of Stem Cell Aggregates Instructs Pluripotency and Lineage Bias. *Scientific Reports*, *7*(1). https://doi.org/10.1038/s41598-017-14325-9

5

CONCLUSION

FINAL CONCLUSION

A significant milestone of this study was the comprehensive transcriptomic analysis conducted at multiple stages of differentiation, which revealed the dynamic gene expression profiles associated with endoderm specification and hepatic development. By identifying distinct gene clusters that peak at various stages of differentiation, the study unveiled novel putative regulators, signaling mediators, and surface markers essential for hepatic development. These insights not only validate the differentiation protocol but also offer a broader understanding of the molecular mechanisms driving endoderm differentiation.

The research further explored the generation of liver bud organoids, emphasizing the limitations and challenges of the traditional co-culture method. Despite efforts to co-culture hepatic endoderm, ECs and STM from hiPSCs, the resulting organoids lacked the necessary complexity and spatial organization characteristic of the liver bud *in vivo*. This method, although demonstrating some degree of vascularization, proved to be labor-intensive and challenging, highlighting the difficulty in replicating the intricate cell interactions required for liver morphogenesis.

To address these limitations, the study investigated the co-emergence strategy, wherein different cell types co-emerge and self-organize within a single hiPSC aggregate. By exposing these aggregates to varying concentrations of activin A, the study demonstrated that morphogen gradients can drive spatial patterning and differentiation within the aggregates, supporting the formation of liver bud organoids that closely mimic *in vivo* liver development. Moreover, the study's approach of using a vertical-wheel bioreactor to generate homogeneous cell aggregates and create spatial gradients of morphogen concentrations proved to be a critical factor in the successful differentiation and organization of the cells into functional liver organoids. The low activin A concentrations facilitated the emergence of posterior foregut-like structures that later mimicked the liver budding process, while higher concentrations led to more extensive endodermal differentiation. This process enables precise regulation of cell fate during liver organoid production by varying the concentration of morphogens like activin A at the initial stages. Consequently, this study has established a versatile platform capable of producing liver organoids tailored to specific research objectives (Figure 5.1). On one hand, this platform allows for the recapitulation of key events in liver organogenesis, facilitating detailed studies of human liver development and the modeling of hepatic diseases for subsequent drug discovery. On the other hand, liver organoids with de novo generated hepatocytes offer a promising tool for assessing hepatotoxicity and serving as a cell source for cell therapy.

The novelty of this approach lies not only in its ability to replicate the developmental processes more accurately but also in its potential to uncover new mechanisms of tissue formation and differentiation. By using activin A gradients, it is possible to investigate how cells interpret and respond to varying morphogen signals, which is crucial for understanding the principles of tissue patterning and organogenesis. Moreover, this approach allows for the future study of heterotypic cell-cell interactions, providing a comprehensive view of the microenvironmental factors that influence cell fate decisions.

However, the co-emergence strategy developed in this study has room for improvement. Cell maturation should be carried out to mimic the entire developmental process from pluripotency to fetal liver and not just the liver bud stage. Additionally, the evaluation of functional properties should be performed to fully leverage the potential of this model, as current models fail to replicate the metabolic properties of the liver, which are crucial for drug discovery.

This work not only advances the field of hepatic differentiation and liver organogenesis but also sets the stage for future research to refine these protocols further. The insights gained from this study can have broad implications for the generation of other organoids derived from the gut tube, such as the pancreas, where similar principles of endoderm-mesoderm interactions and signaling gradients are crucial. By extending these methodologies, researchers can enhance the physiological relevance and functionality of organoids, making them valuable tools for studying development, disease mechanisms, and drug responses.

Overall, this study represents a step forward in the field of stem cell research and organoid technology. The ability to recreate the complexity of liver morphogenesis *in vitro* opens new avenues for understanding liver development, modeling liver diseases, and developing therapeutic applications.

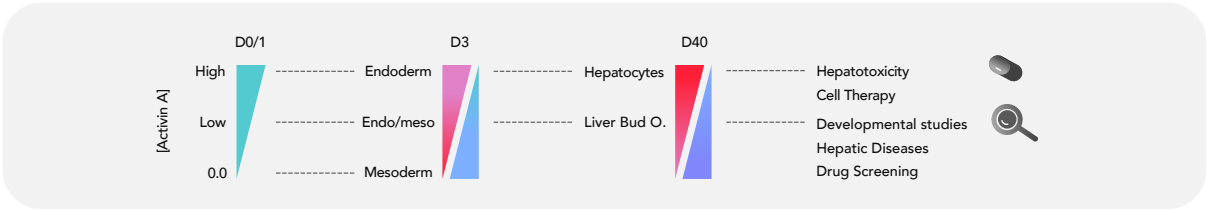

Figure 5.1 - Summary diagram for LO production in the developed platform. Different activin A concentrations lead to different liver organoids with different potential applications, as depicted.